SURFACE HEAT EXCHANGE IN TEMPERATURE DISTRIBUTION IN I-BEAM SECTIONS UNDER STANDARD FIRE CURVE

by

Ahmet Fazıl Kara

B.S., Civil Engineering, Yıldız Technical University, 2007

Submitted to the Institute for Graduate Studies in
Science and Engineering in partial fulfillment of
the requirements for the degree of
Master of Science

Graduate Program in Civil Engineering

Boğaziçi University

2018

ACKNOWLEDGEMENTS

I would like to express my gratitude to my thesis supervisor Assoc. Prof. Serdar Selamet for his help and guide during the preparation of this study.

I would like to express my special thanks to Oğuz Kırkgöz from ENKA construction for his help to supply HEB 300 and HEB 400 sections and insulation materials for the test preparation for this study.

I would like to express my gratitude to my Manager Metehan Çalış from TSE for his help and guide during this study.

ABSTRACT

SURFACE HEAT EXCHANGE IN TEMPERATURE DISTRIBUTION IN I-BEAM SECTIONS UNDER STANDARD FIRE CURVE

Fire is one of the most hazardous, unintentionally events in buildings. Structural engineers deal with fire resistance that might be one of the most important part of structural engineering in case of fire. Estimation of structural temperatures using heat transfer fundamentals is generally neglected by structural engineers. However, the temperature results of steel sections are as important as their mechanical properties and play an important role in thermo-mechanical analyses. Therefore, it is crucial to correctly calculate the temperatures sections of the structural elements. This study aims for a more accurate estimation of average section temperature and thermal gradient in steel column I-sections by considering the heat exchange between flanges and web in the section enclosure. This is generally not taking into account in numerical heat transfer analyses. The thermal behaviour of I sections, which are generally used for perimeter columns, are exposed to two hour ISO 834 standard time-temperature curve in a fire furnace and temperatures at different cross section locations are collected. These results are then validated by finite element analyses.

ÖZET

STANDART YANGIN EĞRİSİ ALTINDA I KESİTLERDEKİ SICAKLIK DAĞILIMINDA YÜZEY ISI DEĞİŞİMİ

Yangın, binalarda en tehlikeli, kasıtsız olaylardan biridir. Yapı mühendisleri, yangın durumunda yapı mühendisliğinin en önemli parçalarından biri olabilecek yangına dayanım konusu ile ilgilenirler. Isı transfer temellerini kullanarak yapısal sıcaklıkların tahmini genellikle yapısal mühendisler tarafından ihmal edilir. Bununla birlikte, çelik kesitlerin sıcaklık sonuçları, mekanik özellikleri kadar önemlidir ve termo-mekanik analizlerde önemli bir rol oynar. Bu nedenle, yapısal elemanların sıcaklık bölümlerini doğru bir şekilde hesaplamak çok önemlidir. Bu çalışma, I kolon kesitlerinin flanş ve gövde arasındaki ısı transferini düşünerek ortalama çelik sıcaklığı ve termal gradyanın daha doğru bir tahminini amaçlamaktadır. Bu genellikle nümerik ısı transfer analizlerinde dikkate alınmaz. Genellikle çevre kolonları için kullanılan I kesitlerin termal davranışı, bir yangın fırını içinde 2 saatlik ISO 834 standart zaman sıcaklık eğrisine maruz bırakılarak, farklı kesit alanlarındaki sıcaklık değerleri toplanmıştır. Bu sonuçlar daha sonra sonlu elemanlar (FE) analizleriyle doğrulanmıştır.

TABLE OF CONTENTS

LIST OF FIGURES

LIST OF TABLES

LIST OF SYMBOLS

A_1	The area of the emitting surface
A_m	The surface area of the member per unit length
A_m/V	The section factor for unprotected steel members
b	Thermal inertia with units
c_a	The specific heat of steel
c_p	The amount of heat required to heat a unit mass of the material by one degree with units
d	Depth of specimen from extreme fibre compression zone to extreme fibre of tension zone
h	Convective heat transfer coefficient
h	Exposed height
$h_{net}^{\cdot}$	The design value of the net heat flux per unit area
$q^{\cdot"}$	Heat flow per unit area
k	Represents the rate of heat transferred through a unit thickness of the material per unit temperature difference
k	Thermal conductivity
k_{sh}	Correction factor for the shadow effect
L	Exposed span length
t	Time
T	Temperature
T_e	The absolute temperature of the emitting surface
T_r	The absolute temperature of the receiving surface
V	The volume of the member per unit length
x	distance in the direction of heat flow
α	Thermal diffusivity
α	Thermal diffusivity
δ	The mass of the material per unit volume
δ_a	The unit mass of steel

ε_e	Emissivity of the emitting surface
ε_r	The emissivity of the receiving surface
σ	The Stefan-Boltzmann constant
φ	Configuration factor
φ_{ij}	View factor coefficient calculated as follows in three-dimensional space
Δt	The time interval
ΔT	Temperature difference between the surface of solid and the fluid
x_{fi}	Reduction factor for flexural buckling in the fire design situation
$k_{y,\theta}$	Reduction factor from EN 1993-1-2 for yield strength of steel at the steel temperature θ_a reached at time t.
$N_{b,fi,t,Rd}$	Buckling resistance
$k_{E,\vartheta}$	reduction factor from EN 1993-1-2 the slope of the linear elastic range at the steel temperature θ_a reached at time t.
λ'_θ	Non dimensional slenderness
f_y	Steel yield stress

LIST OF ABBREVIATIONS

2D	Two Dimensional
3D	Three Dimensional
FE	Finite Element
EN	European Norm

1. INTRODUCTION

Fire is one of the most hazardous, unintentionally events in buildings. Fire resistance in structural elements is one of the topic that structural engineers deal with. Fire resistance is often described as passive fire protection, which is always ready and waiting for a fire (Buchanan, 2001) that prediction of temperatures of structural members are crucial to calculate material internal forces.

This study aims for a more accurate estimation of average steel temperature (ΔT) and thermal gradient in column I (or H) sections ($T_{y,mm}$). The thermal behaviour of I sections, which are generally used for perimeter columns, are exposed to ISO 834 standard time-temperature curve in a fire furnace and temperature at different cross section locations are collected. These results are then validated by finite element (FE) analyses. The main objective is to find the effect of heat exchange between hot, cold steel surfaces on the average temperature, and thermal gradient of I sections.

Heat transfer by radiation is dominant at high temperatures for steel sections, so the radiative heat transfer should be assessed precisely. Steel construction sector often uses wide flange steel sections such as I-H sections. I or H sections have 3 faces in their enclosure. 2 of 3 (bottom and top flange) is parallel to each other, the other one is perpendicular to the top and bottom flanges. When the section is exposed to fire from one side, radiative heat exchange also starts additionally in these three enclosure. If the section is fully engulfed in fire, the radiative heat exchange can be ignored in enclosures. But, if the section exposed to one-sided heating (fire) such as perimeter columns, the heat transfer exchange between these faces shall be taken in to account due to thermal gradient.

In this study, I sections FE models in ABAQUS heated form one side is to be modelled and the actual test results will be compared with those models. The aim of this study is to verify when the heat exchange in enclosure of I section is taken in to account and the thermal gradient of the section is reduced.

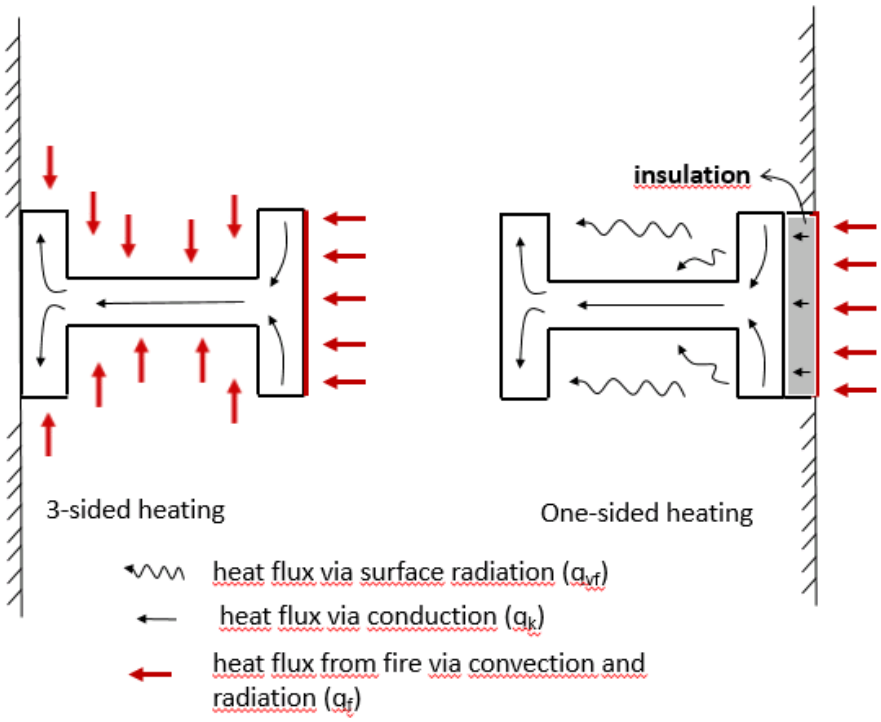

Figure 1.1. One-sided and 3-sided Heating View.

2. PURPOSE OF THE STUDY

In Eurocode 3 - Design of steel structures - Part 1-2: General rules - Structural fire design, three and four-side fire exposure conditions are being determined with shadow effect. However, section heated from one side is not indicated. In this study, columns are heated from one side from flange surface and radiation heat exchange to be considered in FE model and to be validated with fire test.

An efficient calculation methodology is developed by Selamet, 2011 to calculate the radiation heat flux generated by heat exchange between surfaces in the enclosure of uninsulated column I-sections. The heat fluxes are calculated by finding the radiation configuration (view) factors of each surface in the enclosure. First, the general view factor equation for planar surfaces in three-dimensional space is reduced into an equation for two-dimensional space. Hence, the surfaces are treated as finite lines or strips, which could be oriented by an arbitrary angle and spaced from each other by a finite distance. This algorithm is then implemented into the nonlinear heat transfer finite element code FEHEAT (Selamet, 2011) developed by the author (Selamet, 2017).

Purpose of the study is to estimate precisely average steel temperature (ΔT) and thermal gradient (T_y) in I column section. Normally, structural fire engineers do not take in to account the radiation effects on enclosure in one side heating fire exposure assume as adiabatic surface. While they perform one side heating conditions in numerical study, they underestimate the radiation effect on I section enclosure and assume as adiabatic. However, in real case, radiation heat exchange in enclosure surface might have large effects on thermal gradient (T_y) of I sections and average cross section temperature (ΔT) as well. Underestimation of average cross section temperature can cause less axial load demand. In addition, this can cause also less column capacity than expected.

In order to prove the radiation effects on enclosure, in this study, 2 same sections are tested at the same time in furnace. First section enclosure is insulated with ceramic

wool as far as closer to adiabatic surface properties. The latter one is keep as it is, in order to see the effects of radiation on enclosure surface. This uninsulated case simulate the real case. Hence, testing simultaneously insulated (numerical case) and uninsulated (real case) enable to see the difference between numerical and real case of I sections. The test sections are exposed ISO 834 time-temperature curve in a fire furnace. Temperature at different cross section locations are recorded during two-hour fire exposure conditions for one side heating.

In this study, the I-H sections FE models in ABAQUS heated form one side is to be modelled and the actual test results will be compared with those models. The main objective is to investigate the effect of heat exchange between hot and cold surfaces on the average temperature (ΔT) and thermal gradient of I sections (T_y).

3. LITERATURE REVIEW

An accurate estimation of the temperatures in structural member cross sections is the first and most crucial step to calculate fire induced forces and moments and ultimately to evaluate the fire performance of a structural system. (Selamet, 2017). Large thermal gradients within the cross section of structural members cause significant thermal stresses; hence change the mechanical behaviour of the structural system. (Fu *et al.*, 1990). Fire tests of structural elements are over costing and it is difficult to perform fully representative of the construction intendent for use in practice as well. Computational design for material properties known material is crucial to perform both thermal and structural analysis. In most cases, FE modelling is alternative solution to make it inexpensive and easy to see the results. Once the thermal field in the cross section is determined, the load bearing capacity (i.e. combined moment and axial load) of the perimeter columns can be accurately estimated. (Selamet, 2017).

In Eurocode 3 - Design of steel structures - Part 1-2: General rules - Structural fire design, three and four-side fire exposure conditions are being determined with shadow effect. However, section heated from one side is not indicated. In this study, columns are heated from one side from flange surface and radiation heat exchange to be considered in FE model and to be validated with fire test.

An efficient calculation methodology is developed by Selamet, S, 2011 to calculate the radiation heat flux generated by heat exchange between surfaces in the enclosure of uninsulated column I-sections. The heat fluxes are calculated by finding the radiation configuration (view) factors of each surface in the enclosure. First, the general view factor equation for planar surfaces in three-dimensional space is reduced into an equation for two-dimensional space. Hence, the surfaces are treated as finite lines or strips, which could be oriented by an arbitrary angle and spaced from each other by a finite distance. This algorithm is then implemented into the nonlinear heat transfer finite element code FEHEAT (Selamet, 2011) developed by the author (Selamet, 2017).

In the absence of an absorbing medium, radiative heat exchange between surfaces in an enclosure depends on the optical view of each surface to the others, which is generally referred as the geometric effect to the temperature field in the structural member cross section. This geometric effect is calculated by employing the view factor, which is the fraction of radiant energy leaving one surface that is intercepted by another surface. The view factors of any geometry can be calculated by the area (or line) integration algorithm, and the integrals are generally solved using numerical integration techniques (Shapiro 1985; Emery *et al.*, 1991). The geometric effect of radiation in steel I-sections was first investigated by Wickstrom (2001). Wickstrom concluded that the enclosure dimensions and the rate of temperature increase during fire significantly affect the thermal field in the I-section. (Selamet, 2017).

In case of fire expose from three side for open sections, the enclosure radiation does not affect the temperature field. Observations in fire experiments and numerical analyses (Ghojel and Wong 2005; Vacha *et al.*, 2016) suggest that the enclosure radiation does not affect the temperature field if the wide flange sections are subjected to fire on three sides (i.e. all surfaces except the top surface).

In addition, Virdi and Wickstrom (2013) suggested that, further significant reductions in temperature in temperatures are obtained by considering the shadow effect for boxed steel beam exposed three-side with concrete slab. In this study, the perimeter columns are to be heated only the flange surface, thus the radiation heat exchange is crucial and the temperature difference of bottom and top flange will be less than estimated.

3.1. Introduction to Fire Test

The test furnaces as per EN 1363-1 shall be design to work with liquid or gaseous fuels. In this study, Turkish Standards Institution (TSE) indicative furnace was used and is being worked with natural gas. Furnace lining and material density requirements comply with EN 1363-1. Fuel and air ratio shall be approximately 4% when the test sample is non-combustible as per EN 1363-1. In this furnace verifications were done by

TSE as yearly basis. Internal size of TSE indicative furnace is 1,55mx1,55m. Normally as per EN 1363-1 or any other national standards size of the furnace shall generally have dimension minimum 3mx3m in order to simulate actual size of the specimen in real application. But for the research purposes, this furnace is suitable, logical and profitable in order to see the results soon. In fire tests main problem to conduct test is cost of the test and construction. So TSE indicative furnace of TSE is appropriate for such kind of tests.

Temperature-time curves are defined in EN standards as standard temperature-time curve, hydrocarbon curve, external fire exposure curve and slow heating curve.

In case of higher temperature and rapid growing rate of fire, hydrocarbon curve is being used. For instance, in petrochemical and oil industries, structural elements can expose intensive fire conditions such as liquid pool. In this case, hydrocarbon curve should be used. Hydrocarbon fire exposure conditions versus time defined in standards as follows:

$$T = 1080(1.0,325\ e^{(-0,167t)} - 0,675\ e^{(-2,5t)}) +\ 20 \tag{3.1}$$

where is the t time in minutes, is the T Average furnace temperature in °C.

Structural elements may be exposed to fire less than room fire exposure conditions in some cases. For instance, perimeter fire wall in buildings may exposed to fire from external window. In this case, fire exposure conditions are less than compartment fires. External fire exposure curve conditions versus time defined in standards are as follows:

$$T = 660\ (1 - 0,687\ e^{(-0,32t)} - 0,313\ e^{(-3,8t)} + 20) \tag{3.2}$$

where is the t time in minutes, is the T Average furnace temperature in °C.

For some products such as raised floor system fire exposure conditions may be reduced like slow heating curve. In this case for slow heating fire cure conditions versus

time define in standards are as follows.

$$T = 154t^{0,25} + 20 for 0 < t \leq 21 \tag{3.3}$$

$$T = 345\ log\ 10\ (8t + 1) + 20\ t\ >\ 21 \tag{3.4}$$

As per EN 1363-1 furnace temperature equation for standard temperature-time curve shall be satisfied with below equation:

$$T = 345\ log\ 10\ (8t\ +\ 1)\ +\ 20 \tag{3.5}$$

where is the T the average temperature of furnace in ^{o}C, is the t the time in minutes.

The value of 20 in equation is ambient temperature. Average temperature shall be calculated minutely basis derived from plate thermocouples (to be explained later on).

If it is calculated as per logarithmic value, in minute basis, furnace temperature shall be as follows:

Table 3.1. ISO 834 Temperature time curve.

TEMPERATURE-TIME CURVE (ISO 834)	
Time (in minute)	Temperature (in ^{o}C)
0	20
5	576
10	678
15	738
20	781
30	842
45	902
60	945
90	1006
120	1049
150	1082
180	1110
210	1133
240	1153
300	1186
360	1214

Standard Temperature-Time (ISO 834) fire curve shall be shown in Figure 3.1.

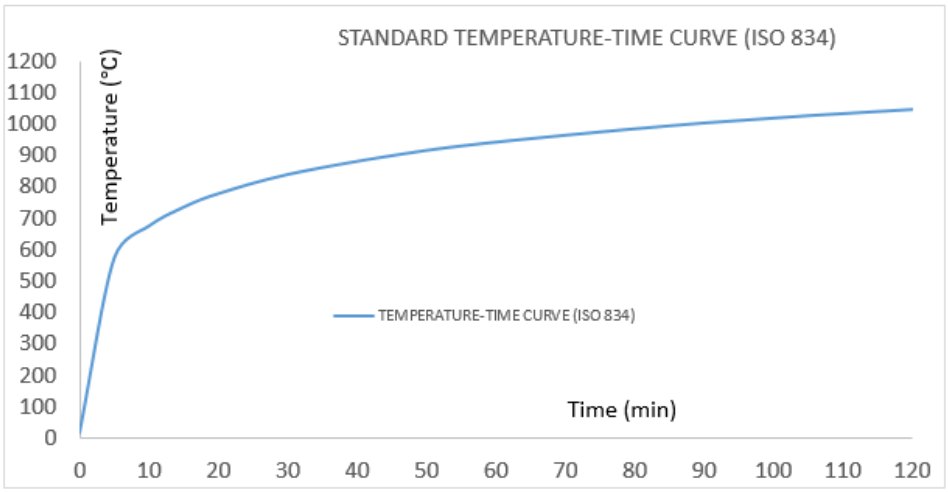

Figure 3.1. Temperature-Time curve (ISO 834).

All Temperature-time curves as per EN standards are shown in Figure 3.2.

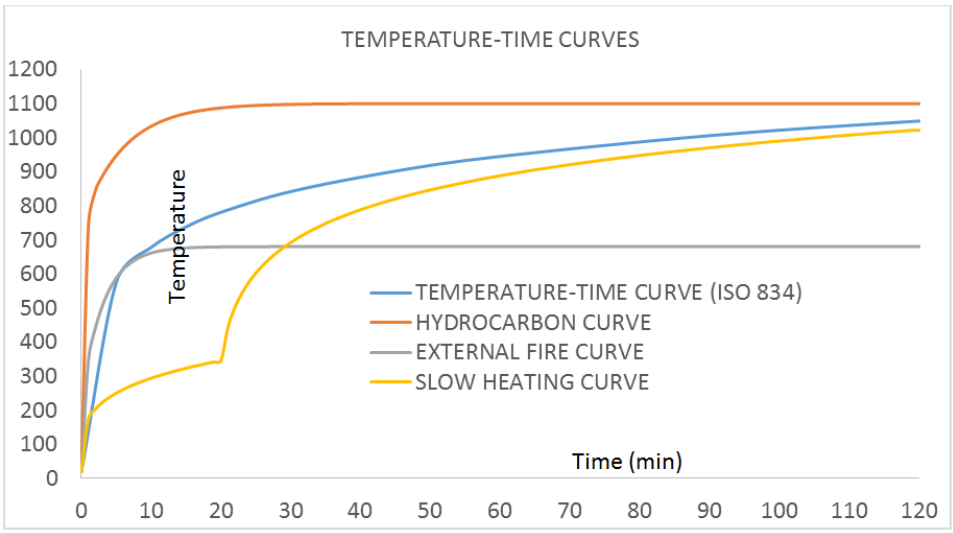

Figure 3.2. Temperature-Time curves (in European Norm).

In this study, the most common use for room fire exposure conditions ISO 834 standard temperature time curve is used. Furnace thermocouple shall be plate thermometers which is (150 ± 1) mm long by (100 ± 1) mm wide by (0,7 ± 0,1) mm folded and shall be made by folded nickel alloy plate. Thermocouple wire (type K) shall be fixed to geometric centre of it. Thermocouple wire properties shall be comply

with EN 60584-1, shall contain mineral insulation in heat resistance steel alloy sheath of nominal diameter 1mm to 3mm. TSE Fire Laboratory uses 1mm diameter Type K thermocouples. Plate thermocouples shall be insulated with a pad of inorganic insulation material nominally (97 ± 1) mm by (97 ± 1) mm by (10 ± 1) mm thick, density (280 ± 30) kg/m^3. Thermocouples calibration is being performed and periodically verified with TSE calibration department and with TSE Fire Resistance Laboratory calibrator. After 50-hour thermocouples shall not be used any more as per EN 1363-1 Fire Resistance-Tests -Part 1 : General Requirements. Thermocouples temperature values is being controlled by software in order to follow the proposed time-temperature curve and recorded by software per second. Furnace plate thermos couples shall be as shown below as per EN 1363-1 EN 1363-1 Fire Resistance-Tests -Part 1: General Requirements.

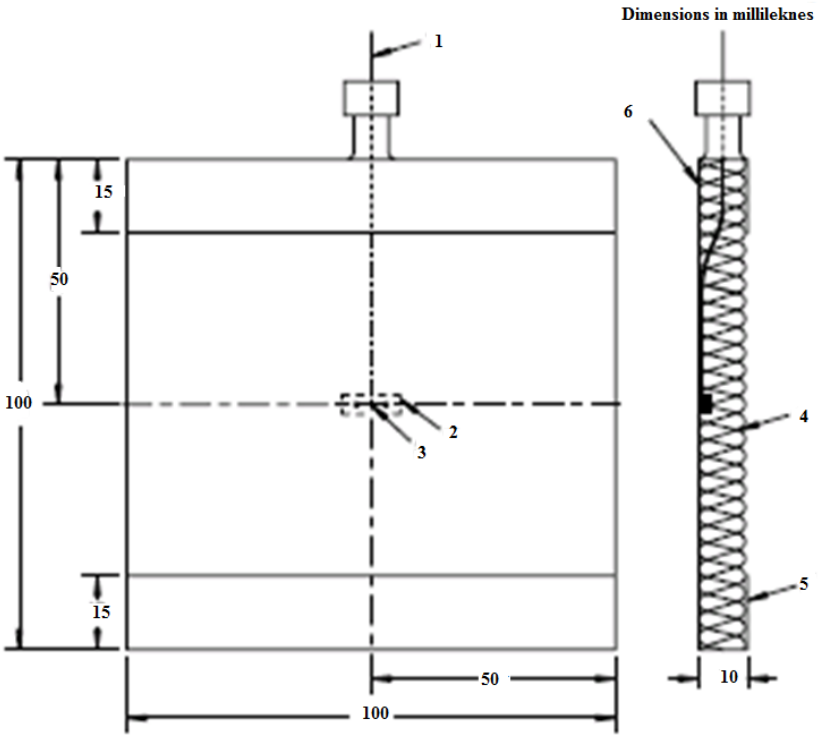

Figure 3.3. Design of plate thermometer.

(i) 1 sheathed thermocouple with insulated hot junction

(ii) 2 spot welded or screwed steel strip

(iii) 3 hot junction of thermocouple

(iv) 4 insulation material (oriented towards the test specimen)

(v) nickel alloy strip (0,7 ± 0,1) mm thick

(vi) face 'A'

Internal thermocouples to measure steel specimen temperatures shall be insulated double glass fibre insulated wire as per EN 1363-1 Fire Resistance-Tests -Part 1: General Requirements. It shall have minimum 0,5 mm diameter. They shall be used once only. In this study 0,8 mm Type K wire is to be used. The thermocouples are double ceramic insulated and 1200 ^{o}C fire retardant. For fixing of thermocouples, steel surface drilled larger in diameter from wire diameter and edge of the hole punched to retain wire inside the steel.

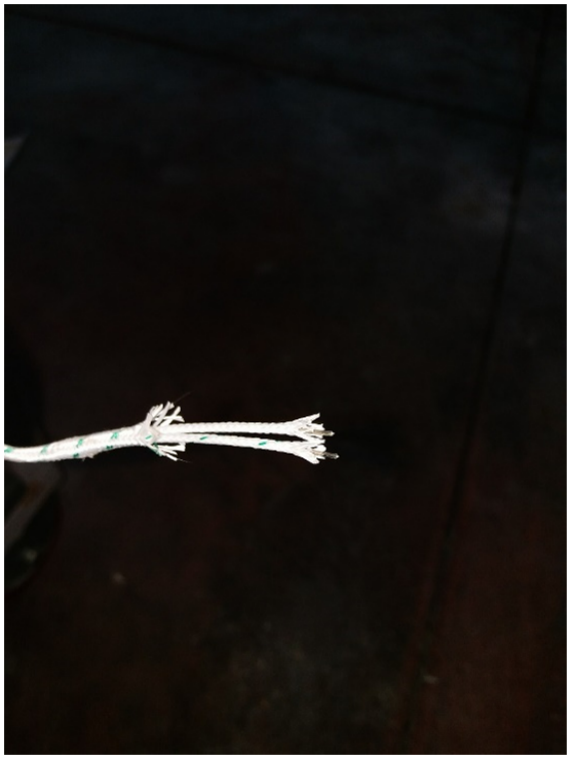

Figure 3.4. 0,8 mm Type K wire thermocouple wire.

The pressure in the furnace shall be measured by sensors described in EN 1363-1 Fire Resistance-Tests -Part 1: General Requirements. The sensors shall operate within the limits specified in EN 1363-1 Fire Resistance-Tests -Part 1: General Requirements. In TSE fire resistance laboratory sensor is being controlled and recorded by software in second bases. It can be accepted that the pressure gradient will be almost 8,5

Pa per meter height of furnace as per for the controlling of the pressure in furnace in EN 1363-1 Fire Resistance-Tests -Part 1 : General Requirements. The furnace pressure shall be maintained relative to the pressure outside the furnace at the same height. The pressure shall be controlled and monitored that it shall be ± 5 Pa upper and lower limit after 5 minutes the test start and shall be ± 3 Pa after 10 minutes. Even if there is no significant effects such kind of specimen, the proposed pressure shall be maintained during the test. In this study, the specimens shall be positioned as horizontally. The nominal pressure on the underside of the specimens shall not exceed 20 Pa during the test as per EN 1363-1 Fire Resistance-Tests -Part 1: General Requirements. The pressure shall be maintained 100 mm below the underside of the specimens. As described before, even if the specimens are not separating element such as beams, columns, the pressure shall be maintained as above. One pressure sensor is enough to control the furnace for horizontal test elements as per EN 1363-1 Fire Resistance-Tests -Part 1: General Requirements. The T type sensors is erected back side of the furnace. The detail of the sensor shall be as follows:

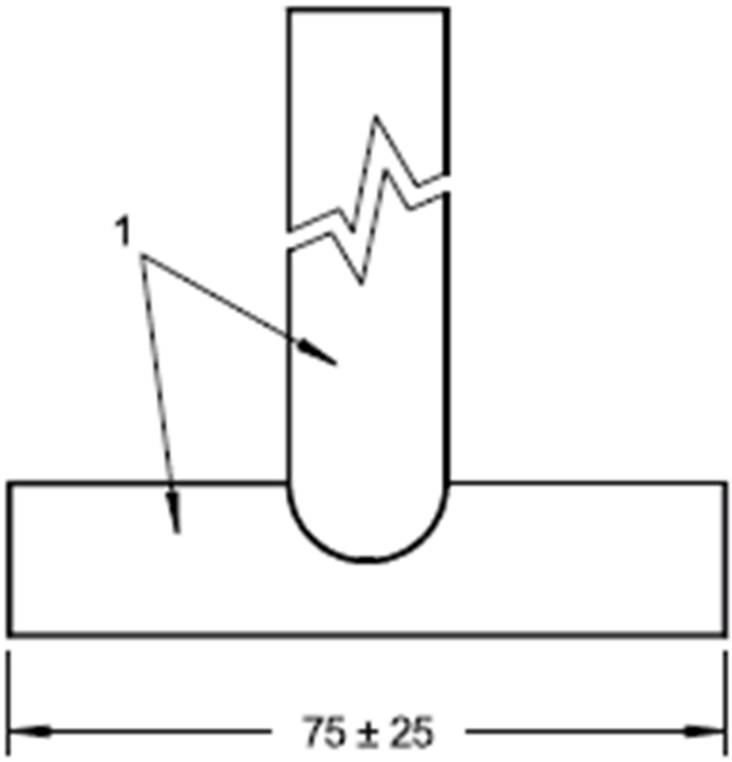

Figure 3.5. Pressure Sensor.

'T' sensor, 1 stainless steel tube (inside diameter (7,5 ± 2,5)mm).

Figure 3.6. Pressure sensor from inside the furnace.

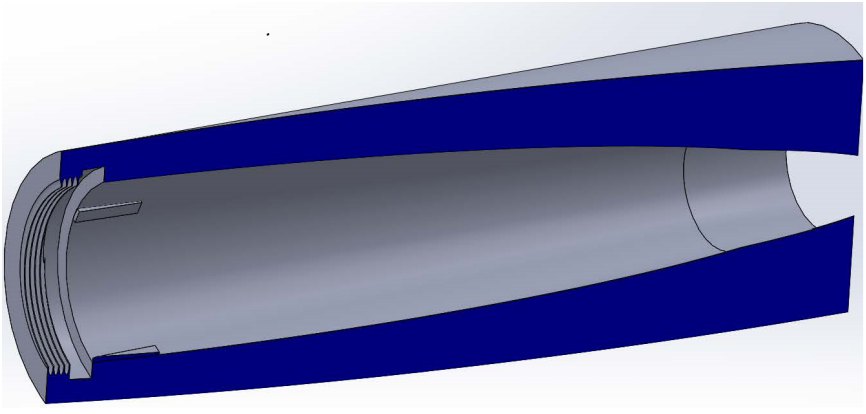

Figure 3.7. Pressure sensor from outside the furnace.

Deviation in furnace as per EN 1363-1 Fire Resistance-Tests -Part 1: General Requirements. Tolerances in furnace temperature is given as follows in EN 1363-1 Fire resistance tests - Part 1: General Requirements:

The deviation percentage in the area of the curve of the average temperature recorded by the plate thermocouples specified in EN 1363-1 against time the standard temperature/time curve area shall be within the below limits:

The percentage deviation (de) in the area of the curve of the average temperature recorded by the specified furnace thermocouples versus time from the area of the standard temperature/time curve shall be within:

(i) 15 % for $5 < t \leq 10$
(ii) (15 - 0,5 (t-10))% for $10 < t \leq 30$
(iii) (5 - 0,083 (t-30))% for $30 < t \leq 60$
(iv) 2,5% for $t > 60$

$$de = \frac{A\ A_s}{A_s} x\ 100 \tag{3.6}$$

where de is the percentage deviation, A is the area under the actual furnace temperature/time curve, As is the area under the standard temperature/time curve, t is the time in minutes.

All areas shall be calculated as not exceeding 1 min intervals. At any time temperature recorded by furnace thermocouples shall not be deviate 100 K from standard temperature/time curve after the 10 minutes start of the test.

Fuel-air ratio of the burners shall have minimum approximately 4% oxygen content as per EN 1363-1 Fire Resistance-Tests -Part 1 : General Requirements. In TSE fire resistance laboratory, this ratio is being controlled periodically in yearly basis. The ambient temperature shall be within the limit 10^oC - 40 ^oC from the beginning of the test. It shall be recorded at a distance of between 1m and 3m horizontally away from outside of the furnace. Under that conditions the sensor shall not be affected by thermal radiation from the test specimen or furnace. The temperature in the test area shall not decline by more than 10 K or shall not raise by more than 20 K during the

test. Recording shall be performed by below device:

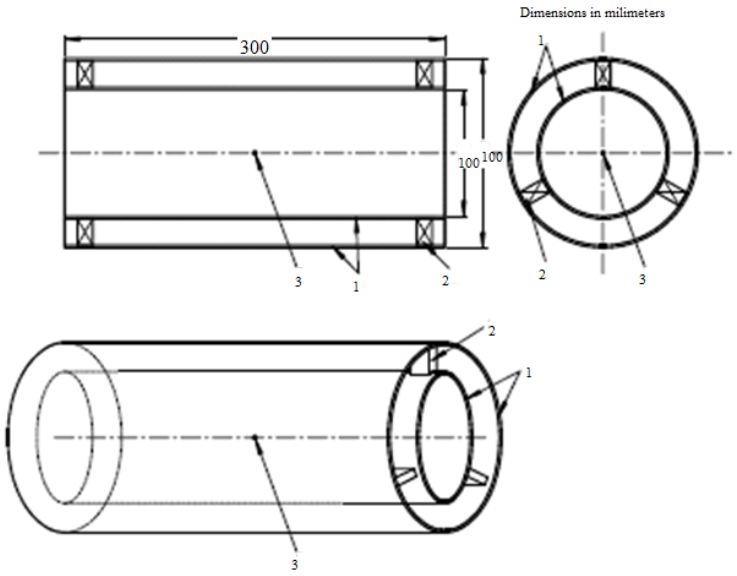

Figure 3.8. Ambient Temperature Measuring Device.

(i) concentric plastic pipes

(ii) spacer

(iii) position of ambient temperature measuring thermocouple

Figure 3.9. TSE Ambient Temperature Measuring Device.

3.2. Heat Transfer Fundamentals

Heat transfer definitions are crucial in order to understand thermal behaviour of structures as well as in fire conditions. Heat transfer can be explained and take place by means of conduction, convection and radiation.

3.3. Conduction

Conduction heat transfer occurs in solid materials. If materials are good conductors of heat, heat passing through the materials by means of interacting of free electrons. It means that, if the materials are good conductors, they are generally also good heat conductors. (Buchanan, 2001). Fire occurrence on solid surface or burning of solid surfaces makes heat conduction crucial.

There are three criteria to be known in order to calculate heat transfer calculations. Density, specific heat and thermal conductivity are main properties to be known. Buchanan, 2001 defined these properties as follows:

Density δ: the mass of the material per unit volume in kg/m^3. Specific heat c_p: the amount of heat required to heat a unit mass of the material by one degree with units J/kgK. Thermal conductivity k: represents the rate of heat transferred through a unit thickness of the material per unit temperature difference, with unit W/Mk. In addition, thermal diffusivity and thermal inertia are also needed properties. Thermal diffusivity $\alpha = k/\delta c_p$ Thermal inertia b $k/\delta c_p$ with units W^2 s/m^{4}K^2. (Buchanan, 2001). Conduction heat transfer is proportional to the temperature gradient between two points in steady state condition. k thermal conductivity is constant and equations defined as follows;

$$q^{"} = k\ dT\ /dx \tag{3.7}$$

where $q^{"}$ heat flow per unit area (W/m^2), k is the thermal conductivity (W/Mk), T is the temperature ^{o}C or K, x is the distance in the direction of heat flow.

Buchanan, 2001 explained that in the steady state calculation material temperature change does not have effects on calculation.

But for the transient analysis, when the temperature changes by time, the heat amount to change material temperature must be taken in to account. Buchanan, 2001 defined this equation as follows.

$$\frac{\delta^2 T}{\delta x^2} = \frac{1}{\alpha} - \frac{\delta T}{\delta t} \tag{3.8}$$

where t time (s), α is the thermal diffusivity (m^2/s).

It can be understood that the lower thermal diffusivity means the more heat conduction occurs. This equation can be extended to two or three dimension as well. Analytical, graphical or numerical methods can be used for calculation. But most of the time, computer based numerical methods is being used as finite-element method.

3.4. Convection

When the heat moves through gases or liquids, it is calculated by convection. Convective heat transfers generally defined between solid surface and fluid around solid that interacts by heating or cooling the solid surface. The convective heat transfer generally take in to account proportionally temperature difference between fluid and solid surface. Heat flow per unit area defined as follows in Buchanan, 2001;

$$q^{"} = h\Delta T \tag{3.9}$$

where h is the convective heat transfer coefficient (W/m^2 K), ΔT is the temperature difference between the surface of solid and the fluid (^{o}C or K).

Heat transfer coefficient can change based on the surface geometry, flow nature and the boundary layer thickness. Buchanan, 2001 defined value for fire-exposed elements is 25 W/m^2 K.

3.5. Radiation

Radiation heat transfer is energy transfer that pass through a vacuum, transparent solid or liquid by electromagnetic waves. Radiation is one of the most crucial point in fires because of the heat transfer pass through from flames to fuel surfaces, because of the fact that hot smoke effects the structural elements. (Buchanan, 2001). The radiation heat flux at a point on a receiving surface;

$$q^{"}(W/m^2) = \varphi \varepsilon_e \sigma T_e^4 \tag{3.10}$$

where φ is the configuration factor, ε_e is the emissivity of the emitting surface, σ is the Stefan-Boltzmann constant (5.67 x 10^{-8} W/m^{2}K^4), T_e the absolute temperature of the emitting surface (K). The radiation heat flux from the emitting surface to the receiving surface;

$$q^{"}(W/m^2) = \varphi \varepsilon \sigma T_e^4 - T_r^4 \tag{3.11}$$

where T_r is the absolute temperature of the receiving surface.

$$\varepsilon \frac{1}{\frac{1}{\varepsilon_e} + \frac{1}{\varepsilon_r} - 1} \tag{3.12}$$

where ε_r is the emissivity of the receiving surface.

The emissivity value changes from 0 to 1.0. For pure black-body, emissivity can be taken 1.0. In structural fire flames emissivity can change from 0.7 to 1.0. (Buchanan, 2001). The emissivity of the material also time dependent. Because after a certain temperature of a solid surface reached, material surface condition changes.

The configuration factor φ (view factor) is a measurement that how much emitter is being seen by the receiving surface. Buchanan, 2001 defined the configuration factor

as follows below; In Figure 3.11 above, configuration factor is as follows;

$$\varphi = \int^{A1} cos\ \theta_1\ cos\ \theta_2\ d\ A1\ /(\pi 2^2) \tag{3.13}$$

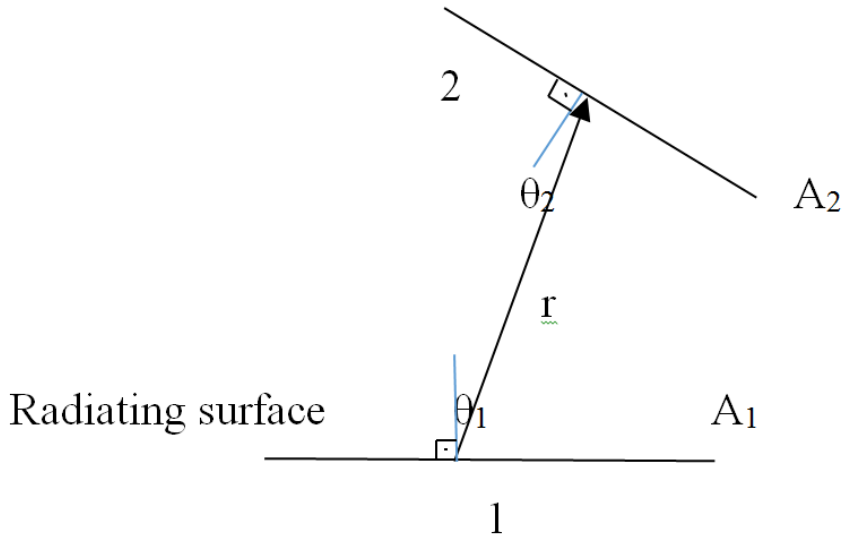

Figure 3.10. Radiation from one surface to another.

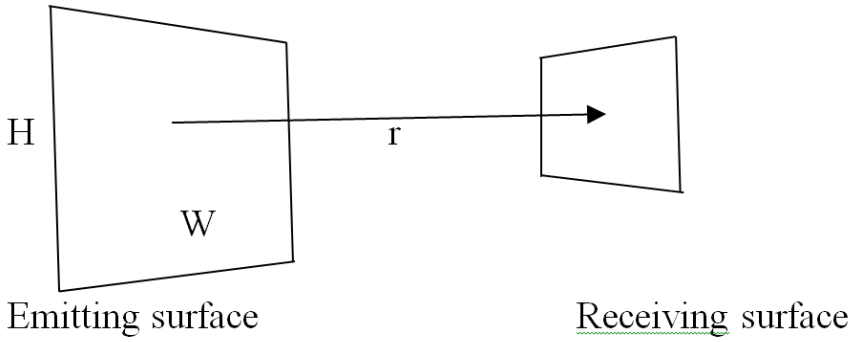

Figure 3.11. Emitting and receiving surface.

$$\varphi = \frac{1}{90}\left[\frac{x}{\sqrt{1+x^2}}tan^{-1}\left(\frac{y}{\sqrt{1+x^2}}\right) + \frac{y}{\sqrt{1+y^2}}tan^{-1}\left(\frac{x}{\sqrt{1+y^2}}\right)\right] \tag{3.14}$$

$$x = H/22 \tag{3.15}$$

$$y = W/2r \tag{3.16}$$

where H is the height of the rectangular source $\tan^{-1}$ is the inverse tangent in degree mode.

If the distance r is large relative to the size of the emitting surface, the configuration factor φ is given approximately by

$$\varphi = A_1/\pi r^2 \tag{3.17}$$

where A_1 is the area of the emitting surface

$$A_1 HW \tag{3.18}$$

Configuration factor defined same manner as in EN 1991-1-2 Annex-G. In EN 1991-1-2 the emissivity of the fire is taken generally as 1.0, but a lower value can be taken because of the "shadow effects" in case fully fire engulfed members. Shadow effects are defined in EN 1993-1-2 as follows; Defined in EN 1993-1-2 as k_{sh} correction factor for the shadow effect. It shall be take in to account in steel temperature development and calculated in code as follows:

For an equivalent uniform temperature distribution in the cross-section, the increase of temperature $\Delta\theta_{a.t}$ in an unprotected steel member during a time interval Δt should be determined from:

$$\Delta\theta_{a.t} = K_{sh}\frac{A_m/V}{c_a\delta_a}h_{\dot{net}}\Delta t \tag{3.19}$$

where k_{sh} is the correction factor for the shadow effect, A_m/V is the section factor for unprotected steel members (1/m), A_m the surface area of the member per unit length (m^2/m), V is the volume of the member per unit length (m^3/m), c_a is the specific heat of steel (J/kgK), $h_{\dot{net}}$ is the design value of the net heat flux per unit area (W/m^2), Δt is the time interval (seconds), δ_a is the unit mass of steel (kg/m^3).

For I-sections under nominal fire actions, the correction factor for the shadow effect can be calculated from:

where k_{sh} is the 0.9 [Am/V]b/[Am/V], $[Am/V]b$ is the box value of the section factor.

The value of k_{sh} should be taken as in other cases: where k_{sh} is the [Am/V]b/[Am/V].

For closed sections such as rectangular or circular hollow sections fully engulfed in fire, shadow effect is not being effected, so k_{sh} shall be taken as 1.0. (EN 1993-1-2).

For open sections, shadow effects shall be taken in to account as per codes, because flanges reduce the fire radiative heat transfer effect to inner enclosure surfaces. Radiative heat flux in fire become dominant compared with convective heat transfer. In this study, I sections are not exposed 3-4 sided exposure conditions, sections are exposed fire one-sided heating from bottom flange. Even if sections are not fully engulfed in fire, the radiative heat transfer between exposed flange and web, exposed flange and top flange become predominant and should be taken in to account.

3.6. View Factor Calculation

Selamet, (2017) defined the thermal field in the steel I-section as following steps:

$$-\left(\frac{\partial q_x}{\partial x}+\frac{\partial q_y}{\partial y}\right)=\rho c\frac{\partial T}{\partial t} \tag{3.20}$$

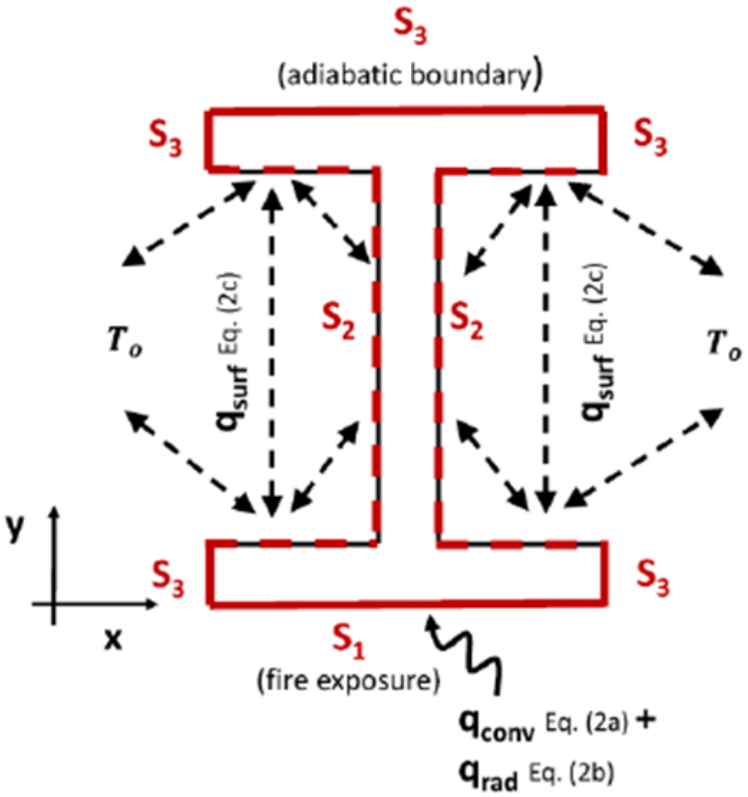

Figure 3.12. I-H section General View (Selamet, 2017).

Above figure exemplifies the three surface conditions S1, S2 and S3 on the I-section. Equation 3.20 and Equation 3.21 determine the convective and radiative heat flux on the fire exposed boundary (Surface S1), respectively. Equation 3.22 determines the radiation surface heat exchange by radiation in the section (Surface S2). (Selamet, 2017).

$$\mathrm{q_{conv}} = \mathrm{h}\,(\mathrm{T_s} - \mathrm{T_{fire}}) \tag{3.21}$$

$$q_{rad} = \sigma \varepsilon_r \left(T_s^4 - T_{fire}^4\right) \tag{3.22}$$

$$q_{surf} = \sigma \varepsilon_{surf} F_{ij} \left(T_i^4 - T_j^4\right) \tag{3.23}$$

The equation $q_{conv} = h\,(T_s - T_{fire})$ governs the heat flux because of convection on the fire exposed boundary.

The equation $q_{rad} = \sigma\varepsilon_r \left(T_s^4 - T_{fire}^4\right)$ governs the heat flux because of the radiation.

The equation $q_{surf} = \sigma\varepsilon_{surf}\varphi_{ij} \left(T_i^4 - T_j^4\right)$ governs the heat exchange by surface radiation.

T_i&T_j the element facet average temperatures in the enclosure.

ε_{surf} is usually taken 1 like as 'black body'. It is assumed that reflection is not considered between the surfaces.

φ_{ij} the view factor coefficient calculated as follows in three-dimensional space.

$$\varphi_{ij} = \frac{1}{A_i} \iint \frac{\cos\theta_i \cos\theta_j}{\pi S^2}\, dA_j dA_i \tag{3.24}$$

For a two-dimensional (2D) heat transfer analysis, the finite surfaces become finite strips (lines) with infinitely long width and new equations to be calculated as follows:

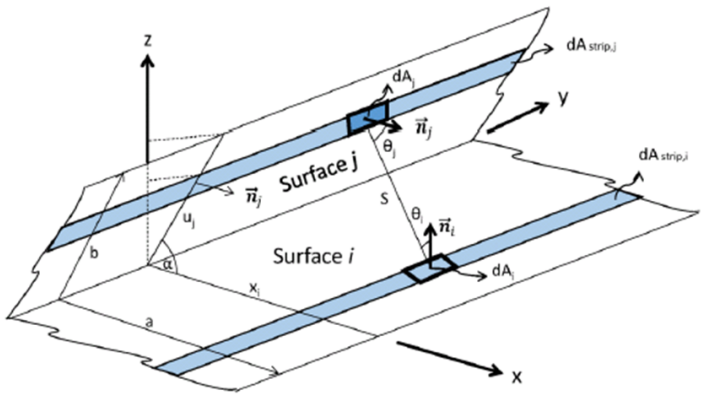

The calculation of the view factor coefficient between finite surfaces in 3D space at arbitrarily angle α with infinite dimension in y-axis.

Figure 3.13. View of Radiating Surface (Selamet, 2017).

bove figure shows two finite surfaces with a common edge at randomly angle α.

$$\vec{\mathbf{s}}_{\mathbf{ij}} = -\vec{\mathbf{s}}_{\mathbf{ji}} = (\mathrm{x_j} - \mathrm{x_i})\,\vec{\mathbf{i}} + (\mathrm{y_j} - \mathrm{y_i})\,\vec{\mathbf{j}} + (\mathrm{z_j} - \mathrm{z_i})\,\vec{\mathbf{k}} \tag{3.25}$$

Let $\vec{s}_{ij}$ be the distance vector from the centre point on Surface dA_i to the center point on Surface dA_i:

The local surface normal (unit) vector can be shown as follows for each finite surface area:

$$\vec{n} = \cos\theta_x \vec{i} + \cos\theta_y \vec{j} + \cos\theta_z \vec{k} \tag{3.26}$$

$\cos\theta_x$, $\cos\theta_y$, $\cos\theta_z$ are direction cosines for the unit vector $\vec{n}$.

The angles between the surface normal and the distance vector $\vec{s_{ij}}$ are shown in Equation 3.27 and Equation 3.28:

$$\cos\theta_{\mathrm{i}} = \frac{\vec{\mathbf{n}}_{\mathbf{i}}.\vec{\mathbf{s}}_{\mathbf{ij}}}{\mathrm{S}} = \frac{1}{\mathrm{S}}\left[(\mathrm{x_j} - \mathrm{x_i})\cos\theta_{\mathrm{x,i}} + (\mathrm{y_j} - \mathrm{y_i})\cos\theta_{\mathrm{y,i}} + (\mathrm{z_j} - \mathrm{z_i})\cos\theta_{\mathrm{z,i}}\right] \tag{3.27}$$

$$\cos\theta_{\mathrm{j}} = \frac{\vec{\mathbf{n}}_{\mathbf{j}}.\vec{\mathbf{s}}_{\mathbf{ji}}}{\mathrm{S}} = \frac{1}{\mathrm{S}}\left[(\mathrm{x_i} - \mathrm{x_j})\cos\theta_{\mathrm{x,j}} + (\mathrm{y_i} - \mathrm{y_j})\cos\theta_{\mathrm{y,j}} + (\mathrm{z_i} - \mathrm{z_j})\cos\theta_{\mathrm{z,j}}\right] \tag{3.28}$$

$S = \sqrt{|\vec{s}_{ji}|^2}$ is the distance length from the center of surface i to the center of surface j.

As seen in Figure 3.13, $z_i = 0; x_j = u_j\ cos(\alpha)$ and $z_j = u_j\ sin\ (\alpha)$ leads to:

$$S^2 = {S_o}^2 + (y_i - y_j)^2 \tag{3.29}$$

where S_o is the projection of S in the x-z plane.

The surface normal $\vec{n_1}$ and $\vec{n_j}$ are shown as shown in Equation 3.30 and Equation 3.31:

$$\vec{n_i} = \vec{k} \tag{3.30}$$

$$\vec{n_j} = \vec{i}\ sin\ \alpha - \vec{k}\ cos\ \alpha \tag{3.31}$$

With the reduction to two dimensional (2D) space, Equation 3.27 and Equation 3.28 change to Equation 3.32 and Equation 3.33:

$$\cos\theta_i = u_j \sin\alpha / S \tag{3.32}$$

$$\cos\theta_j = x_i \sin\alpha / S \tag{3.33}$$

The view factor coefficient from one point m on a differential strip $dF_{m,i}$ to a finite strip $(strip_{,j})$ is therefore:

$$\mathrm{dF_{m,i-strip,j}} = \int \frac{\cos\theta_\mathrm{i}\cos\theta_\mathrm{j}}{\pi \mathrm{S}^2}\mathrm{dA_j} = \frac{\mathrm{du_j}}{\pi}\int_{-\infty}^{\infty}\frac{\mathrm{x_i u_j sin^2}\,(\alpha)}{\left[\mathrm{S_o^2} + (\mathrm{y_i} - \mathrm{y_j})^2\right]^2}\mathrm{dy_j} \tag{3.34}$$

Once θ_{10} and θ_{20} are defined as the projections of θ_i and θ_j, Equation 3.35 is found, which decreases Equation 3.34 to 2D space. As below figure for 2D illustrates, Equation 3.35 shows the view factor coefficient of one point m in finite strip i to a finite strip du_j.

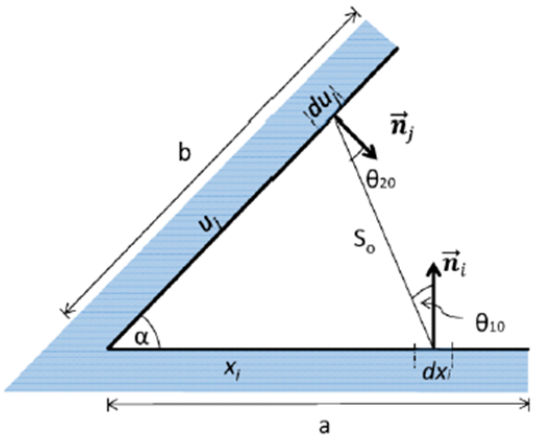

Figure 3.14. 3D View of Radiating Surface (Selamet, 2017).

$$dF_{m,i-strip,j} = \frac{1}{2}\cos\theta_{i0}\cos\theta_{j0}\frac{du_j}{S_o} \tag{3.35}$$

After implementation of FE analysis to I sections and after the parametric study depth of section (d) and width of section (b_f) are crucial that they have significant effects on enclosure heat exchange, thereby effects on thermal gradient. (Selamet, 2017).

4. FIRE TEST SET-UP

4.1. I Sections

INP 400, HEB 300 and HEB 400 steel sections were used in this study. Because the depth of INP 400 and HEB 400 are same, thus the effects of width of section can be evaluate easily. In addition the width of HEB 400 and HEB 300 are same in order to evaluate the effects of depth on thermal gradient. In fire exposure conditions, section factor of specimen is crucial, because the amount and rate of heat input are proportionate to fire exposed area and the volume of steel section. Section factor of steel specimens can be determined by the ratio of heated perimeter to cross section area. Dimensions for these sections are shown below:

Table 4.1. Section dimensions.

SECTIONS TO BE USED IN THE TEST						
No	SECTION	h (mm)	bf (mm)	tf (mm)	tw (mm)	Section factor (1/m)
Test 1	INP 400	400	155	21.6	14.4	13.14
Test 2	HEB 400	400	300	24	14	20.12
Test 3	HEB 300	300	300	19	11	15.17

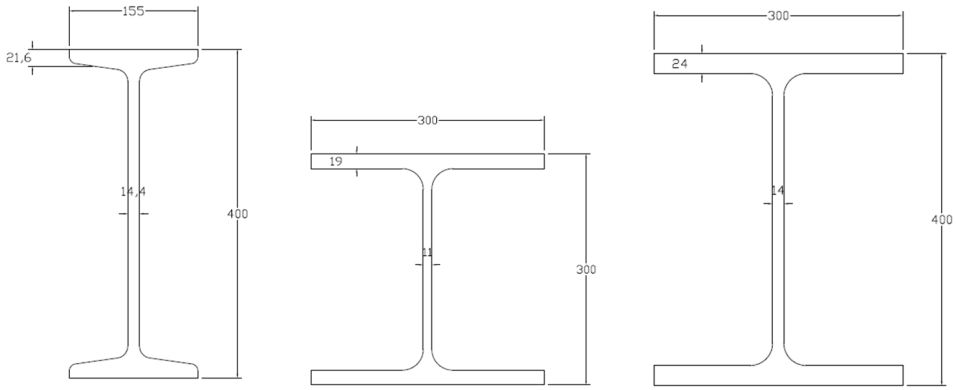

Figure 4.1. Cross sections of INP 400, HEB 300 and HEB 400.

4.2. Insulation Materials

Sections of INP 400 web and flange next to web were insulated with 5 cm ceramic wool. The remaining openings was closed with reinforced autoclaved concrete blocks. After the completion of placement, Gypsum boards were placed to top and bottom flange of the section. Gypsum boards were fixed by self-tapping screws to aerated concrete blocks. Gypsum boards and ceramic wool properties as follows:

Table 4.2. Insulation Material Properties.

Insulation material properties	**Gypsum board**	**Ceramic wool**
Thickness	6.5 mm	50 mm
Reaction to fire class	A2	A1
Thermal conductivity	0.22 W/m.K	0.11 W/m.K
Specific heat (cp)	0.26 cal/gram^{o}C	0.27 cal/gram^{o}C
Density	600 kg/m^3	128 kg/m^3

4.3. Testing Procedure

4.3.1. Test 1: INP 400

16 wire thermocouples were fixed to each specimen. Section exposed fire from bottom flange only. 1st test includes 2 specimen INP 400 steel sections. 16 points at the middle of the specimen was drilled with 2 mm drilling bit. They were fixed to steel section by hammer. Both sections are St 37 structural steel and were cut from same bar. One of the sections of INP 400 web and flange next to web were insulated with 5 cm ceramic wool. Fire retardant stick were used in order to keep in place the insulation material during the test. Both sections placed to indicative furnace horizontally with free end. The remaining openings was closed with reinforced autoclaved concrete blocks. After the completion of placement, Gypsum boards were placed to top and bottom flange of the section. Gypsum boards were fixed by self-tapping screws to aerated concrete blocks. Most of the time in fire tests main problem is the thermocouple falling away during the test. In order to get precise values from each

sections of steel sections, 16 no's thermocouples were fixed symmetrically on sections. In addition, even if in the standards minimum 0,5 mm wire is usually being used in fire tests, in this study 0,8 mm Type K wire was used. Test sections detail as follows for 1^{st} test;

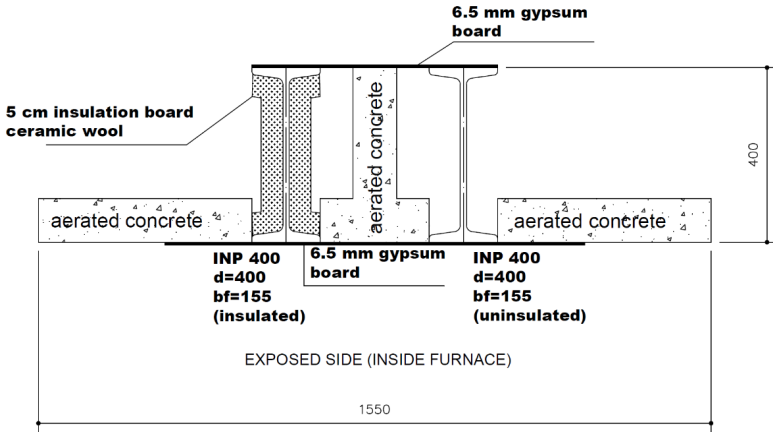

Figure 4.2. Test 1 Section Detail.

The plan view detail as follows for 1^{st} test;

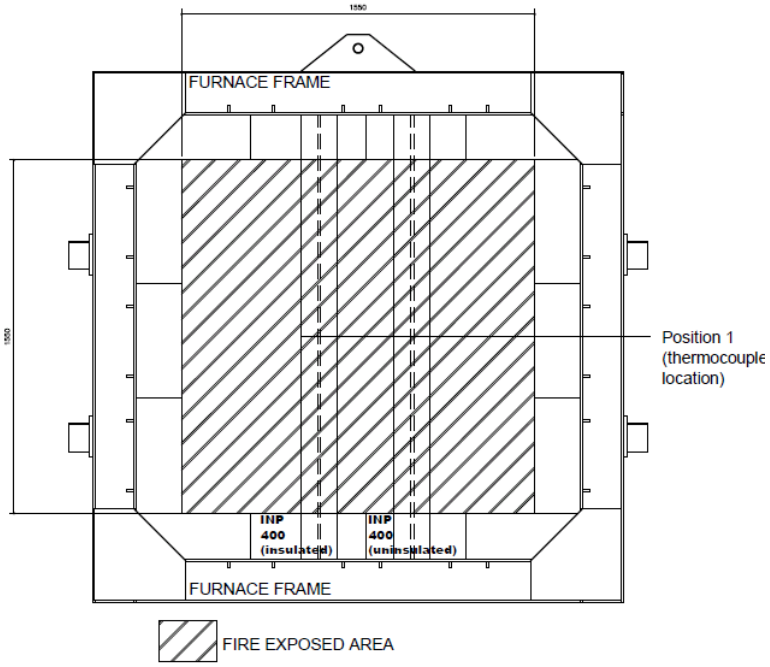

Figure 4.3. Test 1 Plan View.

Thermocouple location detail as follows for 1^{st} test;

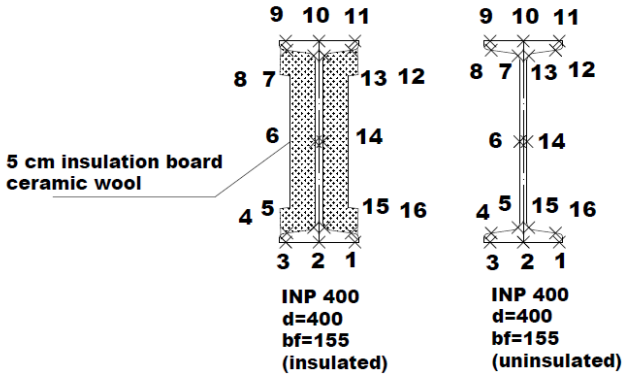

Figure 4.4. Test 1 Thermocouple Detail.

Figure 4.5. Test 1 Thermocouple Detail.

4.3.2. Test 2: HEB 400

16 wire thermocouples were fixed to each specimen. Section exposed fire from bottom flange only. 1st test includes 2 specimen HEB 300 steel sections. 16 points at the middle of the specimen was drilled with 2 mm drilling bit. They were fixed to steel section by hammer. Both sections are St 37 structural steel and were cut from same bar. One of the sections of INP 400 web and flange next to web were insulated with 5 cm ceramic wool. Fire retardant stick were used in order to keep in place the insulation material during the test. Both sections placed to indicative furnace horizontally with free end. The remaining openings was closed with reinforced

autoclaved concrete blocks. After the completion of placement, Gypsum boards were placed to top and bottom flange of the section. Gypsum boards were fixed by self-tapping screws to aerated concrete blocks. Most of the time in fire tests main problem is the thermocouple falling away during the test. In order to get precise values from each sections of steel sections, 16 no's thermocouples were fixed symmetrically on sections. In addition, even if in the standards minimum 0,5 mm wire is usually being used in fire tests, in this study 0,8 mm Type K wire was used. Test sections detail as follows for 2^{nd} test;

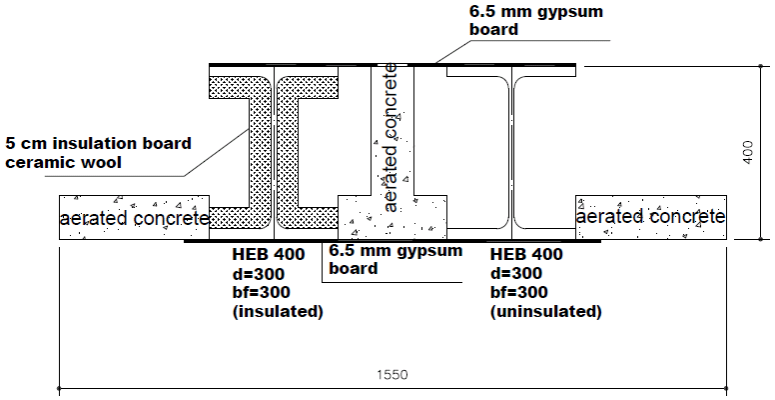

Figure 4.6. Test 2 Section Detail.

The plan view detail as follows for 2^{nd} test;

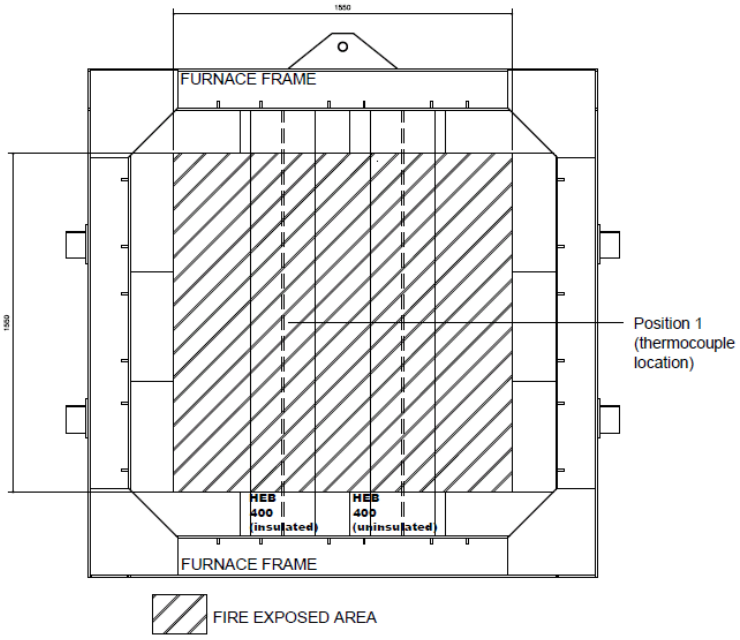

Figure 4.7. Test 2 Plan View.

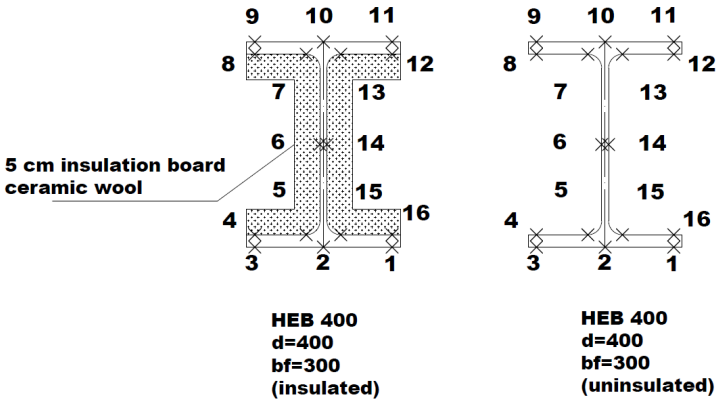

Figure 4.8. Test 2 Thermocouple Detail.

Figure 4.9. Test 2 Assembly.

4.3.3. Test 3 HEB 300

16 wire thermocouples were fixed to each specimen. Section exposed fire from bottom flange only. 1st test includes 2 specimen HEB 300 steel sections. 16 points at the middle of the specimen was drilled with 2 mm drilling bit. They were fixed to steel section by hammer. Both sections are St 37 structural steel and were cut from same bar. One of the sections of INP 400 web and flange next to web were insulated with 5 cm ceramic wool. Fire retardant stick were used in order to keep in place the insulation material during the test. Both sections placed to indicative

furnace horizontally with free end. The remaining openings was closed with reinforced autoclaved concrete blocks. After the completion of placement, Gypsum boards were placed to top and bottom flange of the section. Gypsum boards were fixed by self-tapping screws to aerated concrete blocks. Most of the time in fire tests main problem is the thermocouple falling away during the test. In order to get precise values from each sections of steel sections, 16 no's thermocouples were fixed symmetrically on sections. In addition, even if in the standards minimum 0,5 mm wire is usually being used in fire tests, in this study 0,8 mm Type K wire was used. Test sections detail as follows for 3^{rd} test;

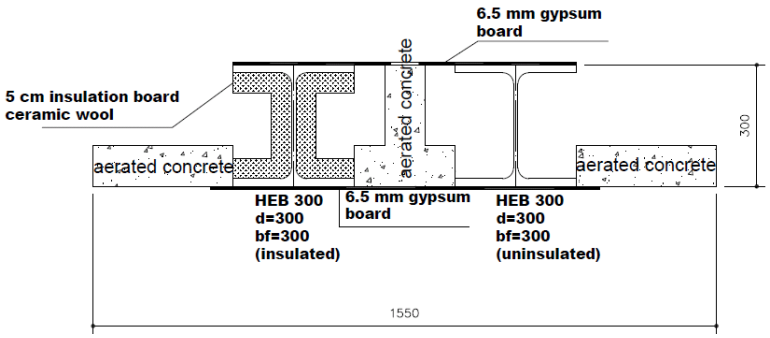

Figure 4.10. Test 2 Assembly.

The plan view detail as follows for 3^{rd} test;

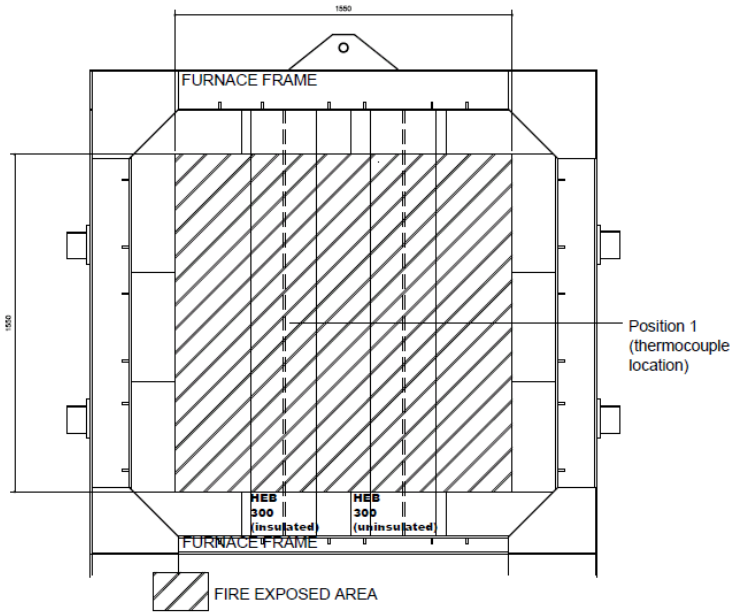

Figure 4.11. Test 3 Plan View.

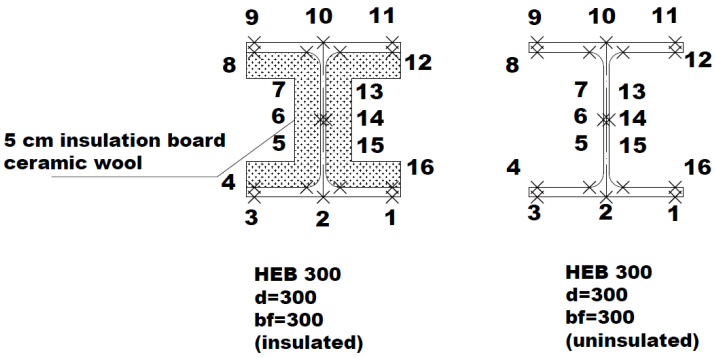

Figure 4.12. Test 3 Thermocouple Detail.

Figure 4.13. Test 3 Assembly.

4.4. Furnace

1.55mx1.55m indicative furnace was used for the test. All test equipment is as specified in EN 1363-1 Fire resistance tests- Part 1- General requirements. Furnace conditions were controlled by furnace plate thermocouples as described in EN 1363-1 and controlled by means of calculating mean temperature of the plate thermocouples. Two natural gas burners were ignited in order to catch ISO-834 temperature-time

curve. Temperature results are to be showed in the following parts for each test.

4.5. Instrumentation

The specimen temperature measurement thermocouple wires are 0.8 mm, Type K, ceramic coated, 1200 ^{o}C fire retardant. The furnace pressure control is performed with "T" sensor as described in EN 1363-1 Fire resistance tests- Part 1- General requirements. Data is transmitted to the furnace software with digital pressure transducers. In order to simulate actual room fire the nominal pressure on the underside of the specimens shall not exceed 20 Pa during the test as per EN 1363-1 Fire Resistance-Tests -Part 1 : General Requirements. So pressure sensor located in the furnace was set up in the software not to exceed 20 Pa by calculating every 1m approximately 8.5 Pa in the furnace. Pressure results are to be shown in the following parts.

5. FIRE TEST RESULTS

5.1. Furnace Readings for 3 Tests

Furnace readings for 3-test packages are shown in Figure 5.1.

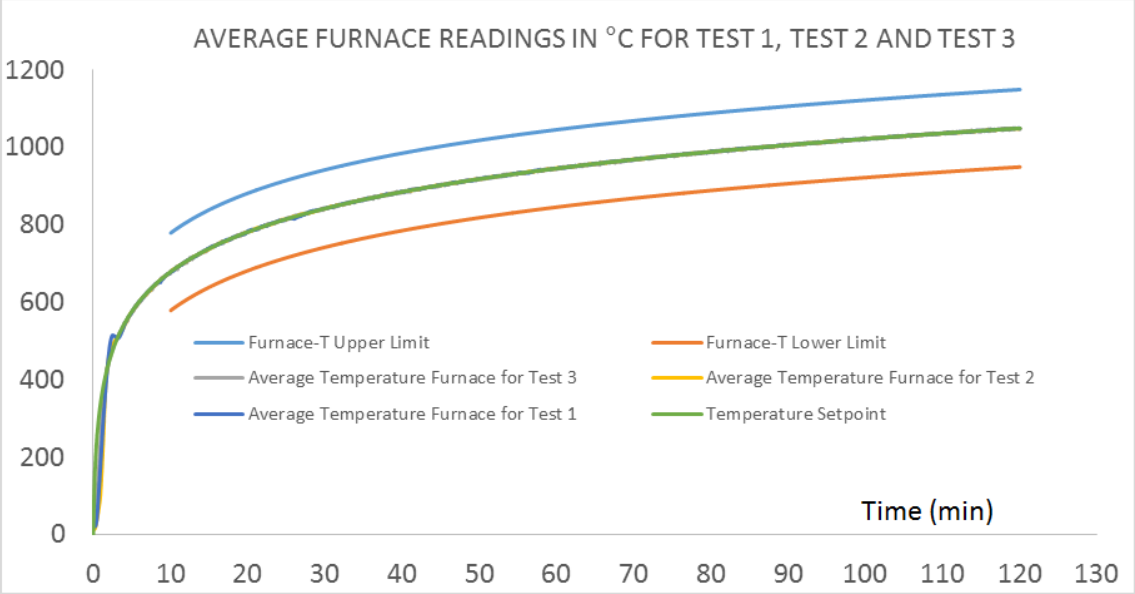

Figure 5.1. Furnace Readings of 3-Test.

Temperature set point defines in the above graph ISO 834 standard temperature-time curve. Average temperature results for Test-1, Test-2 and Test-3 are also shown in graph. As understood from the graph, set point for ISO 834 standard time temperature curve values and Test-1, Test-2 and Test-3 values are so close to each other. It can easily evaluated that the furnace readings at different time for different tests follow ISO 834 standard temperature-time curve precisely. In addition, after the first 10 minutes of the test, the temperature recorded by plate thermocouples did not differ more than 100K at any time from the corresponding temperature of ISO 834 standard temperature-time curve as per EN 1363-1. It means that all values are in limit for 3-test.

5.2. Test 1: INP 400

Thermocouple temperature values for insulated INP 400 is shown in Figure 5.2.

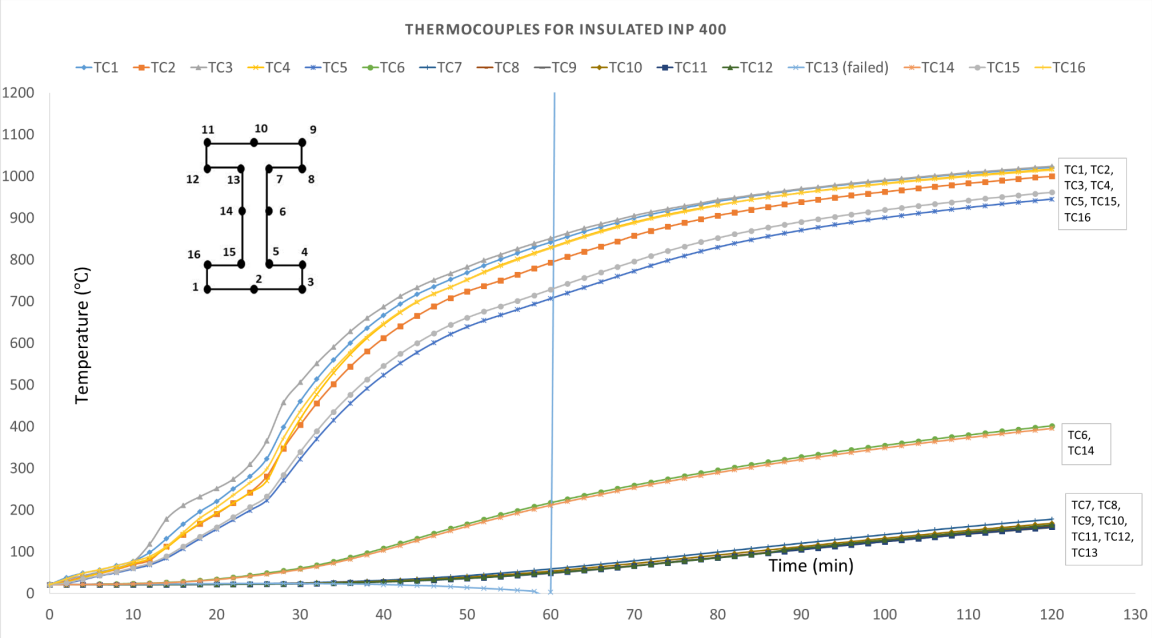

Figure 5.2. Thermocouples for Insulated INP 400 (Test 1).

TC1 to TC16 thermocouples were fixed to the insulated INP 400 sections as defined and illustrated in Figure 4.4. In this figure TC1 to TC3 thermocouples illustrate exposed side of the bottom flange. TC9 to TC11 thermocouples illustrate top side of the top flange. The remaining TC4 to TC8 and TC12 to TC16 illustrate enclosure of I section. TC6 and TC14 are in the middle of the web. All thermocouples were worked properly during the test except TC13. It can be understand from the graph temperature values go down during the test and after 60 minutes TC13 temperature values go to peak and it means that TC13 fell away from the surface. TC1 to TC3 temperature values during the test are very close to each other because of the symmetry of the section and symmetry of the location of the thermocouples. In addition, we can say the same situation for the remaining symmetric thermocouples. It can be easily evaluated form the graph that exposed side temperature values and closer locations are higher than the web and top flange temperature values and top flange less than web temperature values as expected.

Thermocouple temperature values graphic for uninsulated INP 400 is shown in Figure 5.3.

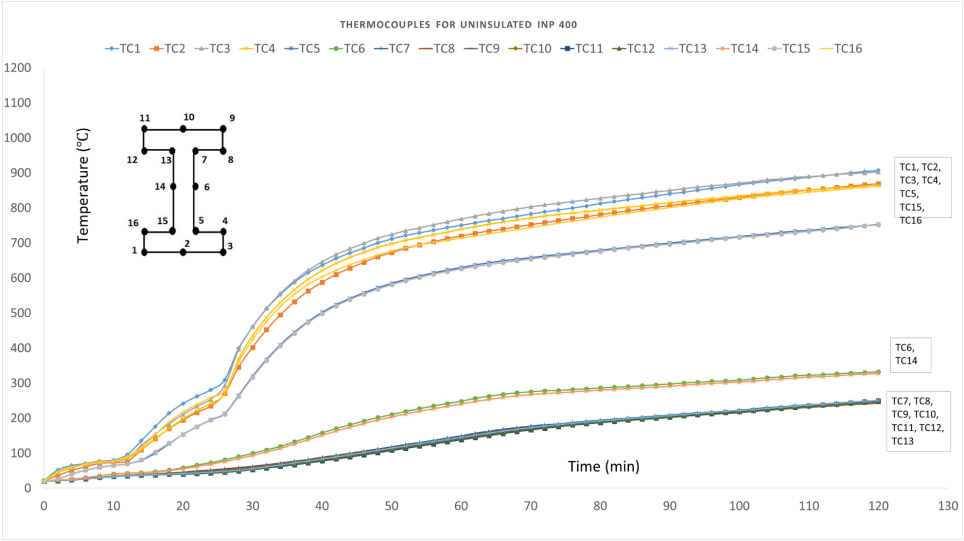

Figure 5.3. Thermocouples for Uninsulated INP 400 (Test 1).

TC31 to TC46 thermocouples were fixed to the insulated INP 400 sections as defined and illustrated in Figure 4.4. In this figure TC1 to TC3 thermocouples illustrate exposed side of the bottom flange. TC9 to TC11 thermocouples illustrate top side of the top flange. The remaining TC4 to TC8 and TC12 to TC16 illustrate enclosure of I section. TC6 and TC14 are in the middle of the web. All thermocouples were worked properly during the test. TC1 to TC3 temperature values during the test are very close to each other because of the symmetry of the section and symmetry of the location of the thermocouples. In addition, we can say the same situation for the remaining symmetric thermocouples. It can be easily evaluated form the graph that exposed side temperature values and closer locations are higher than the web and top flange temperature values and top flange less than web temperature values as expected.

Furnace plate thermocouples temperature values graphic is shown in Figure 5.4.

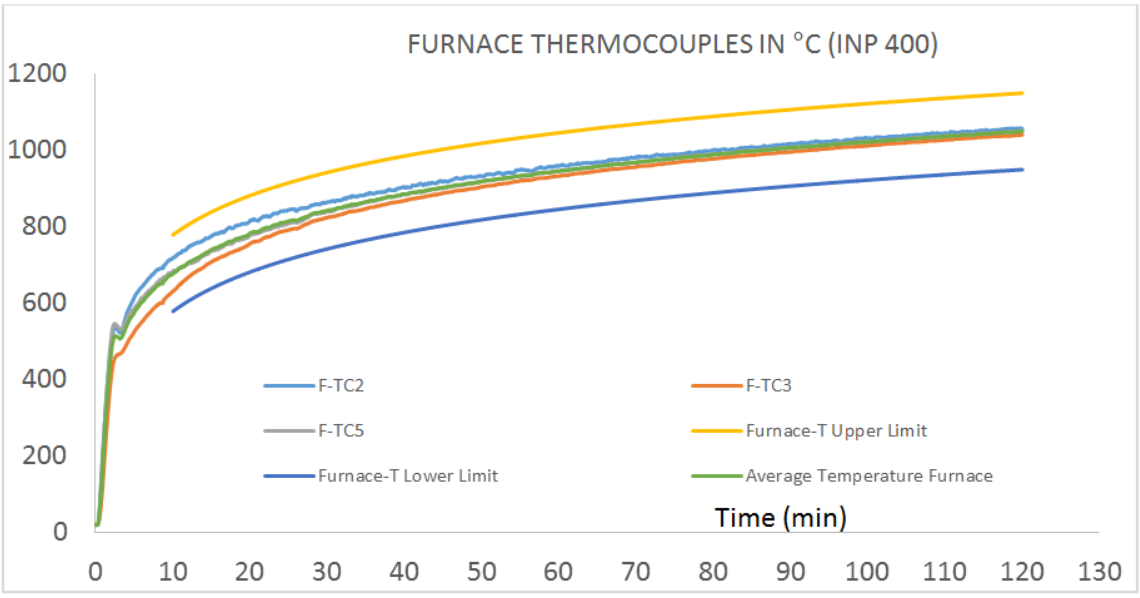

Figure 5.4. Furnace Thermocouples for Test 1.

After the first 10 minutes of the test, the temperature recorded by plate thermocouples did not differ more than 100K at any time from the corresponding temperature of the standard temperature/time curve as per EN 1363-1.

Furnace pressure values graphic is shown in Figure 5.5.

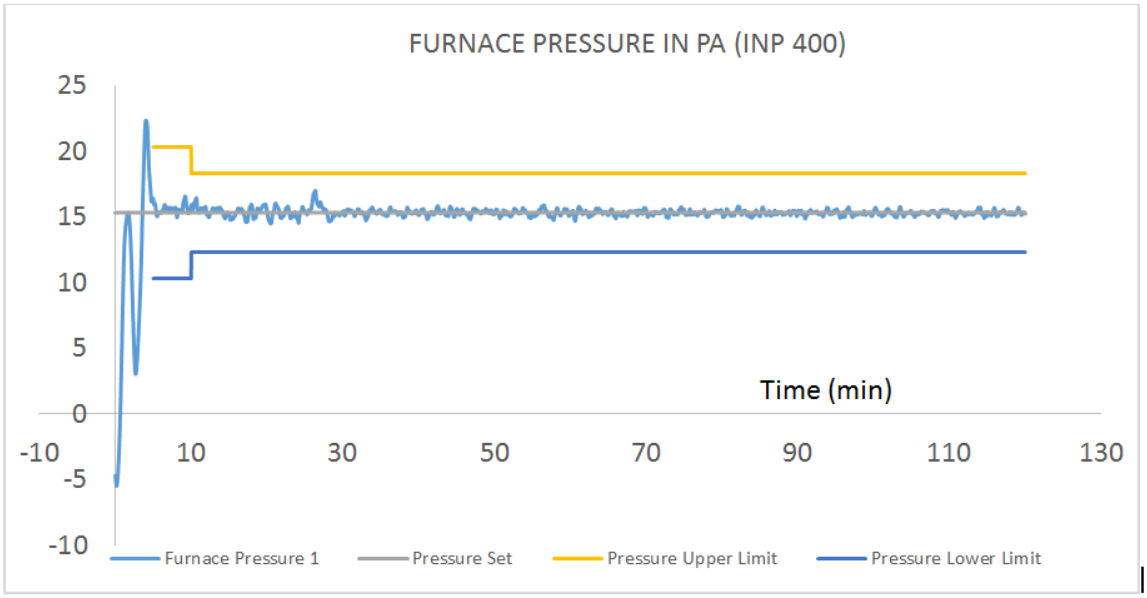

Figure 5.5. Furnace Pressure Test 1.

The furnace pressure recorded so that by 5 minutes from start of the test pressure shall be ±5 Pa of the nominal pressure and pressure shall be ±3 Pa of the nominal pressure from 10 minutes onwards it. All values are in limit at any time.

Furnace deviation graphic is shown in Figure 5.6.

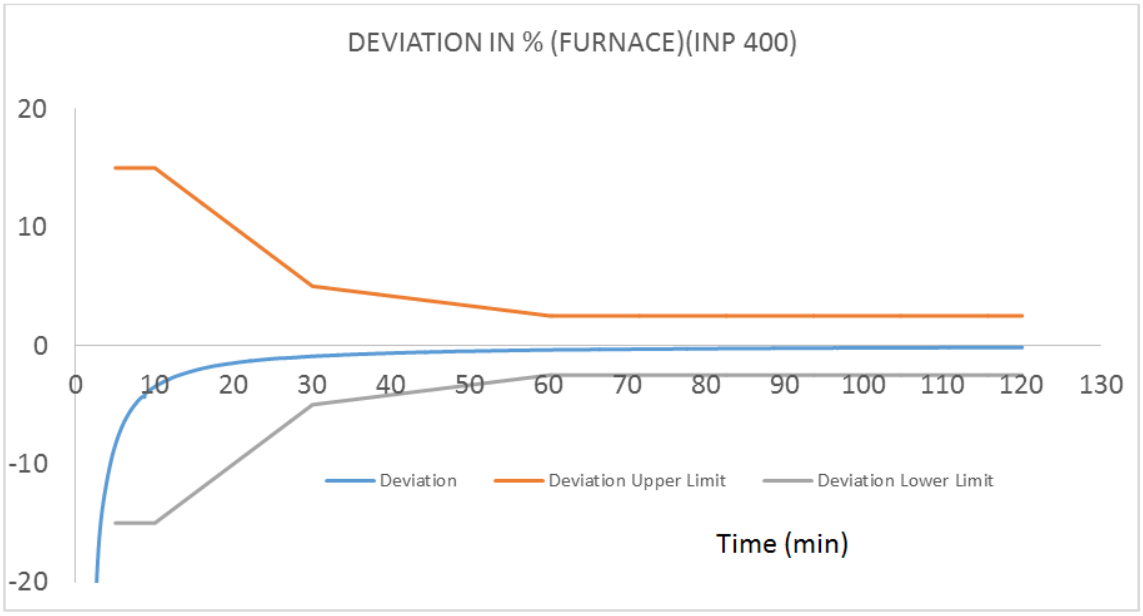

Figure 5.6. Furnace Deviation Test 1.

The deviation percentage in the area of the curve of the average temperature recorded by the plate thermocouples specified in EN 1363-1 against time the standard temperature/time curve area shall be within the below limits: The percentage deviation (de) in the area of the curve of the average temperature recorded by the specified furnace thermocouples versus time from the area of the standard temperature/time curve shall be within:

(i) 15% for $5 < t \leq 10$

(ii) (15 - 0,5 (t-10))% for $10 < t \leq 30$

(iii) (5 - 0,083 (t-30))% for $30 < t \leq 60$

(iv) 2,5% for $t > 60$

$$de = \frac{AA_s}{A_s} x100 \tag{5.1}$$

where de is the percentage deviation, A is the area under the actual furnace temperature/time curve.

All values in this test are in limit as per above. Ambient temperature graphic during the test is shown in Figure 5.7.

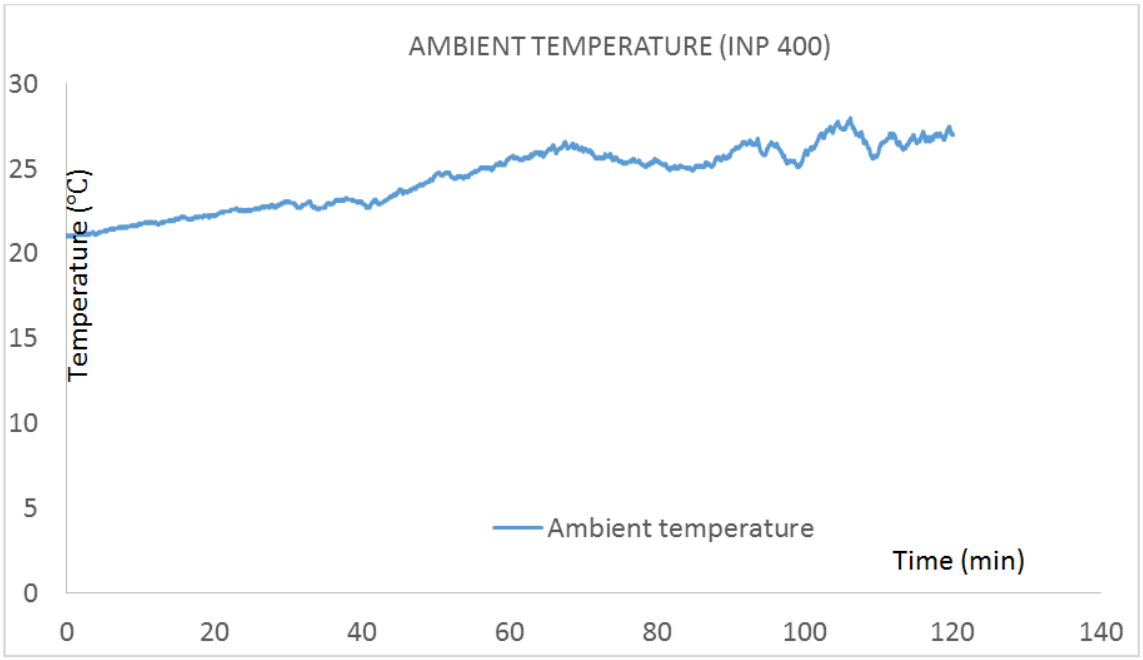

Figure 5.7. Ambient Temperature during the Test 1.

The ambient temperature shall be within the limit 10°C - 40 °C from the beginning of the test. It shall be recorded at a distance of between 1m and 3m horizontally away from outside of the furnace. Under that conditions the sensor shall not be affected by thermal radiation from the test specimen or furnace. The temperature in the test area shall not decline by more than 10 K or shall not raise by more than 20 K during the test. During the test all values are in the limit.

INP 400 test pictures before and during the test are shown in Figure 5.8 to Figure 5.13.

Figure 5.8. Fixed Thermocouples for INP 400.

Figure 5.9. General View before the Test for INP 400.

Figure 5.10. During the Test for INP 400 (1^{st} Minute).

Figure 5.11. During the Test for INP 400 (30^{th} Minute).

Figure 5.12. During the Test for INP 400 (90^{th} Minute).

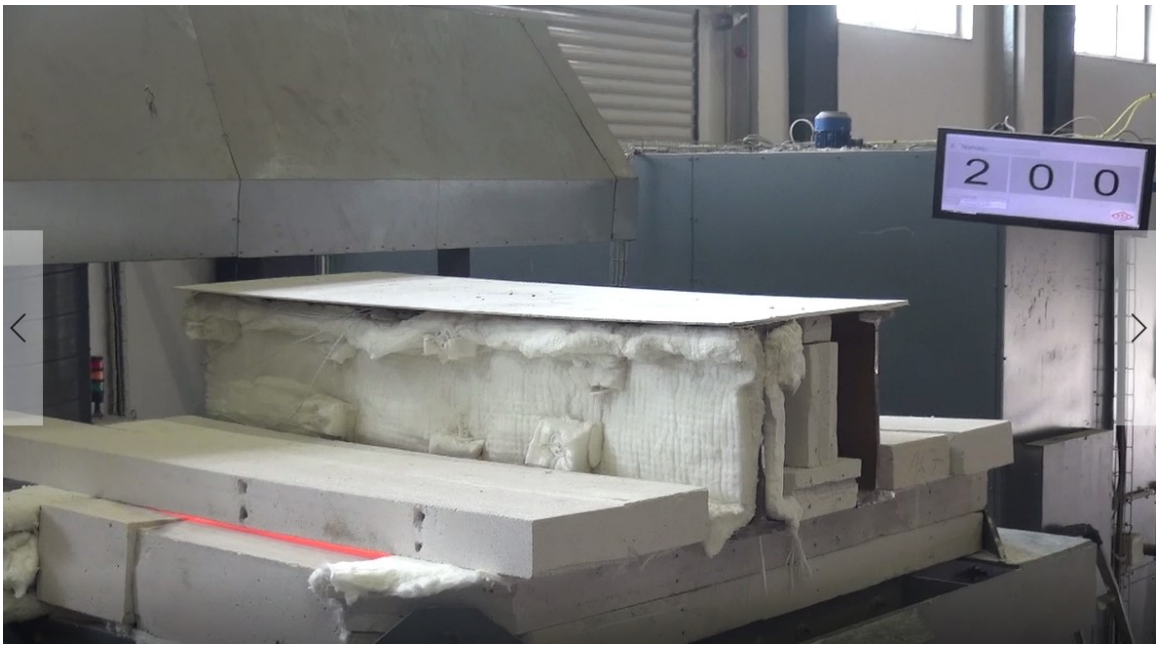

Figure 5.13. During the Test for INP 400 (120^{th} Minute).

5.3. Test 3: HEB 400

Thermocouple temperature values graphic for insulated HEB 400 is shown in Figure 5.14.

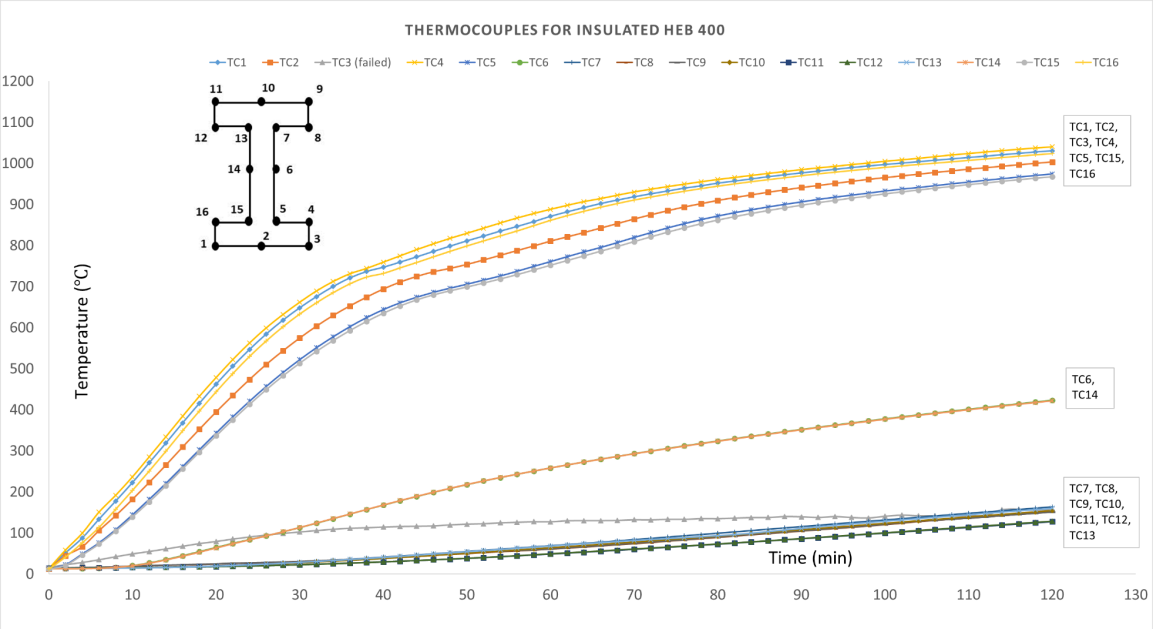

Figure 5.14. Thermocouples for Insulated HEB 400 (Test 2).

TC41 to TC56 thermocouples were fixed to the insulated HEB 400 section as defined and illustrated in Figure 4.8. In this figure TC1 to TC3 thermocouples illustrate exposed side of the bottom flange. TC9 to TC11 thermocouples illustrate top side of the top flange. The remaining TC4 to TC8 and TC12 to TC16 illustrate enclosure of I section. TC6 and TC14 are in the middle of the web. All thermocouples were worked properly during the test except TC3. It can be understand from the graph temperature values go down during the test and it means that TC3 has hot junction outside the furnace. So TC3 temperature values should be ignored. TC1 to TC2 temperature values during the test are very close to each other because of the symmetry of the section and symmetry of the location of the thermocouples. In addition, we can say the same situation for the remaining symmetric thermocouples. It can be easily evaluated form the graph that exposed side temperature values and closer locations are higher than the web and top flange temperature values and top flange less than web temperature values as expected.

Thermocouple temperature values graphic for uninsulated HEB 400 is shown in Figure 5.15.

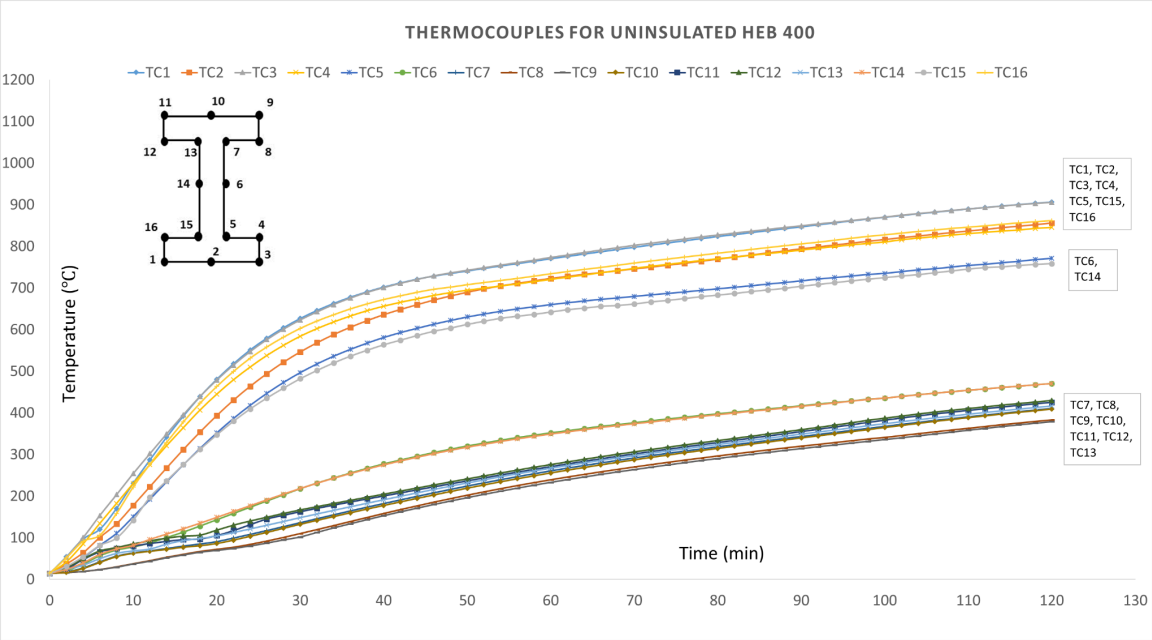

Figure 5.15. Thermocouples for Uninsulated HEB 400 (Test 2).

TC1 to TC16 thermocouples were fixed to the insulated HEB 400 section as defined and illustrated in Figure 4.8. In this figure TC1 to TC3 thermocouples illustrate exposed side of the bottom flange. TC9 to TC11 thermocouples illustrate top side of the top flange. The remaining TC4 to TC8 and TC12 to TC16 illustrate enclosure of I section. TC6 and TC14 are in the middle of the web. All thermocouples were worked properly during the test. TC1 to TC3 temperature values during the test are very close to each other because of the symmetry of the section and symmetry of the location of the thermocouples. In addition, we can say the same situation for the remaining symmetric thermocouples. It can be easily evaluated form the graph that exposed side temperature values and closer locations are higher than the web and top flange temperature values and top flange less than web temperature values as expected.

Furnace plate thermocouples temperature values graphic is shown in Figure 5.16.

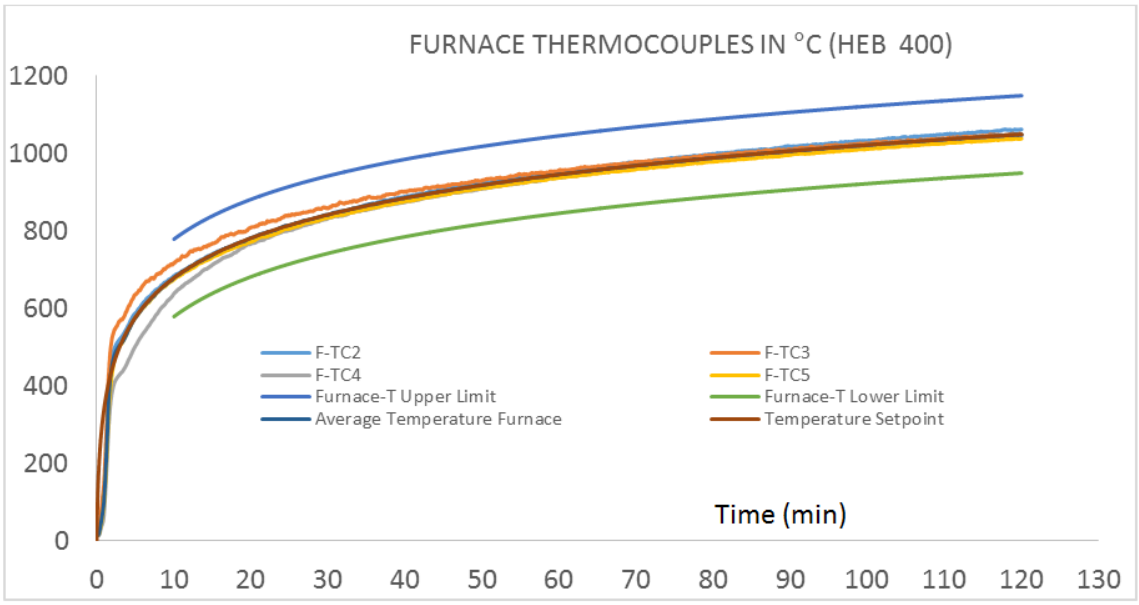

Figure 5.16. Furnace Thermocouples for HEB 400 (Test 2).

After the first 10 minutes of the test, the temperature recorded by plate thermocouples did not differ more than 100K at any time from the corresponding temperature of the standard temperature/time curve as per EN 1363-1. All values are in the limit.

Furnace pressure values graphic is shown in Figure 5.17.

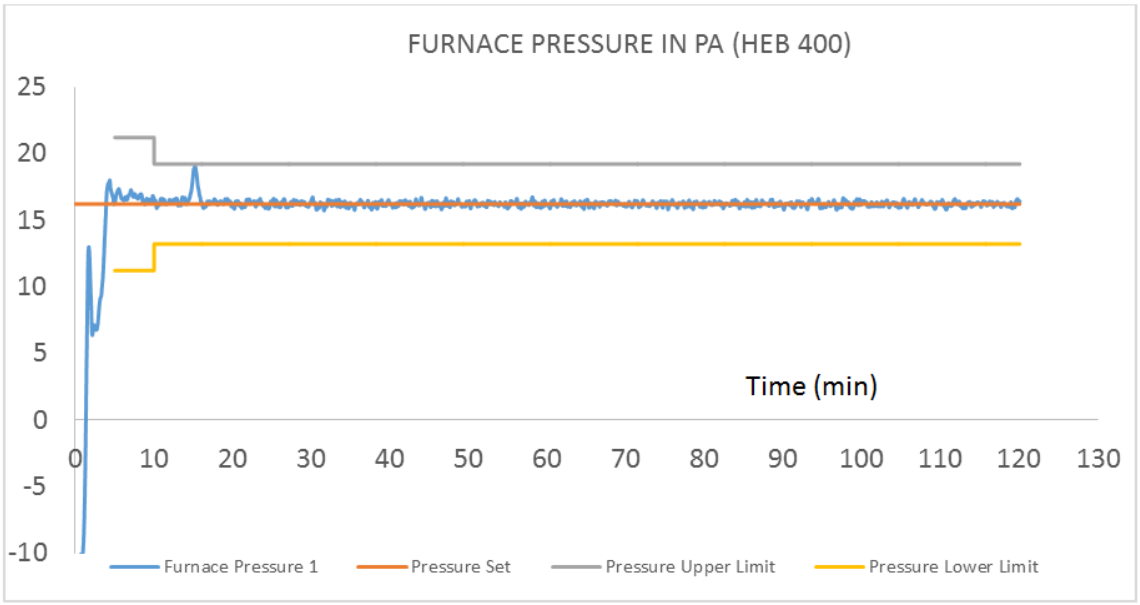

Figure 5.17. Furnace Pressure for HEB 400 (Test 2).

The furnace pressure recorded so that by 5 minutes from start of the test pressure shall be ±5 Pa of the nominal pressure and pressure shall be ±3 Pa of the nominal pressure from 10 minutes onwards it. All values are in limit at any time. Furnace deviation graphic is shown in Figure 5.18.

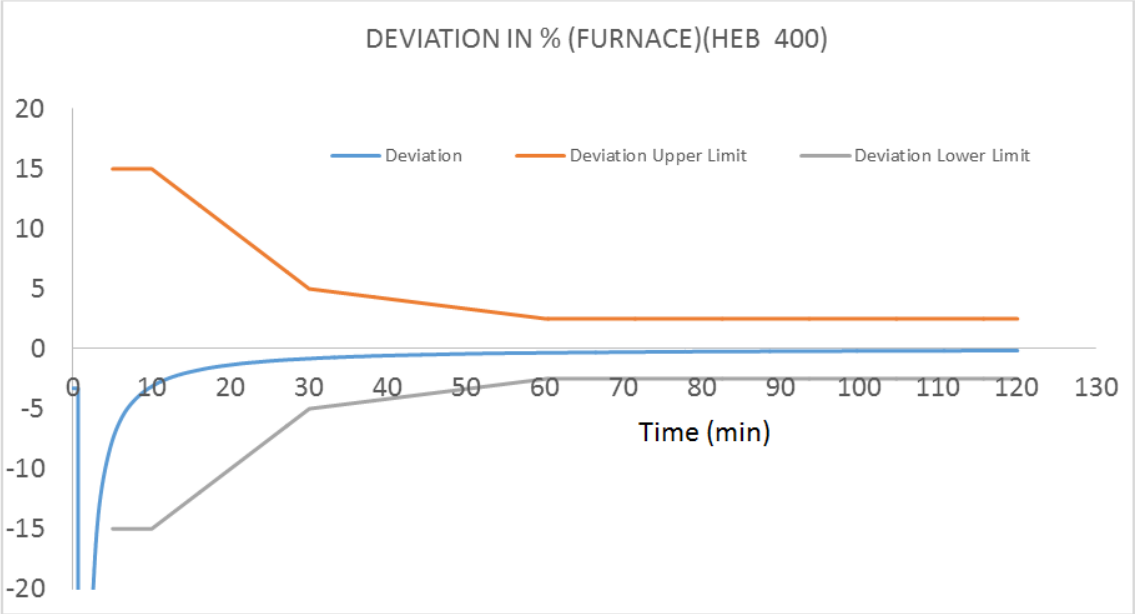

Figure 5.18. Furnace Deviation for HEB 400 (Test 2).

The deviation percentage in the area of the curve of the average temperature recorded by the plate thermocouples specified in EN 1363-1 against time the standard temperature/time curve area shall be within the below limits:

The percentage deviation (de) in the area of the curve of the average temperature recorded by the specified furnace thermocouples versus time from the area of the standard temperature/time curve shall be within:

(i) 15% for $5 < t \leq 10$

(ii) (15 - 0,5 (t-10))% for $10 < t \leq 30$

(iii) (5 - 0,083 (t-30))% for $30 < t \leq 60$

(iv) 2,5% for $t > 60$

$$de = \frac{AA_s}{A_s} x100 \tag{5.2}$$

where de is the percentage deviation, A is the area under the actual furnace temperature/time curve.

All values in this test are in limit as per above. Ambient temperature graphic during the test is shown in Figure 5.19.

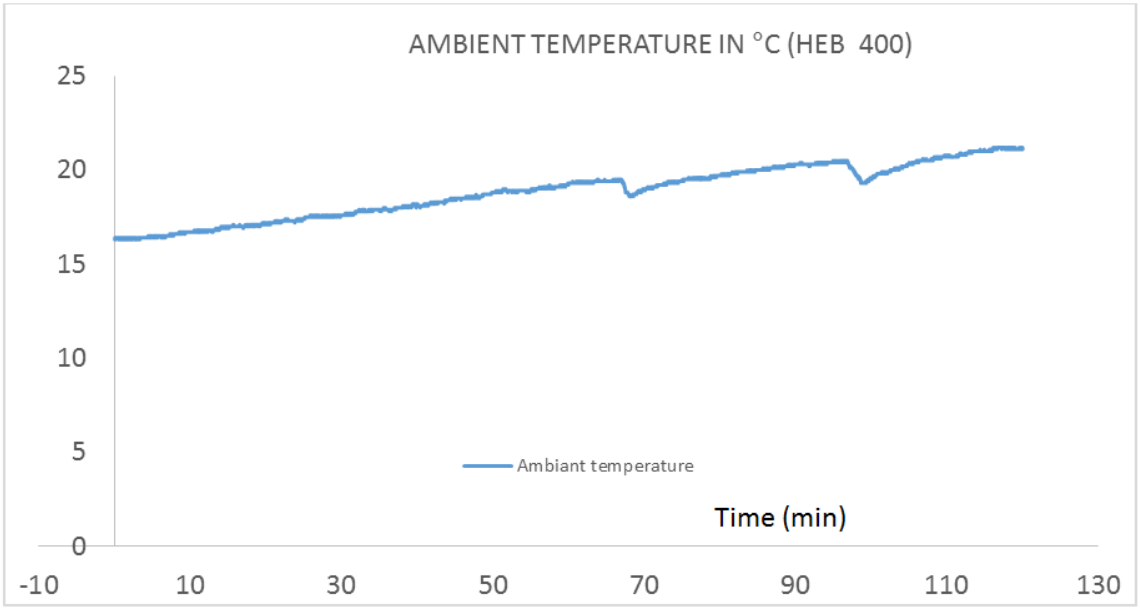

Figure 5.19. Ambient Temperature during the Test for HEB 400 (Test 2).

The ambient temperature shall be within the limit 10^{o}C - 40 ^{o}C from the beginning of the test. It shall be recorded at a distance of between 1m and 3m horizontally away from outside of the furnace. Under that conditions the sensor shall not be affected by thermal radiation from the test specimen or furnace. The temperature in the test area shall not decline by more than 10 K or shall not raise by more than 20 K during the test. During the test all values are in the limit.

HEB 400 test pictures before and during the test are shown in Figure 5.20 to Figure 5.24.

Figure 5.20. General View before the Test for HEB 400.

Figure 5.21. General View during the Test for HEB 400.

Figure 5.22. Section View during the Test for HEB 400 (100^{th} Minute).

Figure 5.23. General View at the End of the Test For HEB 400 (120^{th} Minute).

Figure 5.24. Section View at the End Of The Test For HEB 400 (120^{th} Minute).

5.4. Test 3: HEB 300

Thermocouple temperature values graphic for insulated HEB 300 is shown in Figure 5.25.

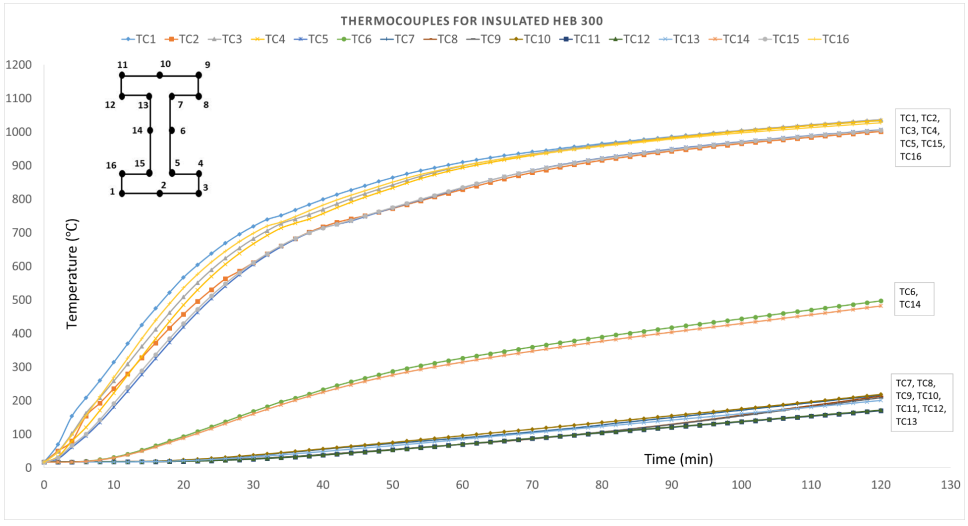

Figure 5.25. Thermocouples for Insulated HEB 300 (Test 3).

TC1 to TC16 thermocouples were fixed to the insulated HEB 300 section as defined and illustrated in Figure 5.12. In this figure TC1 to TC3 thermocouples illustrate exposed side of the bottom flange. TC9 to TC11 thermocouples illustrate top side of the top flange. The remaining TC4 to TC8 and TC12 to TC16 illustrate enclosure of I section. TC6 and TC14 are in the middle of the web. All thermocouples were worked properly during the test. TC1 to TC3 temperature values during the test are very close to each other because of the symmetry of the section and symmetry of the location of the thermocouples. In addition, we can say the same situation for the remaining symmetric thermocouples. It can be easily evaluated form the graph that exposed side temperature values and closer locations are higher than the web and top flange temperature values and top flange less than web temperature values as expected.

Thermocouple temperature values graphic for uninsulated HEB 300 is shown in Figure 5.26.

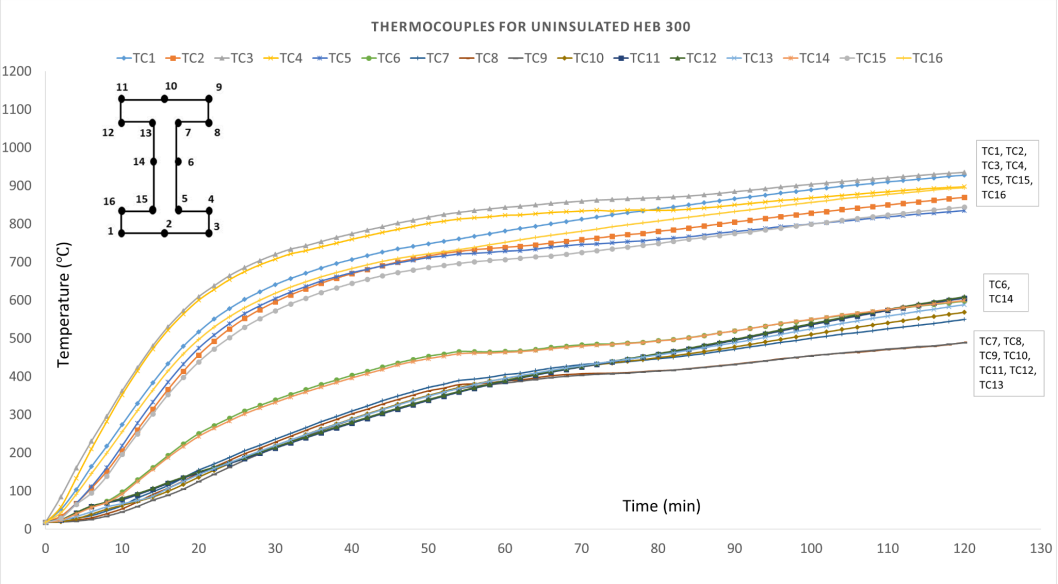

Figure 5.26. Thermocouples for Uninsulated HEB 300 (Test 3).

TC1 to TC16 thermocouples were fixed to the insulated HEB 300 section as defined and illustrated in Figure 4.12. In this figure TC1 to TC3 thermocouples illustrate exposed side of the bottom flange. TC9 to TC11 thermocouples illustrate top side of the top flange. The remaining TC4 to TC8 and TC12 to TC16 illustrate enclosure of I

section. TC6 and TC14 are in the middle of the web. All thermocouples were worked properly during the test. TC1 to TC3 temperature values during the test are very close to each other because of the symmetry of the section and symmetry of the location of the thermocouples. In addition, we can say the same situation for the remaining symmetric thermocouples. It can be easily evaluated form the graph that exposed side temperature values and closer locations are higher than the web and top flange temperature values and top flange less than web temperature values as expected.

Furnace plate thermocouples temperature values graphic is shown in Figure 5.27.

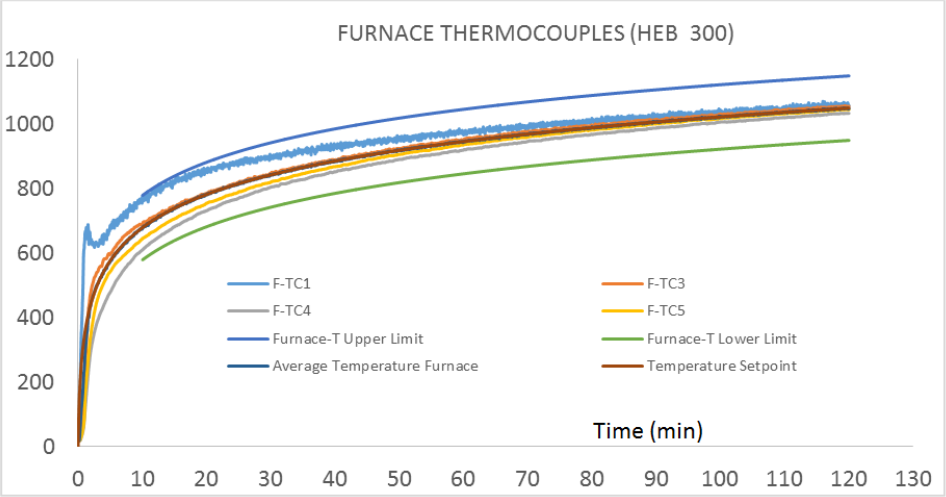

Figure 5.27. Furnace Thermocouples for HEB 300 (Test 3).

After the first 10 minutes of the test, the temperature recorded by plate thermocouples did not differ more than 100K at any time from the corresponding temperature of the standard temperature / time curve as per EN 1363-1. All values are in the limit.

Furnace pressure values graphic is shown in Figure 5.28.

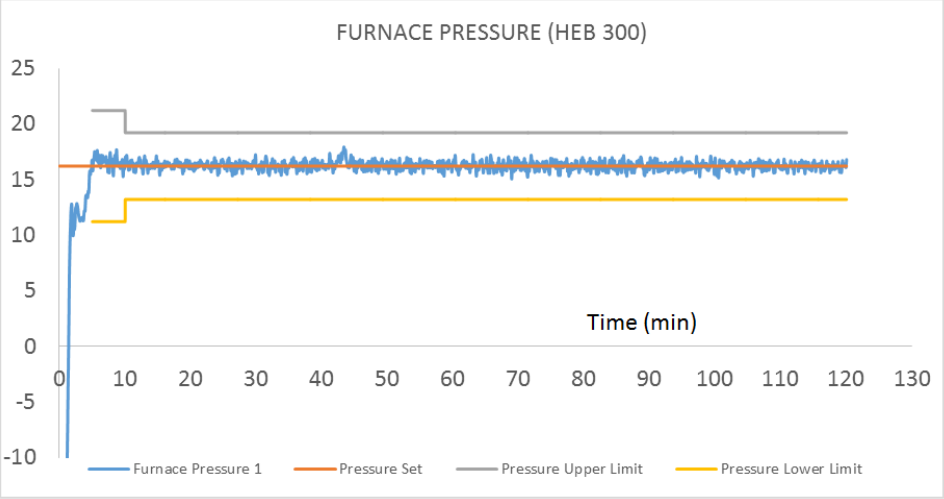

Figure 5.28. Furnace Pressure for HEB 300 (Test 3).

The furnace pressure recorded so that by 5 minutes from start of the test pressure shall be ±5 Pa of the nominal pressure and pressure shall be ±3 Pa of the nominal pressure from 10 minutes onwards it. All values are in limit at any time.

Furnace deviation graphic is shown in Figure 5.29.

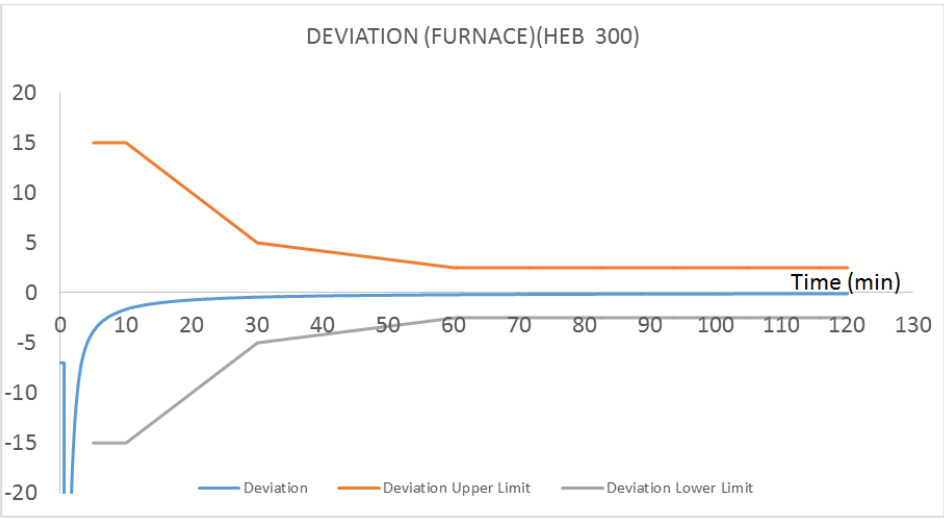

Figure 5.29. Furnace Deviation for HEB 300 (Test 3).

The deviation percentage in the area of the curve of the average temperature recorded by the plate thermocouples specified in EN 1363-1 against time the standard temperature/time curve area shall be within the below limits:

The percentage deviation (de) in the area of the curve of the average temperature recorded by the specified furnace thermocouples versus time from the area of the standard temperature/time curve shall be within:

(i) 15% for $5 < t \leq 10$
(ii) (15 - 0,5 (t-10))% for $10 < t \leq 30$
(iii) (5 - 0,083 (t-30))% for $30 < t \leq 60$
(iv) 2,5% for $t > 60$

$$de = \frac{AA_s}{A_s} x100 \tag{5.3}$$

where de the percentage deviation, A the area under the actual furnace temperature/time curve.

All values in this test are in limit as per above. Ambient temperature graphic during the test is shown in Figure 5.30.

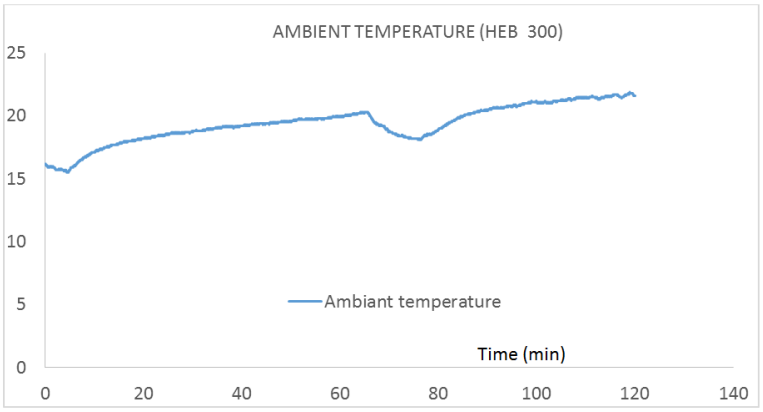

Figure 5.30. Ambient Temperature during the test for HEB 300 (Test 3).

The ambient temperature shall be within the limit 10^{o}C - 40 ^{o}C from the beginning of the test. It shall be recorded at a distance of between 1m and 3m horizontally away from outside of the furnace. Under that conditions the sensor shall not be affected by thermal radiation from the test specimen or furnace. The temperature in the test

area shall not decline by more than 10 K or shall not raise by more than 20 K during the test. During the test all values are in the limit.

HEB 300 test pictures before and during the test are shown in Figure 5.31 to Figure 5.37.

Figure 5.31. General View before the Test for HEB 300.

Figure 5.32. Section View during the Test for HEB 300 (16^{th} Minute).

Figure 5.33. Section View during the Test for HEB 300 (32^{nd} Minute).

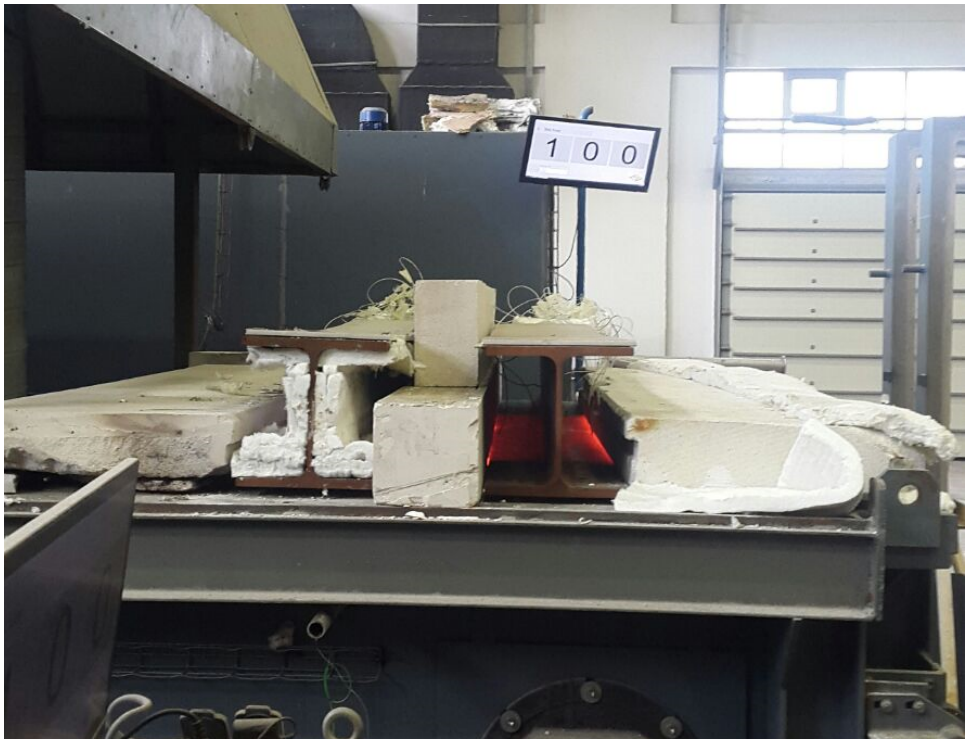

Figure 5.34. Section View during the Test for HEB 300 (60^{th} Minute).

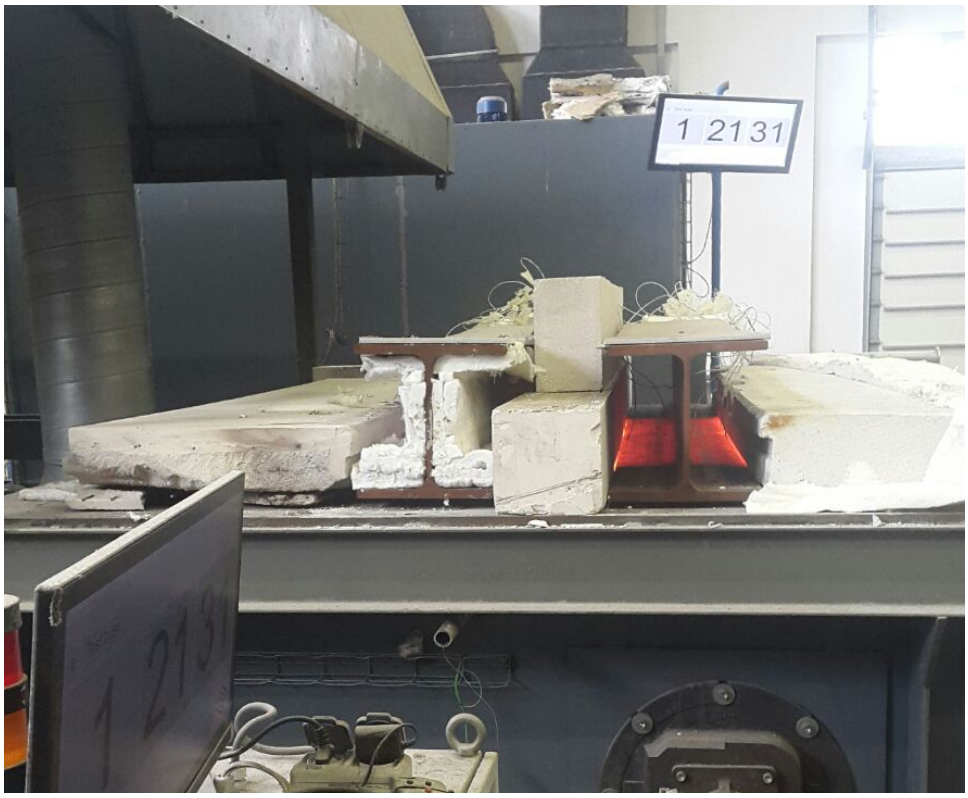

Figure 5.35. Section View during the Test for HEB 300 (80^{th} Minute).

Figure 5.36. Section View during the Test for HEB 300 (100^{th} Minute).

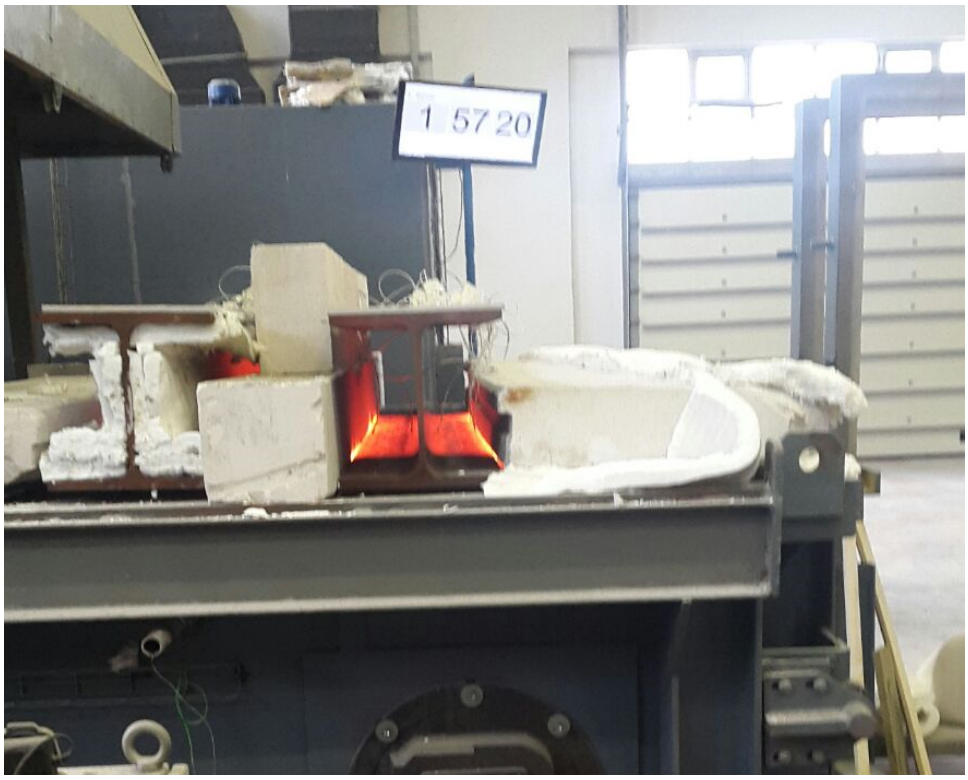

Figure 5.37. Section View during the Test for HEB 300 (120^{th} Minute).

6. FINITE ELEMENT RESULTS

Sections are modelled in ABAQUS FE program in 2D. All sections are exposed to standard temperature-time curve from bottom side of the specimen. In order to meet the test results and evaluate precisely, location 2 (in Figure 4.4, Figure 4.8 and Figure 4.12) test temperature values were applied to all sections as per each test results to bottom part of the bottom flanges. These application from test results facilitate the evaluation and comparison of the enclosure radiation effects in I sections. For the insulated sections, insulated surfaces (enclosure of the sections as shown in Figure 4.2, Figure 4.6 and Figure 4.10 are defined adiabatic FE (ABAQUS) because of the 1200^{o}C fire retardant 5 cm ceramic wool insulation. All locations defined in the FE (ABAQUS) model are same with the thermocouple locations.

6.1. Finite Elements Results for Test 1

For uninsulated INP 400 FE (ABAQUS) results are shown in Figure 6.1 and Figure 6.2.

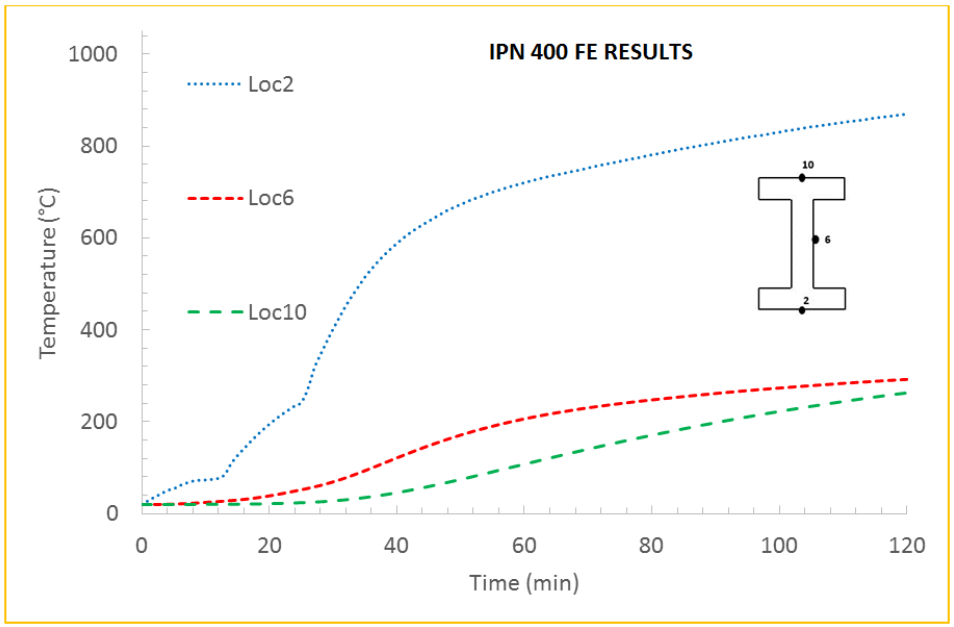

Figure 6.1. Thermocouples for Uninsulated INP 400 (Loc2, Loc6, Loc10).

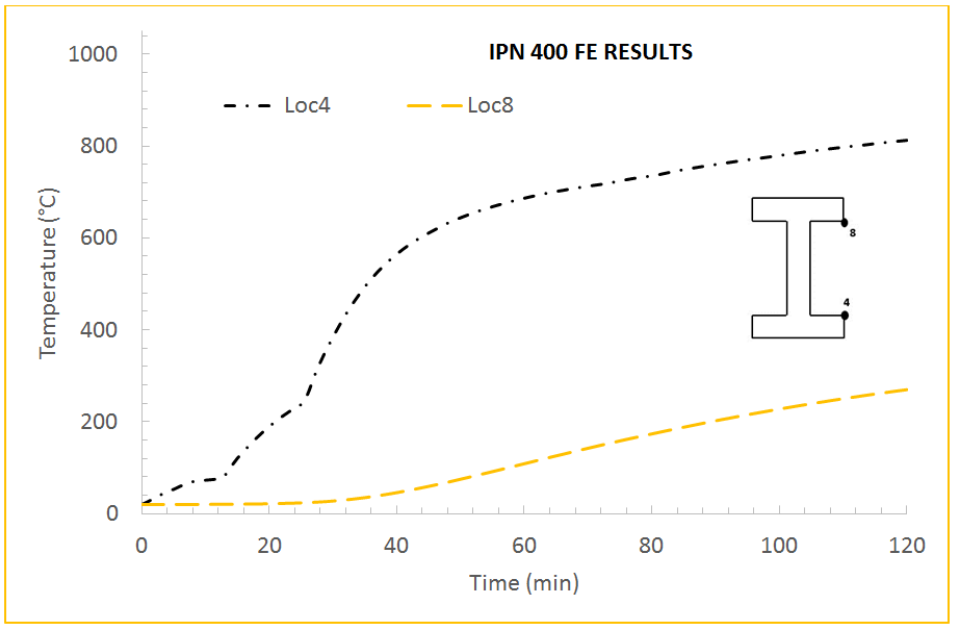

Figure 6.2. Thermocouples for Uninsulated INP 400 (Loc4, Loc8).

Location 2 (Loc2) to Location 10 (Loc10) illustrate the temperature location same as in the tests. Loc2 is temperature location of the bottom flange exposed side middle point. Loc4 is temperature location of the bottom flange unexposed left-hand side. Loc6 is in the surface middle of the web of the section. Loc8 is temperature location of the top flange bottom part left-hand side. Loc10 is temperature location of the top flange unexposed side middle point. The results for uninsulated INP 400 section show that temperature values after 30-minute reach to 402 ^{o}C for Loc2, 385 ^{o}C for Loc4, 69 ^{o}C for Loc6, 28 ^{o}C for Loc8 and 28 ^{o}C for Loc10. After 60-minute temperature values reach 720 ^{o}C for Loc2, 687 ^{o}C for Loc4, 206 ^{o}C for Loc6, 109 ^{o}C for Loc8, 108 ^{o}C for Loc10. After 90-minute temperature values reach 807 ^{o}C for Loc2, 760 ^{o}C for Loc4, 262 ^{o}C for Loc6, 202 ^{o}C for Loc8, 198 ^{o}C for Loc10. After 120-minute temperature values reach 870 ^{o}C for Loc2, 813 ^{o}C for Loc4, 292 ^{o}C for Loc6, 270 ^{o}C for Loc8, 265 ^{o}C for Loc10. The results show that for Loc8 and Loc10 temperature values are close to each other. The remaining temperature values are also logical and reasonable for their location. After 2-hour furnace temperature reach 1049 ^{o}C, so Loc2 temperature value after 2-hour are also reasonable. Temperature difference between Loc2 and Loc10 is 604 ^{o}C after 2 hours.

For insulated INP 400 FE (ABAQUS) results are shown in Figure 6.3 and Figure 6.4.

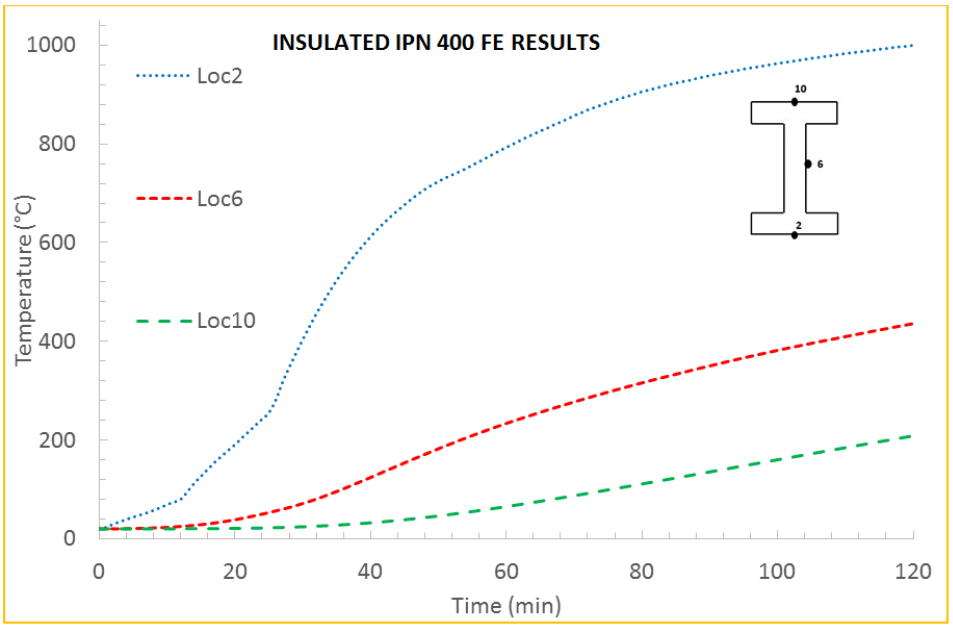

Figure 6.3. Thermocouples for Insulated INP 400 (Loc2, Loc6, Loc10).

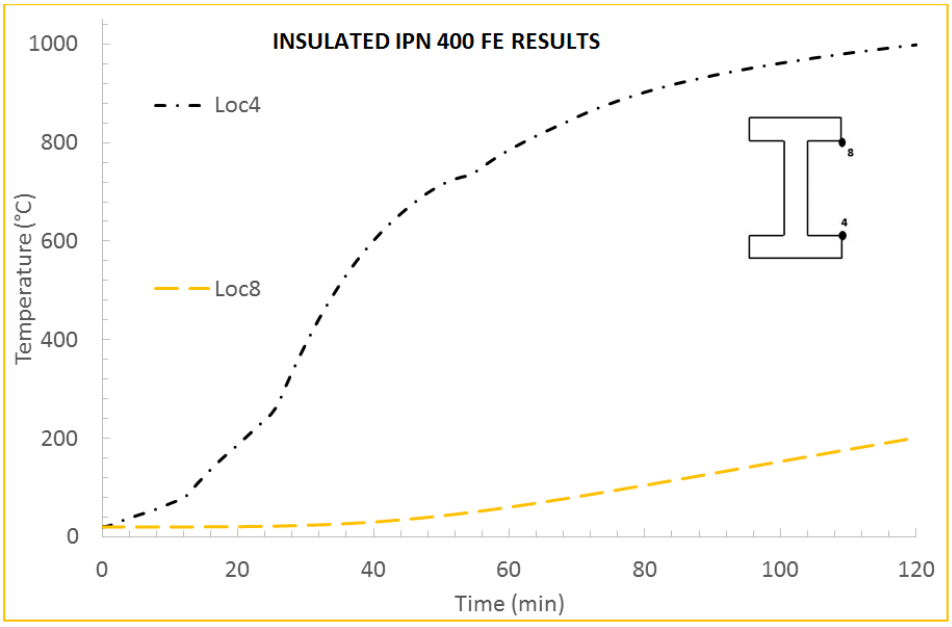

Figure 6.4. Thermocouples for Insulated INP 400 (Loc4, Loc8).

Location 2 (Loc2) to Location 10 (Loc10) illustrate the temperature location same as in the tests. Loc2 is temperature location of the bottom flange exposed side middle

point. Loc4 is temperature location of the bottom flange unexposed left-hand side. Loc6 is in the surface middle of the web of the section. Loc8 is temperature location of the top flange bottom part left-hand side. Loc10 is temperature location of the top flange unexposed side middle point. The results for insulated INP 400 section show that temperature values after 30-minute reach to 404 ^{o}C for Loc2, 391 ^{o}C for Loc4, 71 ^{o}C for Loc6, 23 ^{o}C for Loc8 and 24 ^{o}C for Loc10. After 60-minute temperature values reach 793 ^{o}C for Loc2, 785 ^{o}C for Loc4, 234 ^{o}C for Loc6, 60 ^{o}C for Loc8, 65 ^{o}C for Loc10. After 90-minute temperature values reach 934 ^{o}C for Loc2, 936 ^{o}C for Loc4, 350 ^{o}C for Loc6, 129 ^{o}C for Loc8, 136 ^{o}C for Loc10. After 120-minute temperature values reach 999 ^{o}C for Loc2, 999 ^{o}C for Loc4, 436 ^{o}C for Loc6, 201 ^{o}C for Loc8, 208 ^{o}C for Loc10. The results show that for Loc8 and Loc10 temperature values are close to each other. The remaining temperature values are also logical and reasonable for their location. After 2-hour furnace temperature reach 1049 ^{o}C, so Loc2 temperature value after 2-hour are also reasonable. Temperature difference between Loc2 and Loc10 is 791 ^{o}C after 2 hours.

6.2. Finite Elements Results for Test 2

For uninsulated HEB 400 FE (ABAQUS) results are shown in Figure 6.5 and Figure 6.6.

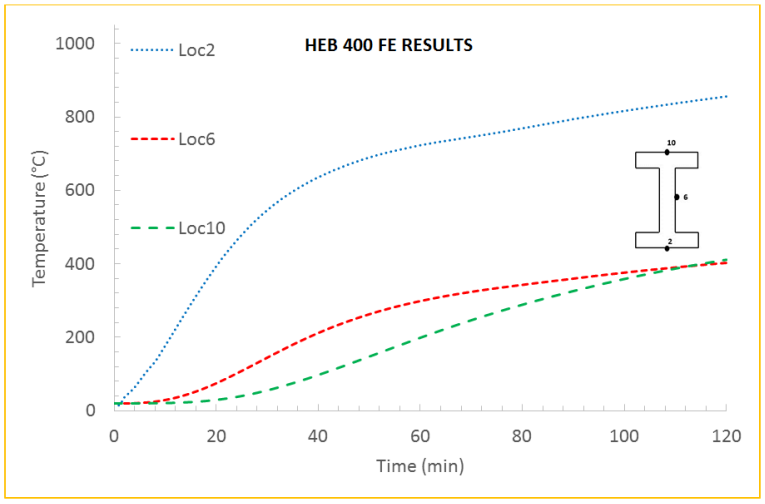

Figure 6.5. Thermocouples for Uninsulated HEB 400 (Loc2, Loc6, Loc10).

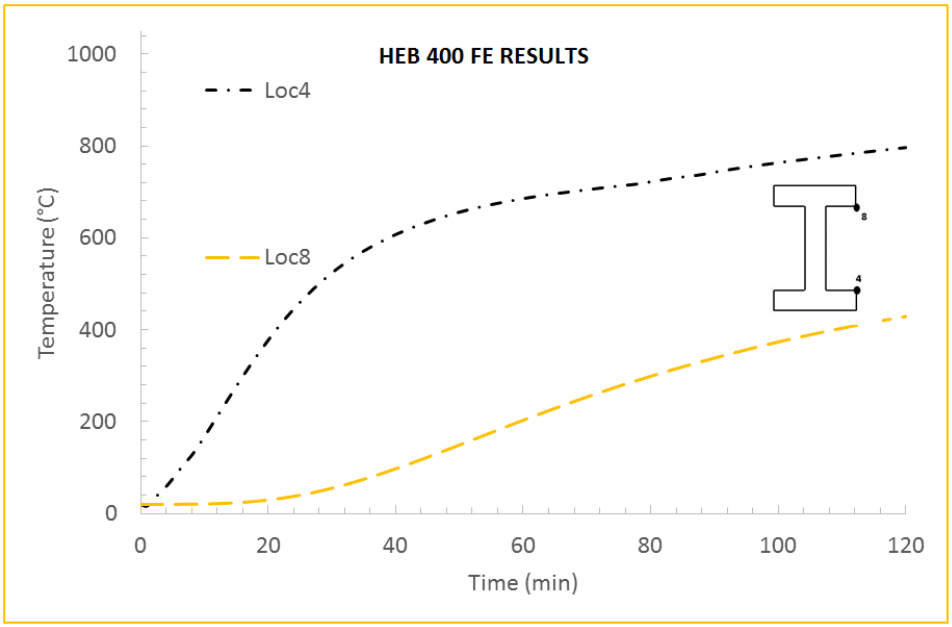

Figure 6.6. Thermocouples for Uninsulated HEB 400 (Loc4, Loc8).

Location 2 (Loc2) to Location 10 (Loc10) illustrate the temperature location same as in the tests. Loc2 is temperature location of the bottom flange exposed side middle point. Loc4 is temperature location of the bottom flange unexposed left-hand side. Loc6 is in the surface middle of the web of the section. Loc8 is temperature location of the top flange bottom part left-hand side. Loc10 is temperature location of the top flange unexposed side middle point. The results for uninsulated HEB 400 section show that temperature values after 30-minute reach to 547 ^{o}C for Loc2, 524 ^{o}C for Loc4, 145 ^{o}C for Loc6, 55 ^{o}C for Loc8 and 55 ^{o}C for Loc10. After 60-minute temperature values reach 723 ^{o}C for Loc2, 685 ^{o}C for Loc4, 298 ^{o}C for Loc6, 203 ^{o}C for Loc8, 198 ^{o}C for Loc10. After 90-minute temperature values reach 794 ^{o}C for Loc2, 742 ^{o}C for Loc4, 359 ^{o}C for Loc6, 338 ^{o}C for Loc8, 325 ^{o}C for Loc10. After 120-minute temperature values reach 856 ^{o}C for Loc2, 796 ^{o}C for Loc4, 403 ^{o}C for Loc6, 428 ^{o}C for Loc8, 411 ^{o}C for Loc10. The results show that for Loc8 and Loc10 temperature values are close to each other. The remaining temperature values are also logical and reasonable for their location. After 2-hour furnace temperature reach 1049 ^{o}C, so Loc2 temperature value after 2-hour are also reasonable. Temperature difference between Loc2 and Loc10 is 445 ^{o}C after 2 hours.

For insulated HEB 400 FE (ABAQUS) results are shown in Figure 6.7 and Figure 6.8.

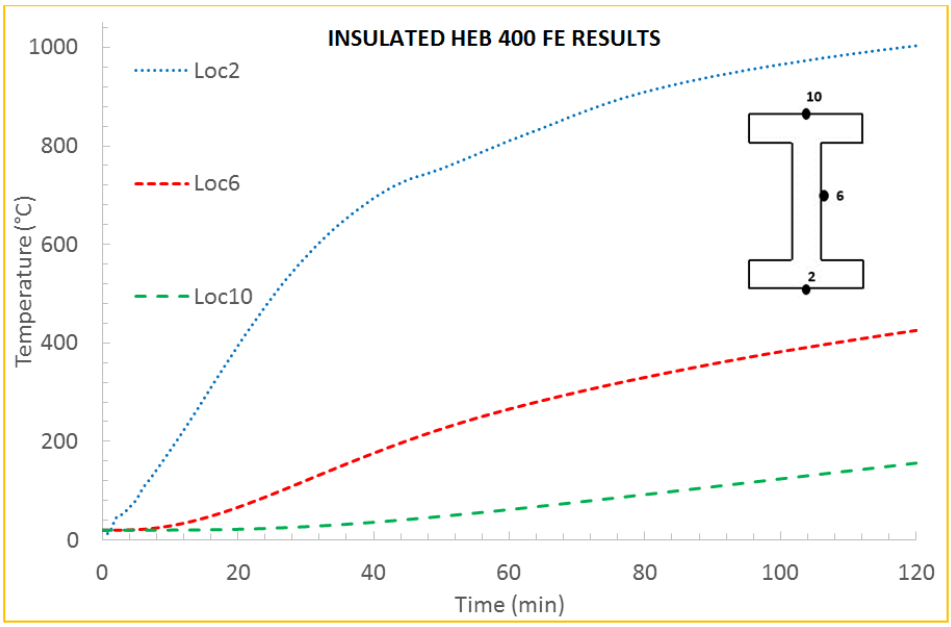

Figure 6.7. Thermocouples for Insulated HEB 400 (Loc2, Loc6, Loc10).

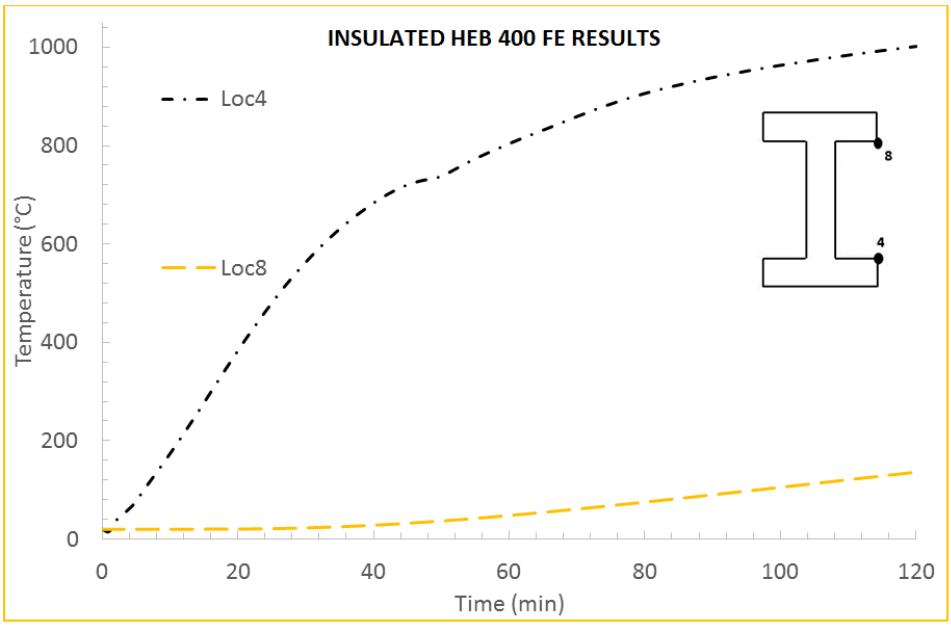

Figure 6.8. Thermocouples for Uninsulated HEB 400 (Loc4, Loc8).

6.3. Finite Elements Results for Test 3

For uninsulated HEB 300 FE (ABAQUS) results are shown in Figure 6.9 and Figure 6.10.

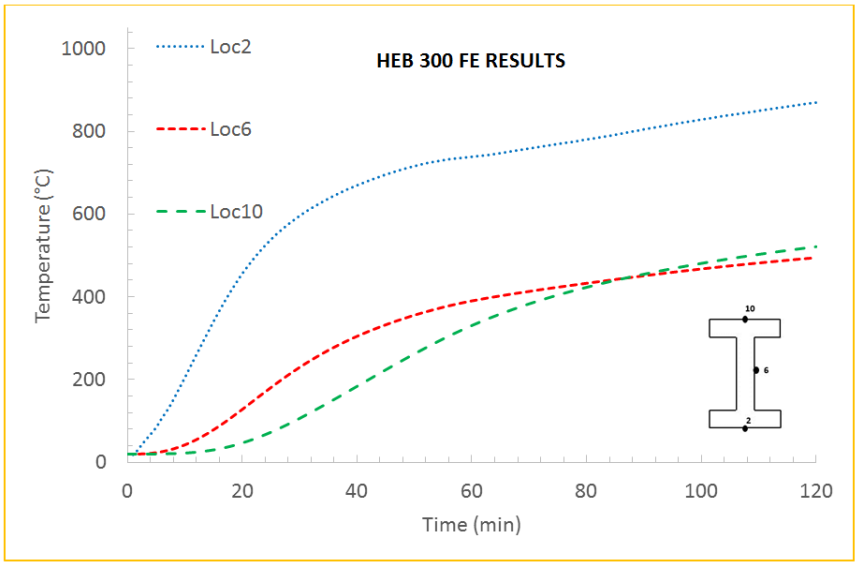

Figure 6.9. Thermocouples for Uninsulated HEB 300 (Loc2, Loc6, Loc10).

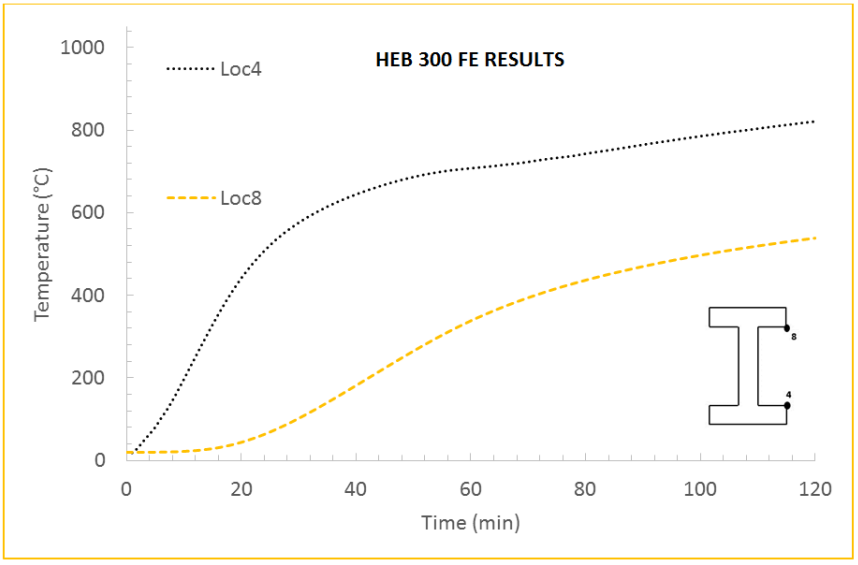

Figure 6.10. Thermocouples for Uninsulated HEB 300 (Loc4, Loc8).

Location 2 (Loc2) to Location 10 (Loc10) illustrate the temperature location same as in the tests. Loc2 is temperature location of the bottom flange exposed side

middle point. Loc4 is temperature location of the bottom flange unexposed left-hand side. Loc6 is in the surface middle of the web of the section. Loc8 is temperature location of the top flange bottom part left-hand side. Loc10 is temperature location of the top flange unexposed side middle point. The results for uninsulated HEB 300 section show that temperature values after 30-minute reach to 595 ^{o}C for Loc2, 576 ^{o}C for Loc4, 230 ^{o}C for Loc6, 102 ^{o}C for Loc8 and 106 ^{o}C for Loc10. After 60-minute temperature values reach 738 ^{o}C for Loc2, 706 ^{o}C for Loc4, 390 ^{o}C for Loc6, 338 ^{o}C for Loc8, 331 ^{o}C for Loc10. After 90-minute temperature values reach 805 ^{o}C for Loc2, 765 ^{o}C for Loc4, 451 ^{o}C for Loc6, 470 ^{o}C for Loc8, 455 ^{o}C for Loc10. After 120-minute temperature values reach 870 ^{o}C for Loc2, 821 ^{o}C for Loc4, 495 ^{o}C for Loc6, 538 ^{o}C for Loc8, 521 ^{o}C for Loc10. The results show that for Loc8 and Loc10 temperature values are close to each other. The remaining temperature values are also logical and reasonable for their location. After 2-hour furnace temperature reach 1049 ^{o}C, so Loc2 temperature value after 2-hour are also reasonable. Temperature difference between Loc2 and Loc10 is 348 ^{o}C after 2 hours.

For insulated HEB 300 FE (ABAQUS) results are shown in Figure 6.11 and Figure 6.12.

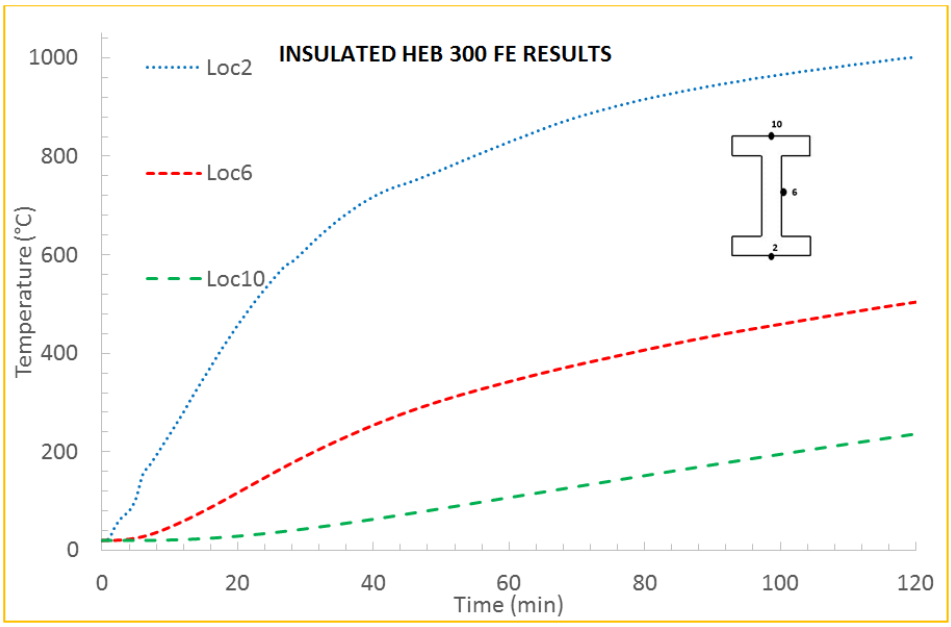

Figure 6.11. Thermocouples for Insulated HEB 300 (Loc2, Loc6, Loc10).

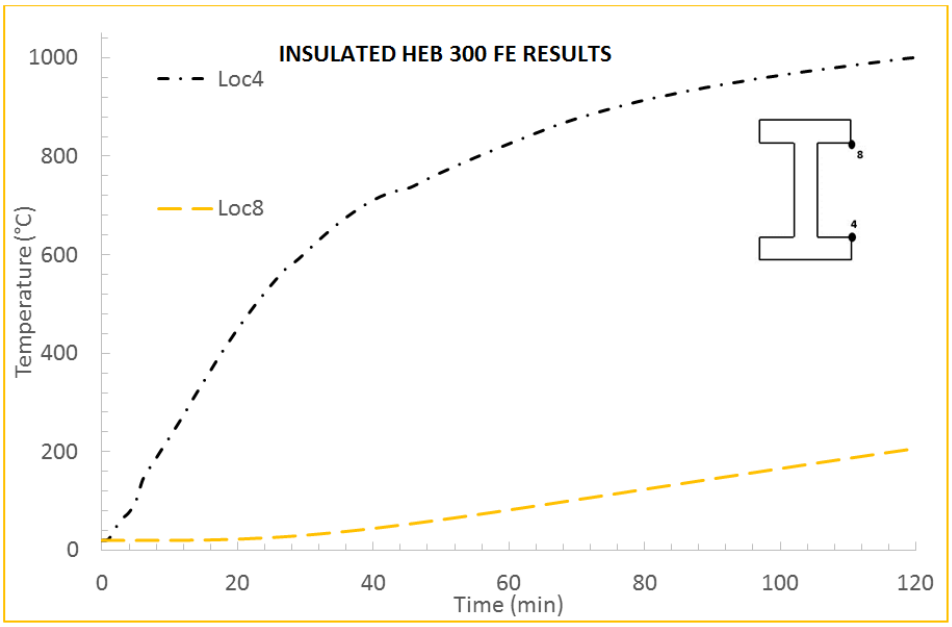

Figure 6.12. Thermocouples for Insulated HEB 300 (Loc4, Loc8).

Location 2 (Loc2) to Location 10 (Loc10) illustrate the temperature location same as in the tests. Loc2 is temperature location of the bottom flange exposed side middle point. Loc4 is temperature location of the bottom flange unexposed left-hand side. Loc6 is in the surface middle of the web of the section. Loc8 is temperature location of the top flange bottom part left-hand side. Loc10 is temperature location of the top flange unexposed side middle point. The results for insulated HEB 400 section show that temperature values after 30-minute reach to 611 ^{o}C for Loc2, 604 ^{o}C for Loc4, 191 ^{o}C for Loc6, 31 ^{o}C for Loc8 and 44 ^{o}C for Loc10. After 60-minute temperature values reach 829 ^{o}C for Loc2, 825 ^{o}C for Loc4, 342 ^{o}C for Loc6, 82 ^{o}C for Loc8, 107 ^{o}C for Loc10. After 90-minute temperature values reach 943 ^{o}C for Loc2, 942 ^{o}C for Loc4, 435 ^{o}C for Loc6, 145 ^{o}C for Loc8, 174 ^{o}C for Loc10. After 120-minute temperature values reach 1001 ^{o}C for Loc2, 1001 ^{o}C for Loc4, 504 ^{o}C for Loc6, 207 ^{o}C for Loc8, 236 ^{o}C for Loc10. The results show that for Loc8 and Loc10 temperature values are close to each other. The remaining temperature values are also logical and reasonable for their location. After 2-hour furnace temperature reach 1049 ^{o}C, so Loc2 temperature value after 2-hour are also reasonable. Temperature difference between Loc2 and Loc10 is 765 ^{o}C after 2 hours.

Thermal gradient for FE results through the section depth can be calculated temperature difference top (Loc10) and bottom flange (Loc2) divided by section depth versus time. Thermal gradient comparison graph for FE results are shown in Figure 6.13.

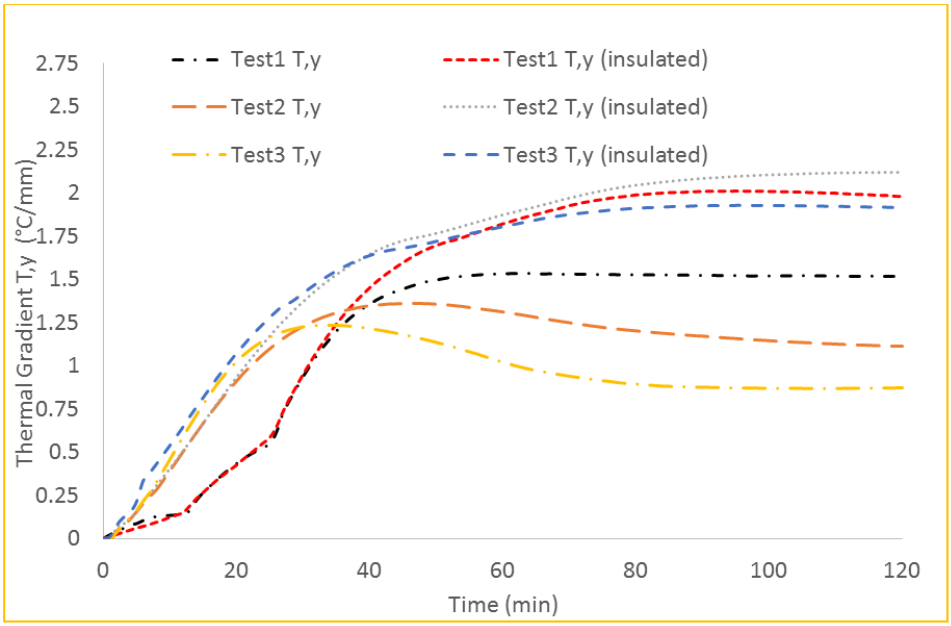

Figure 6.13. Thermal Gradient Comparison for FE.

7. COMPARISON BETWEEN FE AND EXPERIMENTAL RESULTS

7.1. Comparison between FE and Test Results for INP 400

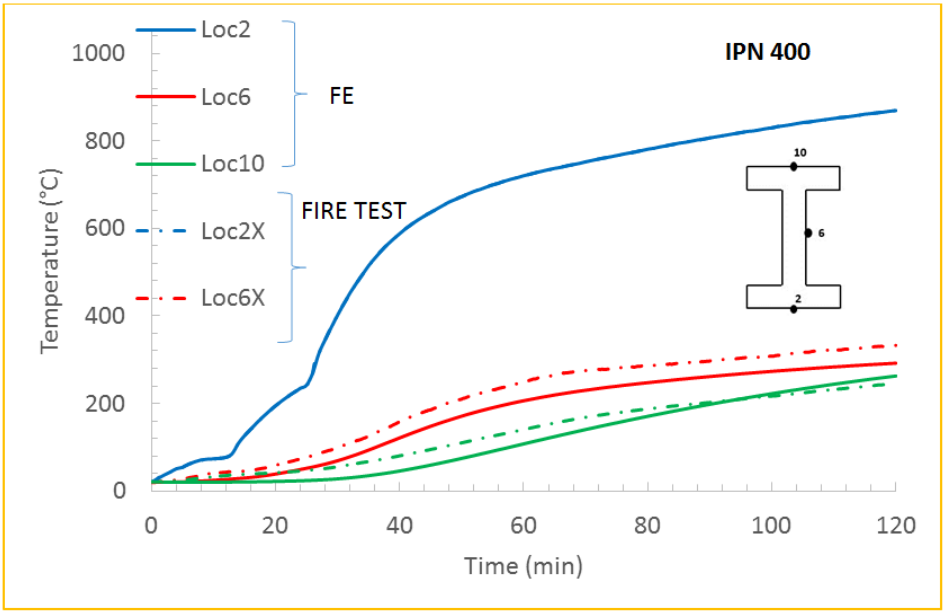

Figure 7.1. Comparison between Fe and Test Results for INP 400 Uninsulated (Loc2, Loc6, Loc10).

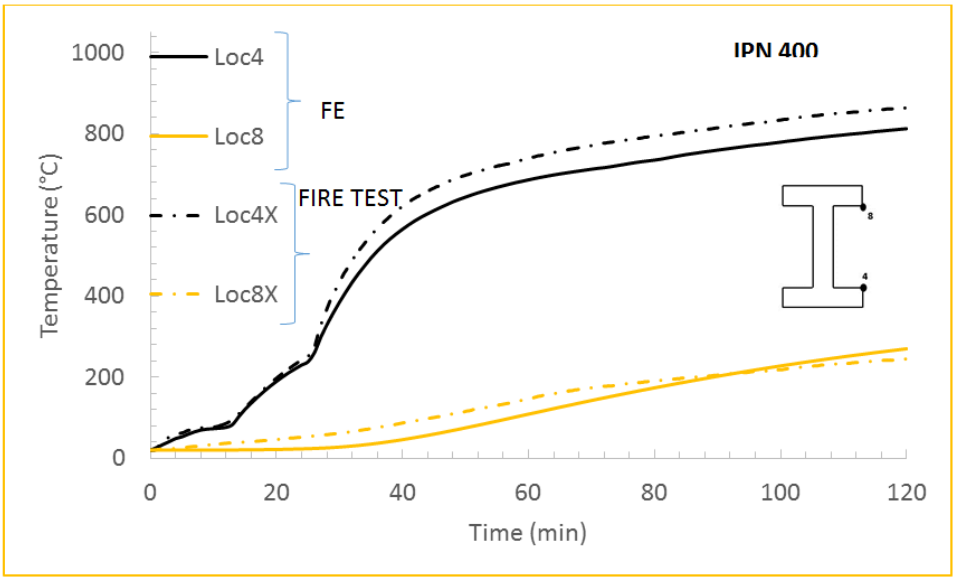

Figure 7.2. Comparison between Fe and Test Results for INP 400 Uninsulated (Loc4, Loc8).

In order to meet the test results and evaluate precisely, location 2 (in Figure 4.4, Figure 4.8 and Figure 4.12) test temperature values were applied to all sections as per each test results to bottom part of the bottom flanges. So it can be understood from the graph Loc2 values are same. At the beginning of the test Loc4 temperature values are also so close each other. After 30-minute difference between FE and test results commence to increase for Loc4. And at the end of the test the temperature difference reach approximately to 50 ^{o}C. For Loc6 at the beginning of the test temperature values are so close to each other. After 30-minute difference between FE and test results increase a little. At the end of the test the temperature difference reaches approximately to 40 ^{o}C. For Loc8 and Loc10, at the beginning of the test temperature values are so close to each other, and behave same manner. After 30-minute difference between FE and test results commence to increase a little. At the end of the test the temperature difference between Loc8 and Loc10 are so close to each other. Generally, the results for FE and test results are so close to each other and temperature values are satisfactory for the comparison. The slight temperature difference for uninsulated sections can be because of the time dependent emissivity coefficient for each temperature.

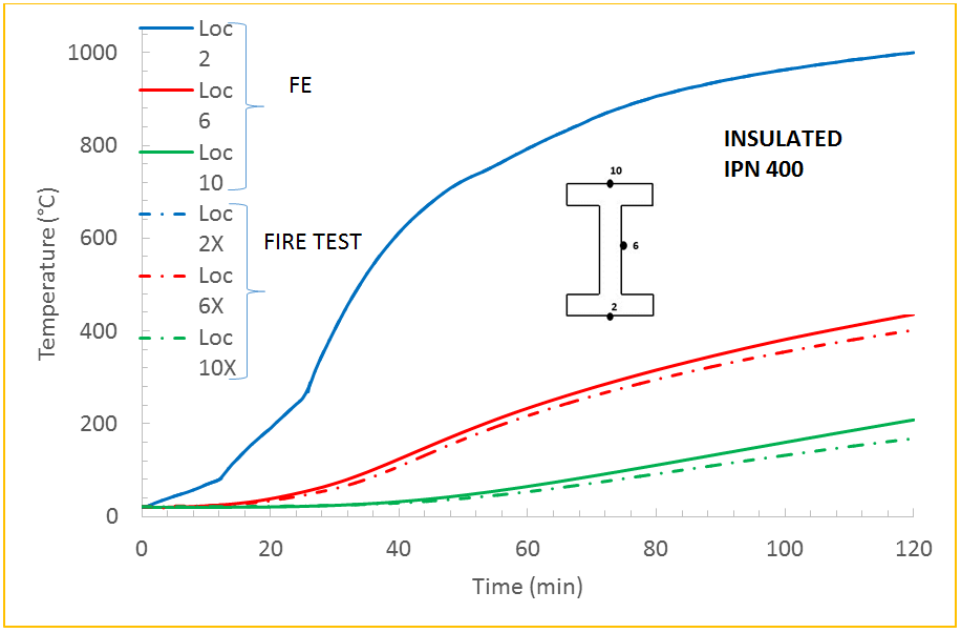

Figure 7.3. Comparison between Fe and Test Results for INP 400 Insulated (Loc2, Loc6, Loc10).

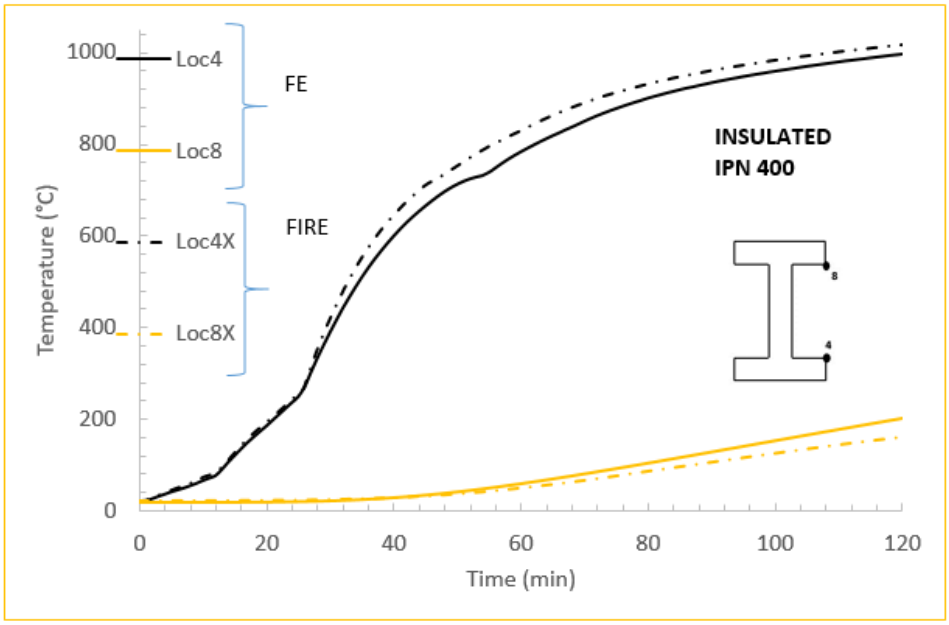

Figure 7.4. Comparison between Fe and Test Results for INP 400 Insulated (Loc4, Loc8).

For insulated INP 400, location 2 (in Figure 4.4) test temperature values were applied to all sections as per each test results to bottom part of the bottom flanges. So it can be understand from the graph Loc2 values are same. At the beginning of the test Loc4 temperature values are also so close each other. After 30-minute difference between FE and test results commence to increase a little bit for Loc4. And at the end of the test the temperature difference are so close to each other. For Loc6 at the beginning of the test temperature values are so close to each other. After 30-minute difference between FE and test results commence to increase a little bit. At the end of the test the temperature difference reach approximately to 30 ^{o}C. For Loc8 and Loc10, at the beginning of the test temperature values are so close to each other, and behave same manner. After 30-minute difference between FE and test results commence to increase a little bit. At the end of the test the temperature difference between Loc8 and Loc10 is approximately to 30 ^{o}C. Generally, the results for FE and test results are so close to each other and temperature values are satisfactory for the comparison.

7.2. Comparison between FE and Test Results for HEB 400

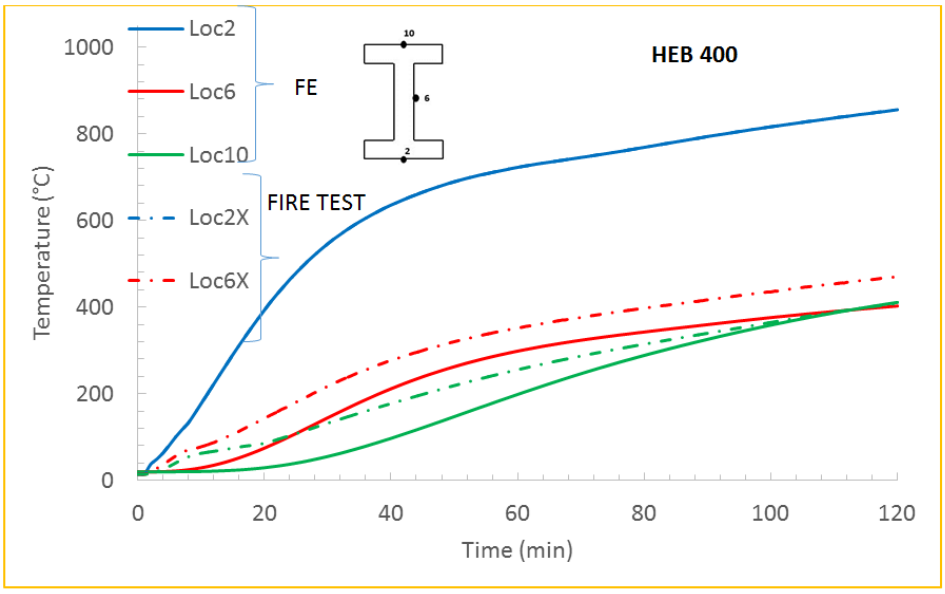

Figure 7.5. Comparison between Fe and Test Results for HEB 400 Uninsulated (Loc2, Loc6, Loc10).

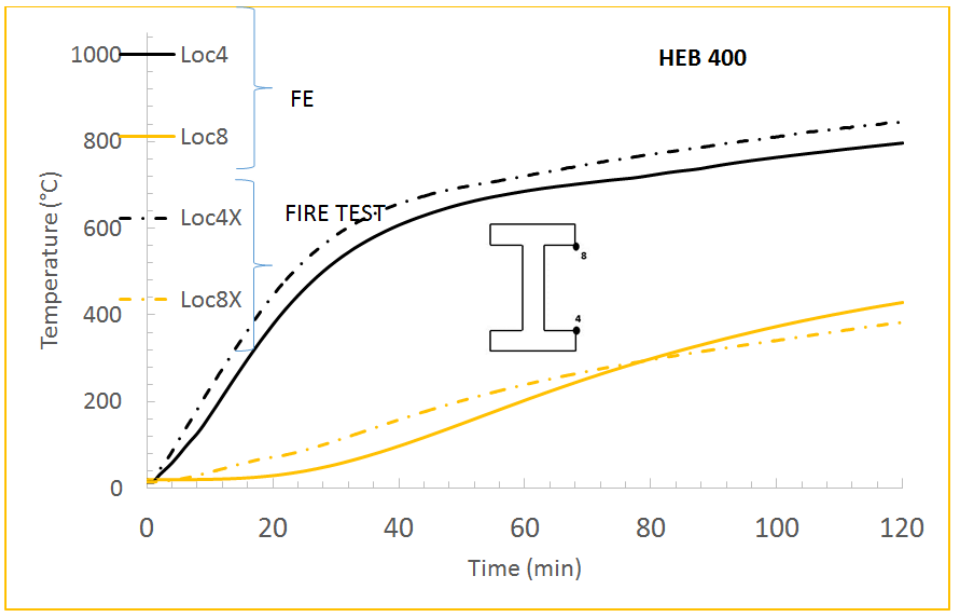

Figure 7.6. Comparison between Fe and Test Results for HEB 400 Uninsulated (Loc4, Loc8).

In order to meet the test results and evaluate precisely, location 2 (in Figure 4.4, Figure 4.8 and Figure 4.12) test temperature values were applied to all sections as per

each test results to bottom part of the bottom flanges. So it can be understand from the graph Loc2 values are same. At the beginning of the test Loc4 temperature values are also so close each other. After 30-minute difference between FE and test results commence to increase a little bit for Loc4. And at the end of the test the temperature difference reached to 30 ^{o}C. For Loc6 at the beginning of the test temperature values are so close to each other. After 30-minute difference between FE and test results commence to increase a little bit. At the end of the test the temperature difference reach approximately to 55 ^{o}C. For Loc8 and Loc10, at the beginning of the test temperature values are so close to each other, and behave same manner. After 30-minute difference between FE and test results commence to increase a little bit. At the end of the test the temperature difference between Loc8 and Loc10 is approximately to 30 ^{o}C. Generally, the results for FE and test results are so close to each other and temperature values are satisfactory for the comparison. The slight temperature difference for uninsulated sections can be because of the time dependent emissivity coefficient for each temperature.

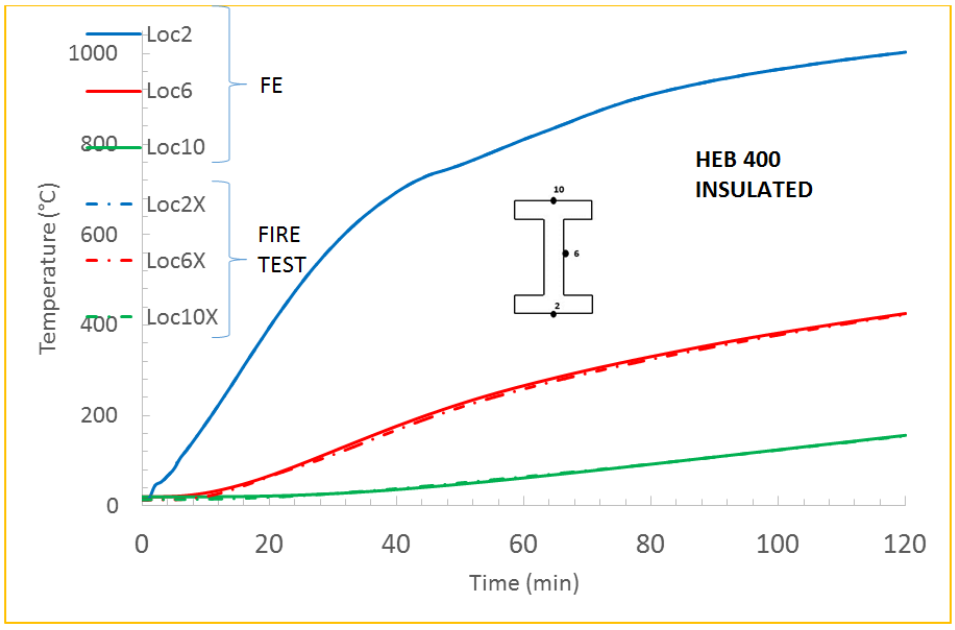

Figure 7.7. Comparison between Fe and Test Results for HEB 400 Insulated (Loc2, Loc6, Loc10).

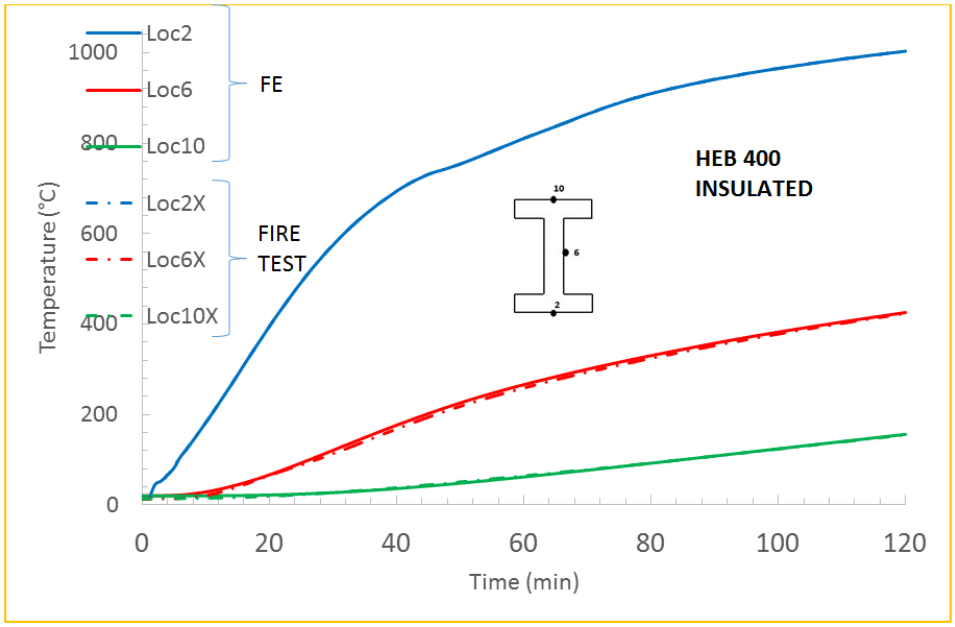

Figure 7.8. Comparison between Fe and Test Results for HEB 400 Insulated (Loc4, Loc8).

For HEB 400, location 2 (in Figure 4.8) test temperature values were applied to all sections as per each test results to bottom part of the bottom flanges. So it can be understand from the graph Loc2 values are same. At the beginning of the test Loc4 temperature values are also so close each other. After 30-minute difference between FE and test results commence to increase a little bit for Loc4. And at the end of the test the temperature difference reached to 30 ^{o}C. For Loc6 at the beginning of the test temperature values are so close to each other. After 30-minute difference between FE and test results commence to increase a little bit. At the end of the test the temperature difference is so close to each other. For Loc8 and Loc10, at the beginning of the test temperature values are so close to each other, and behave same manner. After 30-minute difference between FE and test results commence to increase a little bit. At the end of the test the temperature difference between Loc8 and Loc10 are so close to each other. Generally, the results for FE and test results are so close to each other and temperature values are satisfactory for the comparison.

7.3. Comparison between FE and Test Results for HEB 300

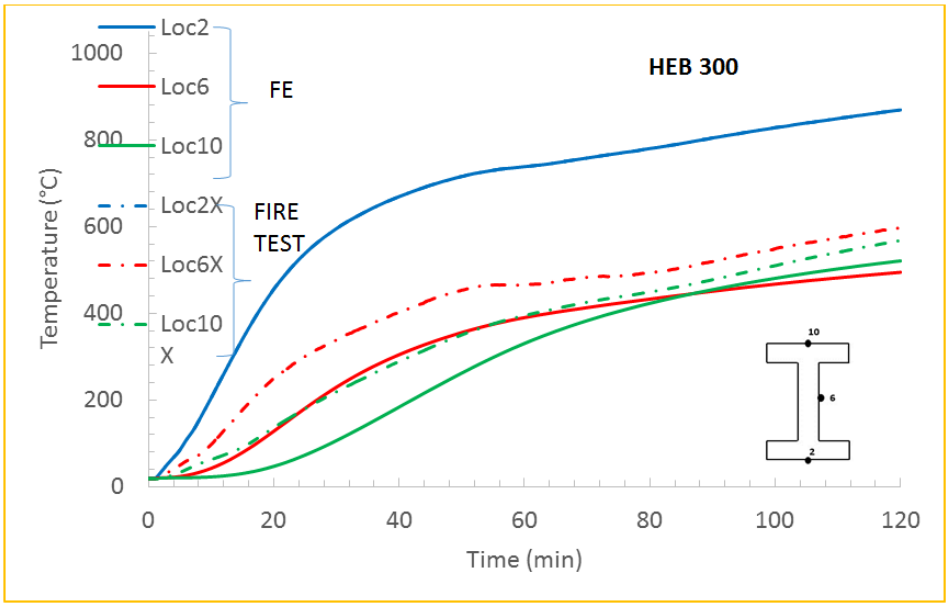

Figure 7.9. Comparison between Fe and Test Results for HEB 300 Uninsulated (Loc2, Loc6, Loc10).

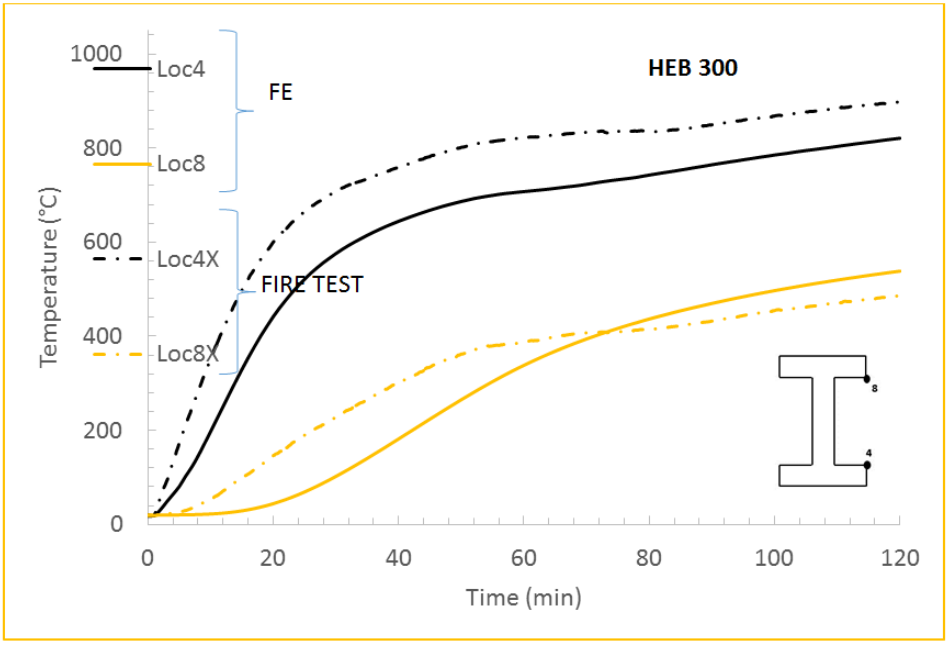

Figure 7.10. Comparison between Fe and Test Results for HEB 300 Uninsulated (Loc4, Loc8).

In order to meet the test results and evaluate precisely, location 2 (in Figure 4.4, Figure 4.8 and Figure 4.12) test temperature values were applied to all sections as per

each test results to bottom part of the bottom flanges. So it can be understand from the graph Loc2 values are same. At the beginning of the test Loc4 temperature values are also so close each other. After 30-minute difference between FE and test results commence to increase a little bit for Loc4. And at the end of the test the temperature difference reached to 70 ^{o}C. For Loc6 at the beginning of the test temperature values are so close to each other. After 30-minute difference between FE and test results commence to increase a little bit. At the end of the test the temperature difference reach approximately to 90 ^{o}C. For Loc8 and Loc10, at the beginning of the test temperature values are so close to each other, and behave same manner. After 30-minute difference between FE and test results commence to increase a little bit. At the end of the test the temperature difference between Loc8 and Loc10 is approximately to 30 ^{o}C. Generally, the results for FE and test results are so close to each other and temperature values are satisfactory for the comparison. The slight temperature difference for uninsulated sections can be because of the time dependent emissivity coefficient for each temperature.

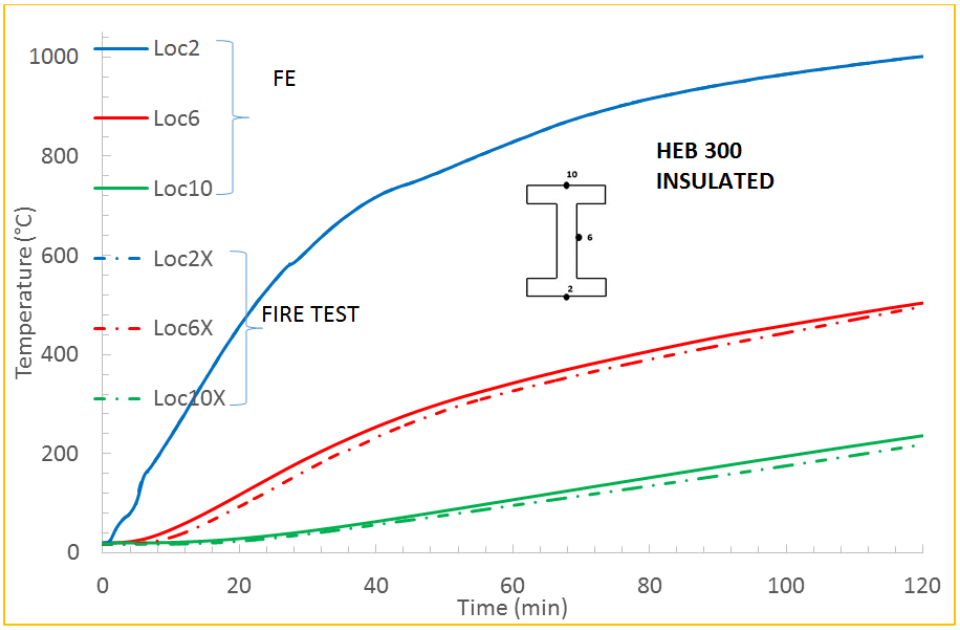

Figure 7.11. Comparison between Fe and Test Results for HEB 300 Insulated (Loc2, Loc6, Loc10).

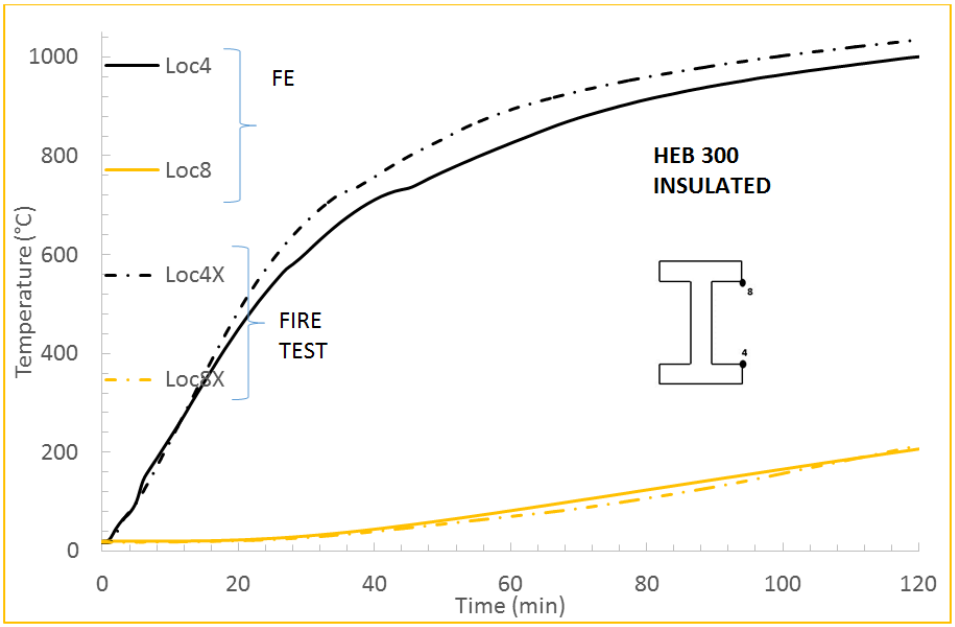

Figure 7.12. Comparison between Fe and Test Results for HEB 300 Insulated (Loc4, Loc8).

For HEB 300, location 2 (in Figure 4.12) test temperature values were applied to all sections as per each test results to bottom part of the bottom flanges. So it can be understand from the graph Loc2 values are same. At the beginning of the test Loc4 temperature values are also so close each other. After 30-minute difference between FE and test results commence to increase a little bit for Loc4. And at the end of the test the temperature difference reached to 20 ^{o}C. For Loc6 at the beginning of the test temperature values are so close to each other. After 30-minute difference between FE and test results commence to increase a little bit. At the end of the test the temperature difference is so close to each other. For Loc8 and Loc10, at the beginning of the test temperature values are so close to each other, and behave same manner. After 30-minute difference between FE and test results commence to increase a little bit. At the end of the test the temperature difference between Loc8 and Loc10 are so close to each other. Generally, the results for FE and test results are so close to each other and temperature values are satisfactory for the comparison.

7.4. Comparison of Test Results for Insulated and Uninsulated Sections

For INP 400 section test results comparison is shown in Figure 7.13.

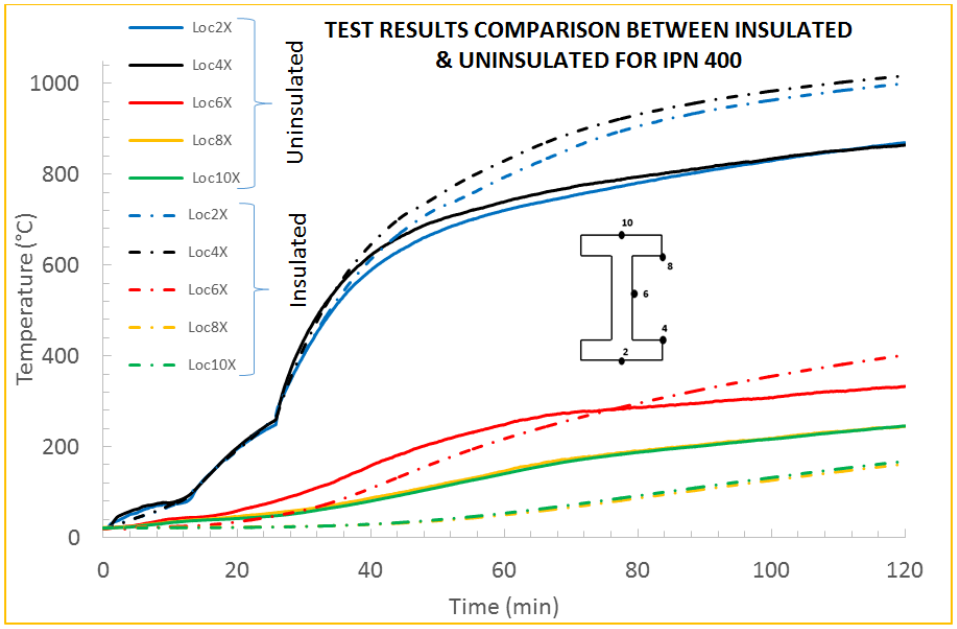

Figure 7.13. Comparison of Test Results for INP 400.

At the beginning of the test, for Loc2 temperature values are so close to each other until 30-minute. After 30-minute temperature difference commenced to differ. At the 60-minute temperature difference reached to 70 ^{o}C for Loc2. After 90-minute temperature difference reached to 130 ^{o}C for Loc2. At the end of the test, temperature difference reached approximately 150 ^{o}C. For Loc4 temperature values are so close to each other until 30-minute. At the 60-minute temperature difference reached to 90 ^{o}C for Loc4. After 90-minute temperature difference reached to 140 ^{o}C for Loc4. At the end of the test, temperature difference reached approximately 155 ^{o}C. For Loc6, at the beginning of the test, temperature values are so close to each other, but after 5 minutes uninsulated (real) section temperature commenced to increase approximately after 75 minutes differences between them decrease and at the end of the test-insulated section temperature was 70 ^{o}C higher than the uninsulated one. For the upper flange Loc8 temperature values are so close to each other until 30-minute. At the 60-minute temperature difference reached to 90 ^{o}C for Loc8. After 90-minute temperature difference approximately same with 60-minute. At the end of the test, temperature difference

was approximately 80 ^{o}C. For the upper flange Loc10 temperature values are so close to each other until 30-minute. At the 60-minute temperature difference reached to 90 ^{o}C for Loc10. After 90-minute temperature difference approximately same with 60-minute. At the end of the test, temperature difference was approximately 80 ^{o}C for Loc10. Overall at the end of the test, bottom flange temperature for Loc2 (bottom) reached 865 and Loc10 (top) was 245 ^{o}C for uninsulated (real) situation, top flange temperature for Loc2 (bottom) reached 1015 and Loc10 (top) was 165 ^{o}C for insulated situation. Thus, it can be understood that at the end of the test, bottom flange temperature difference between Loc2 (bottom) and Loc10 (top) was 620 ^{o}C for uninsulated (real) situation, 850 ^{o}C for insulated situation. Therefore, thermal gradient difference can be easily understood from this comparison and proved for INP 400 section.

For HEB 400 section test results comparison is shown in Figure 7.14.

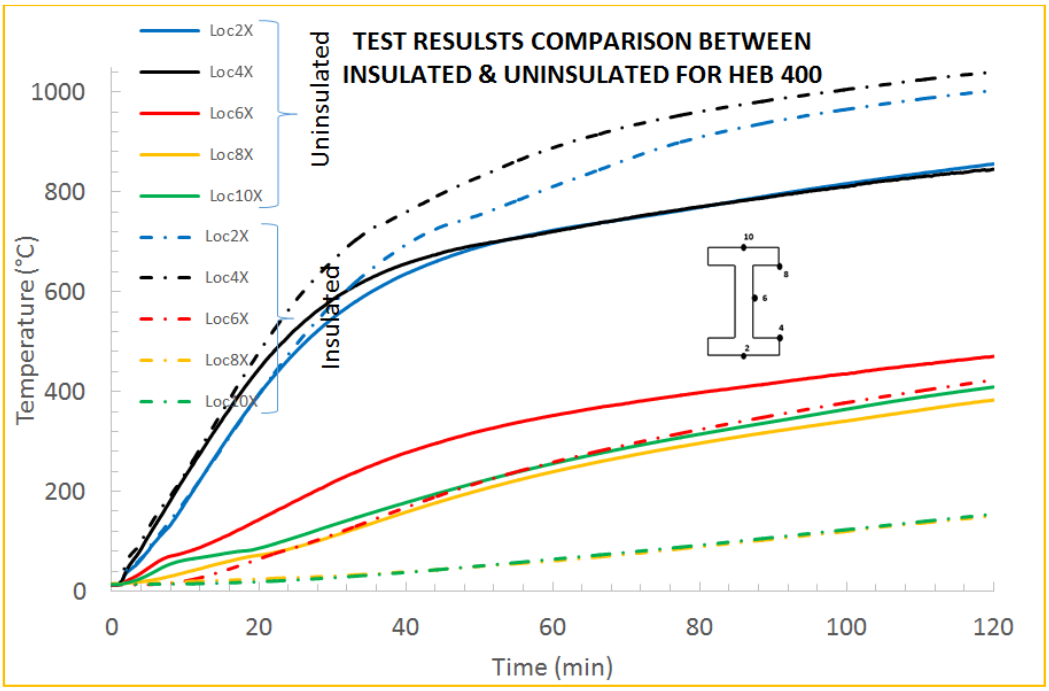

Figure 7.14. Comparison of Test Results for HEB 400.

At the beginning of the test, for Loc2 temperature values are so close to each other until 30-minute. After 30-minute temperature difference commenced to differ. At the 60-minute temperature difference reached to 90 ^{o}C for Loc2. After 90-minute

temperature difference reached to 130 ^{o}C for Loc2. At the end of the test, temperature difference reached approximately 150 ^{o}C. For Loc4 temperature values are so close to each other until 30-minute. At the 60-minute temperature difference reached to 260 ^{o}C for Loc4. After 90-minute temperature difference decreased to 200 ^{o}C for Loc4.

At the end of the test, temperature difference reached approximately 175 ^{o}C. For Loc6, at the beginning of the test, temperature values are so close to each other, but after 2 minutes uninsulated (real) section temperature commenced to increase, after 30-minute difference reach 100 ^{o}C and at the end of the test uninsulated section temperature was 50 ^{o}C higher than the insulated one. For the upper flange Loc8 temperature difference reached to 90 ^{o}C until 30-minute. At the 60-minute temperature difference reached to 200 ^{o}C for Loc8. After 90-minute temperature difference approximately same with 60-minute. At the end of the test, temperature difference was approximately 180 ^{o}C. For the upper flange Loc10 temperature difference reached to 90 ^{o}C until 30-minute. At the 60-minute temperature difference reached to 200 ^{o}C for Loc10. After 90-minute temperature difference approximately same with 60-minute.

At the end of the test, temperature difference was approximately 160 ^{o}C. Overall at the end of the test, bottom flange temperature for Loc2 (bottom) reached 845 and Loc10 (top) was 410 ^{o}C for uninsulated (real) situation, top flange temperature for Loc2 (bottom) reached 1000 and Loc10 (top) was 150 ^{o}C for insulated situation. Thus, it can be understood that at the end of the test, bottom flange temperature difference between Loc2 (bottom) and Loc10 (top) was 435 ^{o}C for uninsulated (real) situation, 850 ^{o}C for insulated situation. Therefore, thermal gradient difference can be easily understood from this comparison and proved for HEB 400 section.

For HEB 300 section test results comparison is shown in Figure 7.15.

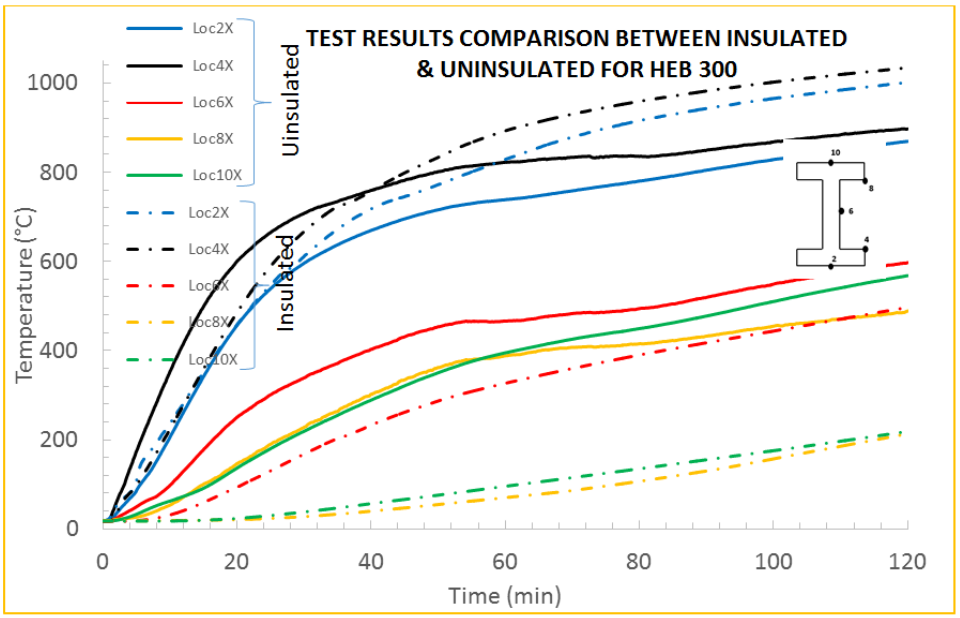

Figure 7.15. Comparison of Test Results for HEB 300.

At the beginning of the test, for Loc2 temperature values are so close to each other until 30-minute. After 30-minute temperature difference commenced to differ. At the 60-minute temperature difference reached to 80 ^{o}C for Loc2. After 90-minute temperature difference reached to 130 ^{o}C for Loc2. At the end of the test, temperature difference was approximately 150 ^{o}C. For Loc4 temperature values are so close to each other until 30-minute. At the 60-minute temperature difference reached to 70 ^{o}C for Loc4. After 90-minute temperature difference reached to 135 ^{o}C for Loc4. At the end of the test, temperature difference reached approximately 140 ^{o}C. For Loc6, at the beginning of the test, temperature values are so close to each other, but after 2 minutes uninsulated (real) section temperature commenced to increase, after 30-minute difference reach 160 ^{o}C and at the end of the test uninsulated section temperature was 100 ^{o}C higher than the insulated one. For the upper flange Loc8 temperature difference reached to 160 ^{o}C until 30-minute. At the 60-minute temperature difference reached to 300 ^{o}C for Loc8. After 90-minute temperature difference approximately same with 60-minute. At the end of the test, temperature difference was approximately 260 ^{o}C. For the upper flange Loc10 temperature difference reached to 90 ^{o}C until 30-minute. At the 60-minute temperature difference reached to 300 ^{o}C for Loc10. After 90-minute temperature difference approximately same with 60-minute. At the end of the test,

temperature difference was approximately 350 ^{o}C. Overall, at the end of the test, bottom flange temperature for Loc2 (bottom) reached 870 and Loc10 (top) was 570 ^{o}C for uninsulated (real) situation, top flange temperature for Loc2 (bottom) reached 1000 and Loc10 (top) was 220 ^{o}C for insulated situation. Thus, it can be understood that at the end of the test, bottom flange temperature difference between Loc2 (bottom) and Loc10 (top) was 200 ^{o}C for uninsulated (real) situation, 780 ^{o}C for insulated situation. Therefore, thermal gradient difference can be easily understood from this comparison and proved for HEB 300 section.

7.5. Thermal Gradient (T_y) for Test 1, Test 2 and Test 3

Thermal gradient through the section depth can be calculated as the temperature difference top (Loc10) and bottom flange (Loc2) divided by the depth.

Thermal gradient (T_y) comparison for Test 1 is shown in Figure 7.16.

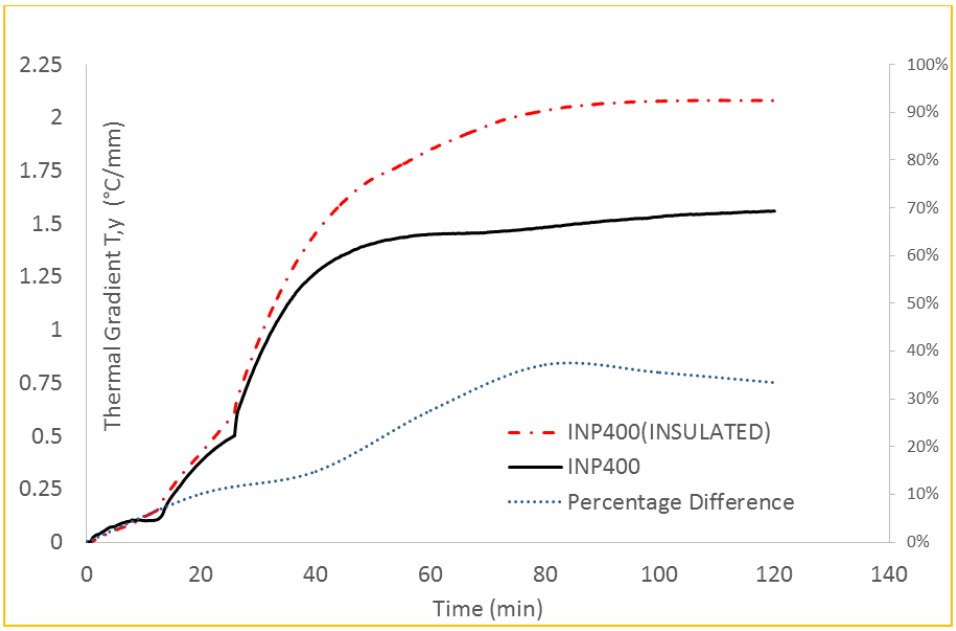

Figure 7.16. Thermal Gradient (T_y) for Test 1 for INP 400.

For INP 400 section (depth 400 mm, width 155 mm), until 30 minutes, the thermal gradient (T_y) is so close to each other for insulated and uninsulated. At 30-minute thermal gradient for INP 400 is 0,87 °C/mm and for INP 400 (insulated) 0,95

^{o}C/mm. At 60-minute thermal gradient for INP 400 is 1,45 ^{o}C/mm and for INP 400 (insulated) 1,85 ^{o}C/mm. At 90-minute thermal gradient for INP 400 is 1,51 ^{o}C/mm and for INP 400 (insulated) 2,1 ^{o}C/mm. At 120-minute thermal gradient for INP 400 is 1,56 ^{o}C/mm and for INP 400 (insulated) is 2,08 ^{o}C/mm. Thermal gradient peak value for 90-minute and 120-minute are so close to each other, it is almost 2,1, it can be evaluated that occurred at the end of the test (120th minute) for fire test insulated specimen. For uninsulated test specimen thermal gradient peak value 1,56 ^{o}C/mm occurred at the end of the test as well. When heat transfer by radiation in the enclosure is allowed, the thermal gradient decrease approximately 34%. It can be evaluated that heat transfer in enclosure should be taken in to account.

Thermal gradient (T_y) comparison for Test 2 is shown in Figure 7.17.

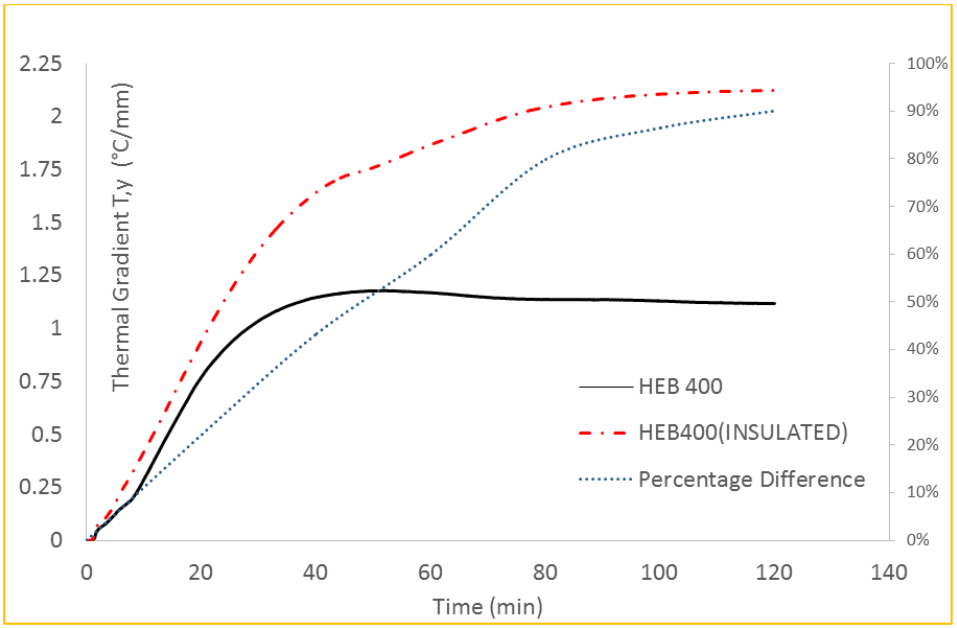

Figure 7.17. Thermal Gradient (T_y) for Test 1 for HEB 400.

For HEB 400 section (depth 400 mm, width 300 mm), until 30 minutes, the thermal gradient (T_y) is so close to each other for insulated and uninsulated. At 30-minute thermal gradient for HEB 400 is 1,04 ^{o}C/mm and for HEB 400 (insulated) 1,37 ^{o}C/mm. At 60-minute thermal gradient for HEB 400 is 1,17 ^{o}C/mm and for HEB 400 (insulated) 1,87 ^{o}C/mm. At 90-minute thermal gradient for HEB 400 is 1,14 ^{o}C/mm and for HEB 400 (insulated) 2,08 ^{o}C/mm. At 120-minute thermal gradient for HEB

400 is 1,12 ^{o}C/mm and for HEB 400 (insulated) is 2,12 ^{o}C/mm. Thermal gradient peak value is 2,12 ^{o}C/mm occurred at the end of the test for fire test insulated specimen. For uninsulated test specimen thermal gradient peak value 1,18 ^{o}C/mm occurred at 52nd minute. When heat transfer by radiation in the enclosure is allowed, the thermal gradient decrease approximately 89% at the end of the specimen. For the peak value for 52nd minute, thermal gradient decrease approximately 50%. It can be evaluated that heat transfer in enclosure should be taken in to account.

Thermal gradient (T_y) comparison for Test 3 is shown in Figure 7.18.

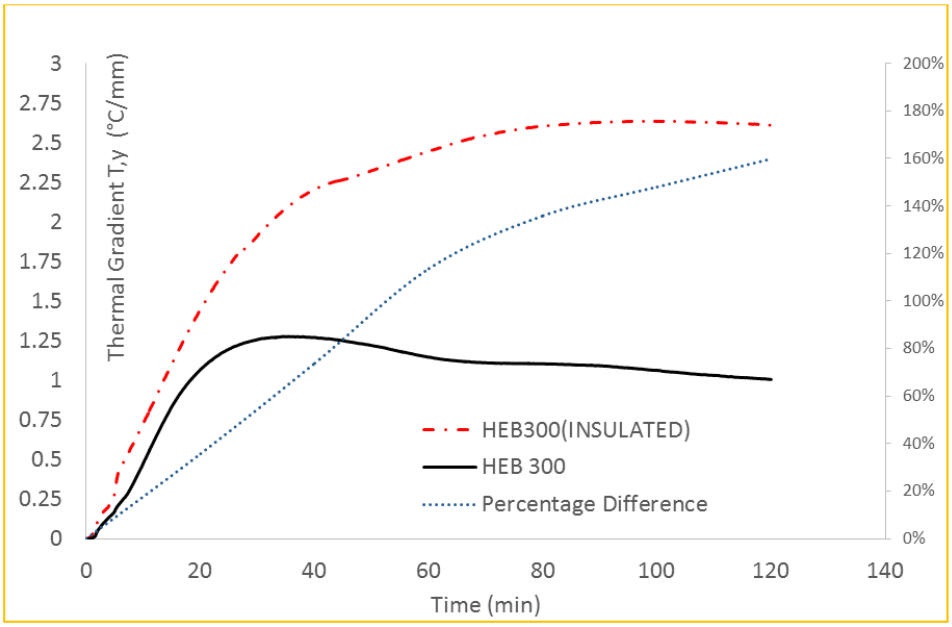

Figure 7.18. Thermal Gradient (T_y) for Test 1 For HEB 300.

For HEB 300 section (depth 300 mm, width 300 mm), until 30 minutes, the thermal gradient (T_y) is so close to each other for insulated and uninsulated. At 30-minute thermal gradient for HEB 300 is 1,26 ^{o}C/mm and for HEB 300 (insulated) 1,91 ^{o}C/mm. At 60-minute thermal gradient for HEB 300 is 1,15 ^{o}C/mm and for HEB 300 (insulated) 2,44 ^{o}C/mm. At 90-minute thermal gradient for HEB 300 is 1,09 ^{o}C/mm and for HEB 300 (insulated) 2,63 ^{o}C/mm. At 120-minute thermal gradient for HEB 300 is 1,01 ^{o}C/mm and for HEB 300 (insulated) is 2,61 ^{o}C/mm. Thermal gradient peak value is 2,636 ^{o}C/mm occurred at 97th minute for fire test insulated specimen. For uninsulated test specimen thermal gradient peak value 1,276 ^{o}C/mm occurred at

35th minute. When heat transfer by radiation in the enclosure is allowed, the thermal gradient decrease approximately 160% at the end of the specimen. For the peak value for 35th minute, thermal gradient decrease approximately 63%. It can be evaluated that heat transfer in enclosure should be taken in to account.

Thermal gradient (T_y) comparison for Test 1, Test 2 and Test 3 is shown in Figure 7.19.

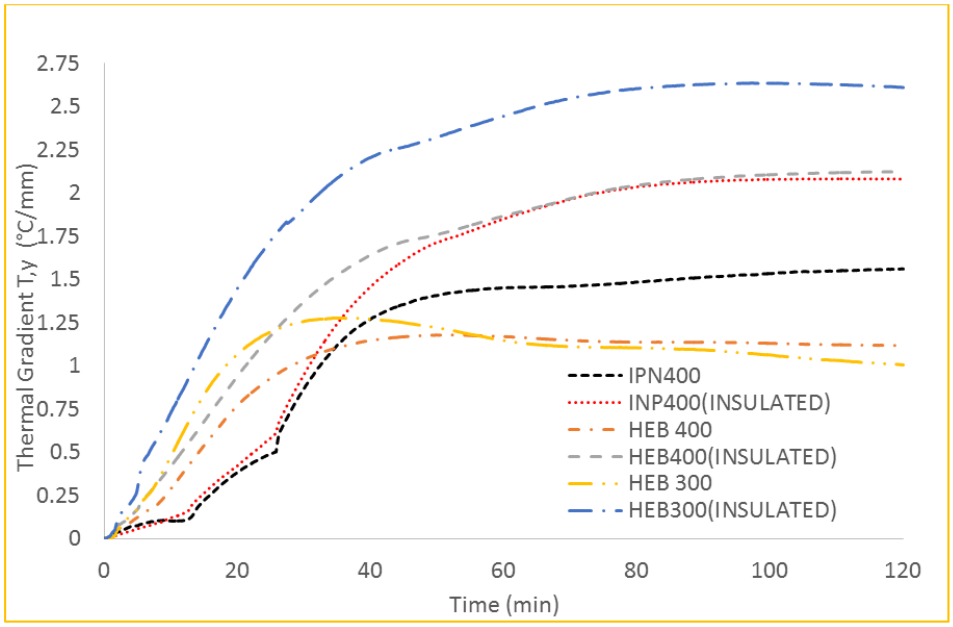

Figure 7.19. Comparison of Thermal Gradient (T_y) for Test 1, Test 2 And Test3.

At the end of the test, thermal gradient (T_y) for INP 400 decay is 34% instead of 89% for HEB 400. It can be evaluated from Figure 7.12. that flange width has significant effect on thermal gradient. In addition, thermal gradient for HEB 300 decay is 160% instead of 89% for HEB 400. Even if they have same flange width, there is significant difference between them due to section depth. When the bottom and top flange is closer to each other, the thermal gradient effect is more the other farther one. It can be evaluated that the more depth decrease the more thermal gradient it has. In other words, when the flange width increase, the radiation effect of enclosure and effects of top-bottom flange and web is more than the less one. Moreover, when the depth decrease, radiation effects from bottom flange to top flange and bottom flange to web is more than the higher one.

In summary, the thermal gradient (T_y) is crucial to accurately estimate the moment demand and capacity in a column section in structural fire engineering. Both experimental and numerical results show that the surface heat exchange significantly changes the thermal gradient. In a realistic scenario, the sections are left bare (i.e. uninsulated). In most of the conventional numerical heat transfer analyses, the section surfaces are adiabatic, hence the flange and web surfaces act as if they are insulated. The results show that the numerical analyses (if surface heat exchange is not taken into account) will always overestimate the thermal gradient, which is on the conservative side. However, this is not cost effective.

8. AVERAGE TEMPERATURE (ΔT) OF SECTIONS FOR TEST1, TEST2 AND TEST3

Average temperature (ΔT) results for all test sections are calculated in order to evaluate the sections overall thermal difference exposed to fire. The average temperature of steel sections are determined with weighted ratio proportional to their area. For instance, all reading from bottom flange are close to each other. Mean value of bottom flange readings are multiplied by its corresponding area and this calculation is performed also for other parts of section. At the end, total value is divided by total area. Average temperature (ΔT) for INP 400 is shown in Figure 8.1.

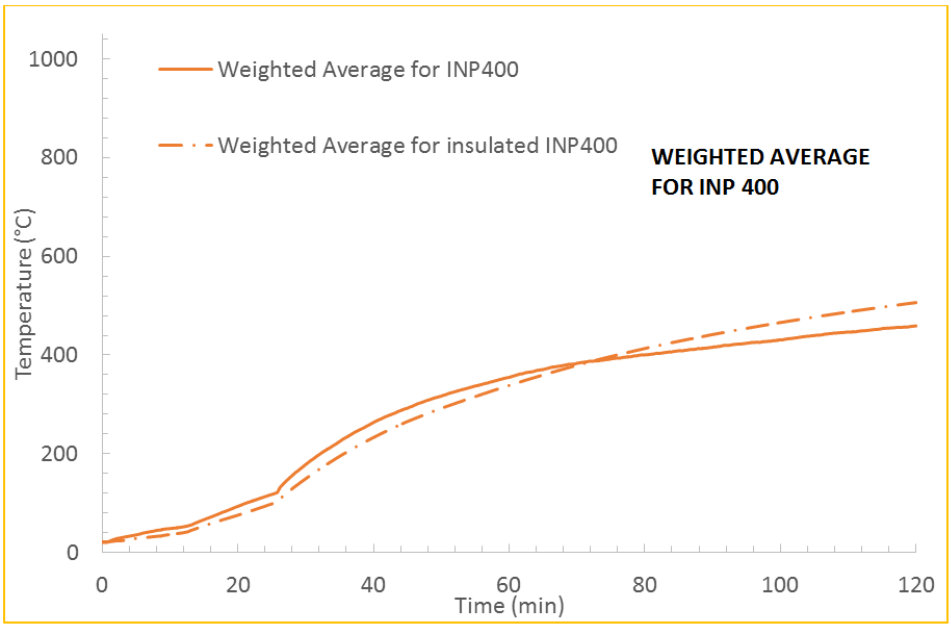

Figure 8.1. Average Temperature (ΔT) for INP 400.

Weighted average temperature for INP 400 in uninsulated case (a realistic scenario) is higher than the insulated cross section until approximately 70^{th} minute. The temperature difference is approximately 30 ^{o}C. After 70th minute, the difference starts to increase. At the end of the test, the difference is approximately 40 ^{o}C. The plot shows that the average temperature in an ınsulated cross section is slightly lower compared to the bare (uninsulated section) for most of the fire duration. Average temperature

(ΔT) for HEB 400 is shown in Figure 8.2.

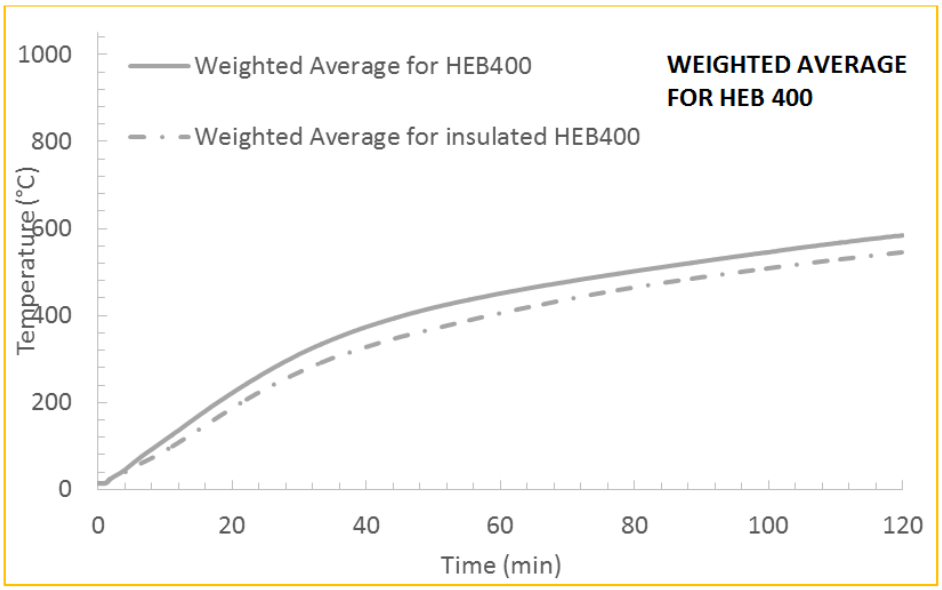

Figure 8.2. Average Temperature (ΔT) for HEB 400.

In Figure 8.2, the temperature difference is approximately 50 ^{o}C. The plot shows that the average temperature in an insulated HEB 400 cross section is lower compared to the uninsulated (bare) section for all of the fire duration. Average temperature (ΔT) for HEB 300 is shown in Figure 8.3.

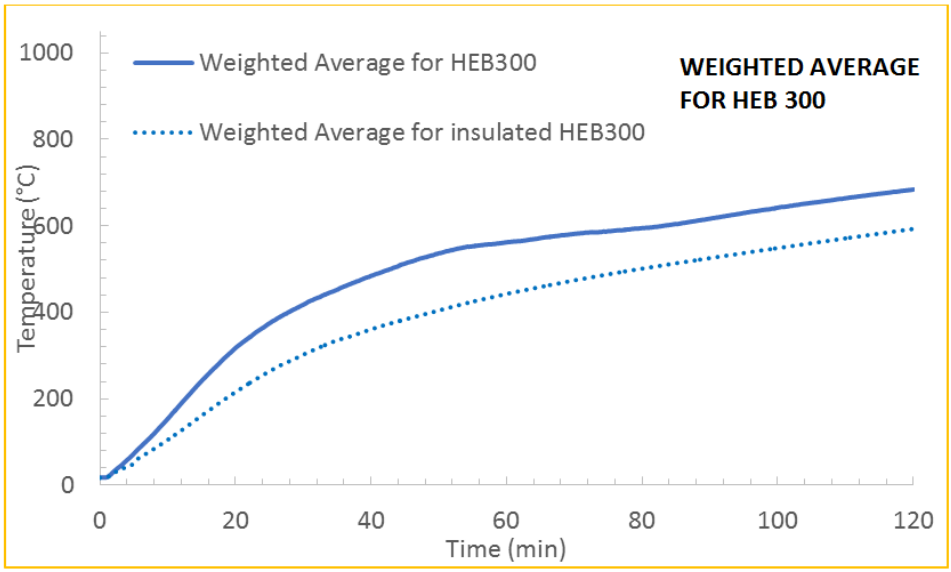

Figure 8.3. Average Temperature (ΔT) for HEB 300.

In Figure 8.3, the temperature difference is approximately 100 ^{o}C. The plot shows that the average temperature in an insulated HEB 300 cross section is lower compared to the bare (uninsulated section) for all of the fire duration.

In summary, the average temperature (ΔT) is crucial to accurately estimate the axial load demand and capacity in a column section in structural fire engineering. Both experimental and numerical results show that the surface heat exchange changes the average temperature. In a realistic scenario, the sections are left bare (i.e. uninsulated). In most of the conventional numerical heat transfer analyses, the section surfaces are adiabatic, hence the flange and web surfaces act as if they are insulated. The results show that the numerical analyses (if surface heat exchange is not taken into account) will underestimate the average temperature, which is on the unconservative side and therefore cannot be permitted.

9. STRUCTURAL ENGINEERING IMPLICATIONS OF THE RESEARCH FINDINGS

In intermediate storey or top storey columns in case of braced frame in which each storey has fire compartment with enough fire resistance, buckling resistance of columns shall be determined for average temperature of columns for related fire resistance time. In order to understand the effect of average temperature changes observed in the research findings to the structural behaviour of columns, the buckling resistance design as per EN 1993-1-2 for compression members at time of t is shown below:

$$N_{b,fi,t,Rd} = x_{fi}\ A\ k_{y,\theta} f_y /\ \gamma_{M,fi} \tag{9.1}$$

where x_{fi} is the reduction factor for flexural buckling in the fire design situation, $k_{y,\theta}$ is the reduction factor from EN 1993-1-2 for yield strength of steel at the steel temperature θ_a reached at time t, x_{fi} lesser value should be taken:

$$x_{fi} = 1/(\varphi_\theta + ((\varphi_\theta^2 - \lambda_\theta'^2)^{0,5})) \tag{9.2}$$

$$\varphi_\theta = 0,5(1 + \alpha\lambda_\theta' + \lambda_\theta'^2) \tag{9.3}$$

$$\alpha = 0,65(235/f_y) \tag{9.4}$$

Non-dimensional slenderness λ_θ' for elevated temperature calculated as follows:

$$\lambda_\theta' = \lambda'(k_{y,\theta}/k_{E.\theta})^{0,5} \tag{9.5}$$

where $k_{E,\theta}$ is the reduction factor from EN 1993-1-2 the slope of the linear elastic range at the steel temperature θ_a reached at time t.

If the HEB 300 properties applied to above equations for 500 ^{o}C;

$$x_{fi} = 0,73 \tag{9.6}$$

where $N_{b,fi,t,Rd} = x_{fi}\ A\ k_{y,\theta} f_y / \gamma_{M,fi}$= 0,73*14910*0,78* 220 N/mm^2 for (St.37 class steel yield strength 220 N/mm^2) =1866,3 kN.

If the HEB 300 properties applied to above equations for 600^{o}C;

$$x_{fi} = 0,47 \tag{9.7}$$

where $N_{b,fi,t,Rd} = x_{fi}\ A\ k_{y,\theta} f_y / \gamma_{M,fi}$= 0,73*14910*0,78* 220 = 1092,8 kN.

It can be evaluated from above equations that buckling resistance of steel columns reduce approximately 40% if the column average temperature is 600 ^{o}C instead of 500 ^{o}C. In a typical heat transfer analysis, the column temperatures will be 500 ^{o}C. However, when the surface heat exchange in the enclosure is taking into account, the average temperature will be 600 ^{o}C. This means that the numerical heat transfer analysis will lead to 40% overestimation of the column strength. Therefore, it can be understood that heat exchange between enclosure surfaces has significant role in fire resistance of columns exposed one side fire exposure. It can be understood that underestimation of axial load capacity cannot be accepted from structural analysis point of view.

10. CONCLUSIONS

There are some important conclusions of this research and they are highlighted below. The research is based on experimental results of IPN400, HEB400 and HEB300 cross sections backed by numerical analyses conducted in commercial finite element software Abaqus. Here, cross sections without insulation in the enclosure represents a realistic scenario. Cross sections with insulation in the enclosure represents the adiabatic surface conditions usually assumed in numerical analysis.

(i) Radiation heat transfer of steel I sections exposed to one side heating is generally not taken into consideration in structural fire engineering. However, the results show that one side heating with adiabatic surface enclosure (insulated case) underestimates the average cross section temperature (ΔT). This can result in underestimation of axial load demand and capacity of column sections, which cannot be accepted from structural analysis point of view.

(ii) Surface heat exchange in enclosure has large effects on thermal gradient (T, y) on steel structures such as perimeter steel columns. The tests confirm that the thermal gradient significantly reduces when the cross sections are left unprotected in the enclosure. The numerical analyses which represent insulated (adiabatic) surfaces in the enclosure always largely overestimate the thermal gradient (T, y). This can result in overestimation of moment demand and capacity of column sections. This is safe from the structural analysis point of view but costly from steel industry point of view.

(iii) When cross sections with different depth and flange width are compared, it is seen that flange width has a larger effect on the thermal gradient. HEB400, which has a larger flange width has a smaller thermal gradient compared with INP 400 has same depth and smaller flange width. HEB 300, which has a smaller depth, has a smaller thermal gradient compared with HEB 400 has same flange width and smaller depth.

(iv) INP 400 thermal gradient ($T_{,y}$) decrease in real unprotected case is approximately 33%, while in HEB 400 decrease is 90%. Therefore, bf (flange width of section)

has a greater effect on thermal gradient. In addition, even if HEB 300 has same flange width thermal gradient ($T_{,y}$) decrease is 160%. If HEB 300 and HEB 400 compared with each other, it can be evaluated that thermal gradient ($T_{,y}$) decrease is approximately 70% (depth difference is 100 mm). Overall, it can be understood that the bf effects on thermal gradient ($T_{,y}$) is more than depth of the section effect.

(v) Design Recommendations: In buildings, one side heating exposure conditions can take place in perimeter columns and also internal columns separated by left and right side non-load bearing fire compartment walls that fire occurs from one side only. When design is performed as per EN 1993-1-2 Structural fire Eurocode 3 - Design of steel structures -Part 1-2: General Rules -Structural fire design, the reduction factor for yield stress is 0,78 for 500 ^{o}C and 0,47 for 600 ^{o}C. Linear interpolation shall be done for interim temperatures. Therefore, it can be evaluated for HEB 300 (larger flange width, smaller depth) that there is significant effects on design when enclosure effects are taken into account when the average cross section temperature (ΔT) is considered. Even if the results show that for HEB 400 average cross section temperature is close to each other, the reduction factor differ approximately 12%, so this difference can cause problem during the design. Therefore, the radiation heat transfer between flanges and web in the enclosure have significant effects in structural design.

REFERENCES

Buchanan, A.H., "Structural Design for Fire Safety", *Univercity of Canterbury*, New Zealand, 2001.

Emery, A.F., O. Johansson, M. Lobo, A. Abrous, "A Comparative Study of Methods for Computing the Diffuse Radiation view Factors for Complex Structures", *Journal of Heat Transfer*, Vol. 113, No. 2, pp. 413-422, 1991.

Fu, H.C., S.F. Ng, and M.S. Cheung, "Thermal Behavior of Composite Bridges", *Journal of Structural Engineering*, Vol. 116, No.12, pp. 3302-3323, 1990.

Ghojel, J.I., M.B. Wong, "Heat Transfer Model for Unprotected Steel Members in A Standard Compartment Fire with Participating Medium", *Journal of Constructional Steel Research*, Vol. 61, No. 6, pp. 825-833, 2005.

Huebner, K.H., D.L. Dewhirst, D.E. Smith, and T.G. Byrom, *The Finite Element Method for Engineers*, John Wiley and Sons, 2008.

Rao, V.R., V.M.K. Sastri, "Efficient Evaluation of Diffuse View Factors for Radiation", *International Journal of Heat and Mass Transfer*, Vol. 39, No. 6, pp. 1281-1286, 1996.

Selamet S., M. Garlock, "Plate Buckling Strength of Steel Wide-Flange Sections at Elevated Temperatures", *Journal Structutal Engineering*, Vol. 139, No. 11, pp. 1853-1865, 2013.

Selamet S., M. Garlock, "Fire Resistance of Steel Shear Connections", *Fire Safety Journal*, Vol. 68, pp. 52-60, 2014.

Selamet, S., *Behavior, Design and Finite Element Modeling of Shear Connections Under Fire Hazard*, Ph.D. Thesis, Princeton University, NJ USA, 2011.

Selamet, S., "Thermal Gradient Estimation due to Surface" *Heat Exchange in Steel I-Sections*, 2017.

Shapiro, A.B., "Computer İmplementation, Accuracy, and Timing of Radiation View Factor Algorithms", *Journal of Heat Transfer*, Vol. 107, No. 3, pp. 730-732, 1985.

Siegel, R., J.R. Howell, "Thermal Radiation Heat Transfer", *Taylor and Francis*, Vol. 1, pp. 155-192, 2002.

Sparrow E.M., R.D. Chess, "Radikal Heat Transfer, Augmented" *Hemisphere Publishing Corporation*, Vol. 81, No. 144, pp. 339-349, 1978.

Tan, Kang-Hai, and Zhan-Fei Huang, "Structural Responses of Axially Restrained Steel Beams With Semirigid Moment Connection İn Fire", *Journal of Structural Engineering*, Vol. 131, No. 4, pp 541-551, 2005.

Türkiye Standartları Enstitüsü 13501-2, "Fire Classification of Construction Products and Building Elements" - Part 2: "Classification Using Data From Fire Resistance Tests, Excluding Ventilation Services, Brussels", *European Committee for Standardization.*

Türkiye Standartları Enstitüsü 1363-1, "Fire resistance- Tests- Part 1: General Requirements", Brussels, *European Committee for Standardization.*

Türkiye Standartları Enstitüsü 1363-2, "Fire Resistance Tests"- Part 2: "Alternative and Additional Procedures", Brussels, *European Committee for Standardization.*

Türkiye Standartları Enstitüsü 1991-1-2, Eurocode 1: "Actions on Structures" - Part 1-2: General actions "Actions on Structures Exposed to Fire", Brussels, *European Committee for Standardization.*

Türkiye Standartları Enstitüsü 1993-1-2, Eurocode 3: "Design of Steel Structures" - Part 1-2: "General Rules -Structural Fire Design", Brussels, *European Committee for Standardization.*

Usmani, A.S., J.M. Rotter, S. Lamont, A.M. Sanad, M. Gillie, "Fundamental Principles of Structural Behaviour Under Thermal Effects", *Fire Safety Journal*, Vol. 36, No. 8, pp. 721-744, 2001.

Vacha, J., P. Kyzlik, I. Both, F. Wald, "Beams with Corrugated Web at Elevated Temperature, Experimental Results", *Thin Walled Structures*, Vol. 98, pp. 19-28, 2016.

Virdi, K.S., U. Wickstrom, "Influence of Shadow Effect on The Strength of Steel Beams Exposed to Fire", In 20th *International Conference on Computer Methods in Mechanics*, 2013.

Walz, J, L. Choe, A. Surovek, A. Varma, "Section Characterization of Wide-Flange Steel Sections Subjected to Combined Thermal and Mechanical Loading", *Journal of Structural Engineering*, Vol. 141, No. 6, pp. 014-162, 2014.

Wickstrom U., "Heat Transfer by Radiation and Convection in Fire Testing", *Fire and Materials*, Vol. 28, No. 5, pp. 411-415, 2004.

Wickstrom, U., "Calculation of Heat Transfer to Structures Exposed to Fire - Shadow Effects", Proceedings of the Ninth International Conference, *Interscience Communication*, Vol. 1, pp. 451-458, 2001.